Université de Montréal

Localized Electronic States of a Centrosymmetric SSH Soliton

par

Maude Bédard

Département de physique
Faculté des arts et des sciences

Mémoire présenté en vue de l'obtention du grade de
Maître ès sciences (M.Sc.)
en Physique

December 23, 2022

Université de Montréal

Faculté des arts et des sciences

Ce mémoire intitulé

Localized Electronic States of a Centrosymmetric SSH Soliton

présenté par

Maude Bédard

a été évalué par un jury composé des personnes suivantes :

David London
(président-rapporteur)

Richard MacKenzie
(directeur de recherche)

Manu Paranjape
(membre du jury)

Résumé

La matière condensée moderne porte un intérêt particulier pour la classe de matériaux formée par les isolants topologiques. Ils sont différents des isolants typiques par leurs intéressantes propriétés quantiques; ils se comportent comme des isolants dans leur intérieur, mais contiennent des états conducteurs sur leur surface. On peut mieux comprendre le comportement de certains systèmes en matière condensée, tel que les chaînes de polyacétylène, en étudiant un système unidimensionnel simple : le modèle de Su-Schrieffer-Heeger (SSH). Le modèle SSH décrit des fermions sans spin sautant sur un réseau unidimensionnel où les amplitudes de saut alternent d'un site à l'autre. Ce modèle, bien que simpliste, expose les propriétés clés des isolants topologiques tel que les états délocalisés dans tout le réseau ainsi que les états exponentiellement localisés aux frontières du réseau. Dans ce projet, nous étudions le modèle SSH, mais en ajoutant un défaut central dans le réseau qu'on appelle un soliton. Dans notre cas, le soliton consiste en un site central donc les amplitudes de saut sont les mêmes d'un côté et de l'autre. Nous trouvons un ensemble de solutions complet incluant des états de basse énergie localisés aux frontières ainsi que des états de haute énergie localisés au soliton.

mots clés: matériaux topologiques, modèle Su-Schrieffer-Heeger (SSH), états de surface, soliton

Abstract

Topological insulators are a class of materials that have attracted much attention in modern condensed matter. They are different from typical insulators as they exhibit interesting quantum properties; they behave as insulators in their interior but have conducting states on their surface. We can better understand the properties of low dimensional condensed matter systems (like poly-acetylene chains) by studying a toy model known as the Su-Schrieffer-Heeger (SSH) Model. The SSH model describes spinless fermions hopping on a one-dimensional lattice with staggered hopping amplitudes. Such a toy model exhibits key properties of topological insulators, such as bulk states (delocalized states across the lattice) and edge states (exponentially localized states at the boundaries of the lattice). In this project, we study the SSH model with an added central defect to the chain, which we call a soliton. In our case, the soliton consists of a central site with the same hopping amplitude on either side. We study the impact of such a defect on the properties of the system; we find a complete set of solutions including near-zero-energy edge states as well as high-energy states localized at the soliton.

keywords: topological materials, Su-Schrieffer-Heeger (SSH) model, edge states, soliton

Contents

List of tables

List of figures

Acknowledgements

First and foremost, I want to thank Richard MacKenzie for giving me the opportunity to complete this work under his supervision. With his guidance, I learned more than I could have ever thought possible about physics, of course, but, even more so, about myself.

To Nic, the most heartfelt and grateful thank you. I truly could not have done any of this work without your precious help as a mentor, but even more so, as a friend.

To my chosen family, Aude, Chloé, Javier, and Maggie (in alphabetical order, because I could not choose): you are my rocks forever and ever. Thank you for the laughs, the cries and the rants. Je vous aime mes cabochons.

To Maggie, I could not have gotten to do a masters without you by my side throughout undergrad. I will always cherish those years we got to spend together.

To my physics boys, Charles, Jo, Nic, LP and Will: I never, ever, thought I would get to make precious friends like you during this time. Thank you for welcoming me into your group with open arms (and introducing me to mead).

A big thank you to my parents who have always believed in me and encouraged me, even when it seemed impossible.

Finally, to my partner Mo, thank you for your endless support: nobody does a pep talk quite like you do.

Introduction

The emergence of the field of topological materials can be traced back to the observation of the quantum Hall effect where conducting electrons at fixed quantized levels of conductance move along the surface of a material that is insulating in its interior [1]. Topological materials are a classification of materials that can host topological states, which are states confined to the boundaries (edges, surface) of the system and are robust to disorder and deformations [2]. From topological superconductors to topological insulators, there is a variety of such materials that have caught researchers' attention mostly due to the stability of topological states. Topological insulators differ from classical insulators by the existence of conducting states on their surface while maintaining insulating states in their bulk. These metallic states have been the focus of much research as they have various useful and surprising properties such as having the ability to assure light transport in nanophotonics systems [3], to magnify the sound intensity at photonic crystal interfaces [4], to enable a stable one-way propagation [5] and to permit the observation of the anomalous quantum hall effect [6]. The Su-Schrieffer-Heeger model (SSH) was first introduced in 1979 to describe the formation of solitons in polyacetylene chains [7]. In this context, the soliton refers to the boundary between two domains with different ground states, which arises when these states are degenerate [8]. In this work, a soliton will refer to a spatial boundary between two domains. The SSH model is one of the simplest models to showcase topological insulator properties such as topological edge states [9, 10, 11, 12]. It may feel like we have been throwing around the term 'topological' up to this point, so let's briefly discuss what this label actually means. The existence of topological states in one-dimensional materials is explained through the calculation of the Zak Phase [13]. This non-vanishing phase is picked up by particles in systems with a periodic parameter space (for the SSH model, the Brillouin Zone) and changes for different topological configurations. Phase differences are gauge-invariant, which allows

for topological classifications of different configurations of the system. At the domain wall between configurations with different Zak phases (distinct topological arrangements), robust states localized at the system's boundaries emerge [14]. In the context of the SSH model, we call these states topological edge states when they are localized at the edges of the chain and topological solitonic modes when they are localized at a spatial domain wall. A topology-oriented analysis of SSH-analogous models has been widely discussed in various works [9, 15, 16]. The focus of this work will be to provide a full description of the energy solutions and wave functions of both an infinite and finite SSH chain, each with an added soliton (defect, domain wall). We aim to find solitonic modes as well as edge states in both of these systems as it will show that the presence of conducting states is robust to disorder; a signature of topological insulators. In Chapter 1, we provide a detailed analysis of the SSH model's energy spectrum and wave functions. Chapter 2 introduces the effect of a soliton on an infinite SSH chain through the calculation of all wave functions of the Hamiltonian. Studying the infinite system allows us to essentially study the effect of a defect on a continuous system analogous to solitons in quantum fields [17]. Chapter 3 considers both possible configurations of a finite SSH chain with a central soliton; we provide a complete description of the solutions to such systems. Notably, we find that, in addition to edge states with near-zero energies, there are also high-energy states in the presence of a soliton. Finally, we present concluding remarks as well as discuss possible applications of the work presented in this thesis.

Chapter 1

The Su-Schrieffer-Heeger Model

The Su-Schrieffer-Heeger model (SSH model) is named after the three authors who introduced it in the highly influential 1979 paper to describe a polyacetylene chain [7] and has been of interest for its intriguing properties such as the existence of solitons [7, 18] and charge fractionalization [19]. More recently, the model has attracted attention for being one of the simplest examples of topological insulators due to its one-dimensional structure. Fig. 1.1 illustrates an SSH chain.

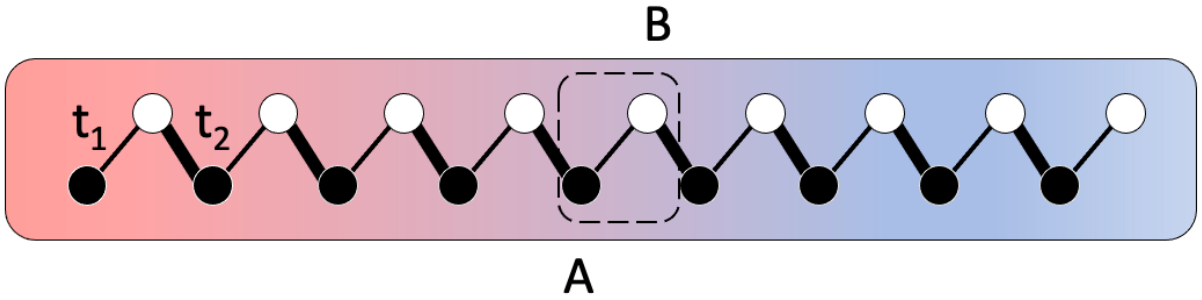

Fig. 1.1. SSH Chain with $N = 18$ with staggered hopping parameters t_1 and t_2. The chain being even, the hopping parameter at the edges of the chain is t_1. The dotted square defines a unit cell with the dark (light) site corresponding to sublattice A (B).

1.1. Hamiltonian and solutions

In this section, we will find the states and the energy spectrum of the SSH model as well as discuss some of its properties that will be relevant to what follows. The SSH model is

a tight-binding model that describes a spinless (or spin-polarized) electron moving along a one-dimensional lattice (chain). In the work that follows, we will use the terms electron, fermion, and particle interchangeably. The dashed region in Fig. 1.1 represents a unit cell, which contains two sites labeled A and B. The unit cell being the periodic structure of the chain, we can create a chain of any length by translating this region as many times as necessary. We will also refer to unit cells as dimers since the SSH model was originally developed to describe a chain of polyacetylene, which is composed of a series of dimers. The chain is commonly described as having staggered hopping amplitudes. This simply means that the chain has alternating tunneling amplitudes, which correspond to bond strengths between atoms due to the overlap of electronic orbitals from neighbouring sites. The chain being composed of two staggered and connected sublattices A and B, we distinguish the hopping parameters by having an inter-cell and an intra-cell hopping parameter. In Fig. 1.1, t_1 (t_2) is the intra-cell (inter-cell) hopping amplitude. However, please note that these roles are not rigidly assigned to either parameters and will change as we move through this work. Moreover, t_1 (t_2) is drawn with a thin (thick) line, but the thickness doesn't necessarily indicate the bond strength of inter/intra-cellular parameters, but instead serves as a visual label. Fig. 1.2 illustrates a simplified representation of an SSH chain that from now on will be the preferred visualization.

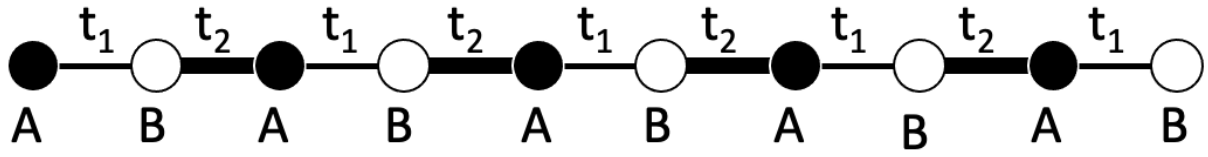

Fig. 1.2. Simplified representation of an SSH Chain with $N = 10$ and alternating hopping parameters t_1 and t_2. Note that we don't specify a value for either hopping parameter; both cases $t_1 < t_2$ and $t_1 > t_2$ are considered. The thicker/thinner lines don't indicate the strength of the coupling, but serve as visual labels for t_1 and t_2. This representation will be used for the rest of the work.

As the work in subsequent chapters is based on the SSH model, we now derive its well-known results closely following the formalism in [20]. We start by considering an SSH chain with an even number of sites; the case of an odd chain will be discussed in less detail in section

1.1.3. As shown in Fig. 1.2, there are two sites, A and B, per unit cell, labeled m. For an even chain, we have a total number of sites $N = 2M$, where M is the total number of unit cells. We start by writing the Hamiltonian describing our system

$$H_{\text{SSH}} = t_1 \sum_{m=1}^{M} \Big(|m,B\rangle\langle m,A| + h.c. \Big) + t_2 \sum_{m=1}^{M-1} \Big(|m+1,A\rangle\langle m,B| + h.c. \Big), \tag{1.1.1}$$

for which we will find the eigenenergies and eigenstates. Expressing the Hamiltonian in matrix form,

$$H_{\text{SSH,Even}} = \begin{pmatrix} 0 & t_1 & & & & \\ t_1 & 0 & t_2 & & & \\ & t_2 & 0 & t_1 & & \\ & & t_1 & 0 & \ddots & \\ & & & \ddots & \ddots & t_1 \\ & & & & t_1 & 0 \end{pmatrix}. \tag{1.1.2}$$

where the last hopping parameter is t_1 as we are considering an even chain. We search for solutions of the Schrödinger equation $(H_{\text{SSH}} - E)\,|\psi\rangle = 0$. Since the system is invariant under translation by an even number of sites, we have the following ansatz

$$|\psi\rangle = \sum_{n=1}^{N} \psi_n |n\rangle = \sum_{m=0}^{M-1} \Big(A|2m+1\rangle + B|2m+2\rangle \Big) e^{i2mk}, \tag{1.1.3}$$

where $n \in \{1,...,N\}$ and $m \in \{0,1,...,M-1\}$ denotes the unit cells. The odd sites are denoted by $|n_{\text{odd}}\rangle = |2m+1\rangle$ and the even sites, $|n_{\text{even}}\rangle = |2m+2\rangle$. A and B are constants to be determined. The last site's oscillatory factor is $e^{i2(M-1)k} = e^{i(2M-2)k} = e^{i(N-2)k}$ since an even-length chain has a total of $N = 2M$ sites. The Schrödinger equation in matrix form is then

$$(H_{\text{SSH}} - E)\,|\psi\rangle = \begin{pmatrix} -E & t_1 & & & & \\ t_1 & -E & t_2 & & & \\ & t_2 & -E & t_1 & & \\ & & t_1 & -E & \ddots & \\ & & & \ddots & \ddots & t_1 \\ & & & & t_1 & -E \end{pmatrix} \begin{pmatrix} A \\ B \\ Ae^{i2k} \\ Be^{i2k} \\ \vdots \\ Ae^{i(N-2)k} \\ Be^{i(N-2)k} \end{pmatrix} = 0, \tag{1.1.4}$$

of which all but the first and last equations are of the form

$$\begin{aligned} t_1\psi_{n-1} - E\psi_n + t_2\psi_{n+1} = 0\,, \\ t_2\psi_{n-1} - E\psi_n + t_1\psi_{n+1} = 0\,, \end{aligned} \tag{1.1.5}$$

for n even and odd respectively. From here on out, these will be referred to as the bulk equations. This system of equations is attributed to the periodicity of the Brillouin Zone over a unit cell. Since every neighbouring unit cell's oscillatory term differs by e^{i2k}, these two equations can be reduced to

$$\begin{aligned} t_1 A - EB + t_2 A e^{i2k} = 0, \\ t_2 B - EA e^{i2k} + t_1 B e^{i2k} = 0, \end{aligned} \tag{1.1.6}$$

which we express in matrix form as

$$\begin{pmatrix} t_1 + t_2 e^{i2k} & -E \\ -E & t_1 + t_2 e^{-i2k} \end{pmatrix} \begin{pmatrix} A \\ B \end{pmatrix} = 0. \tag{1.1.7}$$

The determinant must vanish for a nontrivial solution, which yields the dispersion relation

$$E^2 = t_1^2 + t_2^2 + 2t_1 t_2 \cos 2k, \tag{1.1.8}$$

which has energy bands from $\pm(t_1 + t_2)$ to $\pm|t_1 - t_2|$.

1.1.1. The Dispersion Relation

The dispersion relation (1.1.8) deserves a closer look as it illustrates the most important features of the model; in the thermodynamic limit $N \to \infty$ the chain has no edges. From the dispersion relation (1.1.8), it is clear that there are positive and negative energy solutions, which will yield two bands. For a given energy solution, there is an equal and opposite k solution; we define k to be the positive solution such that solutions take the form $\pm k$. Since the ansatz (1.1.3) is invariant under a phase shift $k \to k + \pi$, we choose k to take values in the range $[-\frac{\pi}{2}, \frac{\pi}{2}]$. The positive and negative energy bands are symmetric due to the chiral symmetry of the Hamiltonian [21]. It is informative to look at a few different configurations of the energy bands for several values of the hopping parameters t_1 and t_2 as shown in Fig. 1.3.

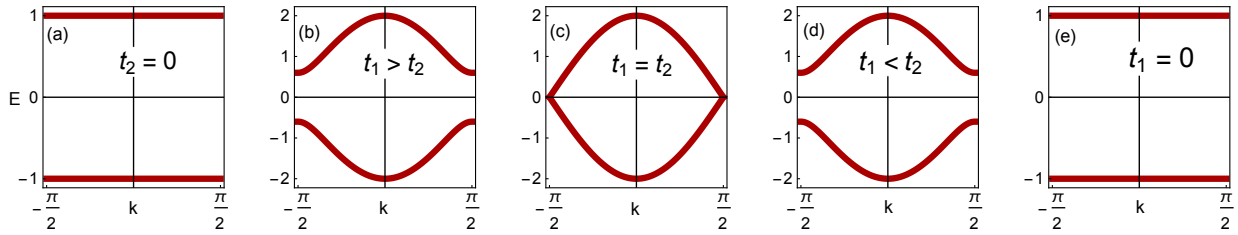

Fig. 1.3. Dispersion relation (1.1.8) for various choices of parameters t_1 and t_2: (a) t_1=1, t_2=0 ; (b) t_1=1.3, t_2=0.7; (c) t_1=1, t_2=1; (d) t_1=0.7, t_2=1.3; (e) t_1=0, t_2=1. We acknowledge that this figure is heavily inspired by Fig. 1.2 of [22].

The case where one of the hopping parameters is zero corresponds to the chain breaking into a series of disconnected dimers. When $t_1 = t_2$, the model reduces to a linear tight-binding chain. We let $t_1 = t_2 = t$ in (1.1.8) to get the well-known dispersion relation of the tight-binding model

$$E^2 = 2t^2(1 + \cos 2k), \tag{1.1.9}$$

where it is easy to see that the energy bands go from $-2t$ to $2t$. Since there is no band gap, this describes a conductor. Finally, we have the cases where $t_1 \neq t_2$ where the gap is open. It is clear that it is necessary to have staggered hopping parameters to describe an insulator. This resulting energy gap, 2Δ, in terms of the hopping parameters is given by [7]

$$\Delta = |t_1 - t_2|. \tag{1.1.10}$$

Back to the Search for Wave Functions

The following constants satisfy the pair of equations (1.1.6)

$$\begin{pmatrix} A \\ B \end{pmatrix} = \begin{pmatrix} t_1 + t_2 e^{-i2k} \\ E \end{pmatrix}. \tag{1.1.11}$$

The first expression of the dispersion relation (1.1.8) allows us to define

$$|E|e^{i2\varphi} \equiv (t_1 + t_2 e^{i2k}), \tag{1.1.12}$$

where the phase φ takes values $0 < \varphi < \pi/2$. Using this definition, we rewrite (1.1.11) such that

$$\begin{pmatrix} A \\ B \end{pmatrix} = \begin{pmatrix} |E|e^{-i2\varphi} \\ E \end{pmatrix}, \tag{1.1.13}$$

which is further simplified by multiplying by $e^{i\varphi}/|E|$ to get the final form

$$\begin{pmatrix} A \\ B \end{pmatrix} = \begin{pmatrix} e^{-i\varphi} \\ \pm e^{i\varphi} \end{pmatrix}, \tag{1.1.14}$$

where the upper (lower) sign corresponds to positive (negative) energy. We now obtain the general form of the solution to the bulk equations $|\psi_\pm\rangle$ by substituting (1.1.14) in (1.1.3) and combining solutions for (k,φ) and $(k,\varphi) \to (-k,-\varphi)$

$$\begin{aligned} |\psi_\pm\rangle = \sum_{m=0}^{M-1} \Big\{ &\left(C_+ e^{-i\varphi} e^{i2mk} + C_- e^{i\varphi} e^{-i2mk}\right) |2m+1\rangle \\ &\pm \left(C_+ e^{i\varphi} e^{i2mk} + C_- e^{-i\varphi} e^{-i2mk}\right) |2m+2\rangle \Big\}, \end{aligned} \tag{1.1.15}$$

where $C_\pm$ are constants to be determined, which are associated with the positive and negative solutions of k and φ. To solve for $C_\pm$, we use this general form of the wave function to rewrite the Schrödinger equation (1.1.4)

$$\begin{pmatrix} -E & t_1 & & & & \\ t_1 & -E & t_2 & & & \\ & t_2 & -E & t_1 & & \\ & & t_1 & -E & \ddots & \\ & & & \ddots & \ddots & t_1 \\ & & & & t_1 & -E \end{pmatrix} \begin{pmatrix} C_+ e^{-i\varphi} + C_- e^{i\varphi} \\ \pm(C_+ e^{i\varphi} + C_- e^{-i\varphi}) \\ C_+ e^{-i\varphi} e^{i2k} + C_- e^{i\varphi} e^{-i2k} \\ \pm(C_+ e^{i\varphi} e^{i2k} + C_- e^{-i\varphi} e^{-i2k}) \\ \vdots \\ C_+ e^{-i\varphi} e^{i(N-2)k} + C_- e^{i\varphi} e^{-i(N-2)k} \\ \pm(C_+ e^{i\varphi} e^{i(N-2)k} + C_- e^{-i\varphi} e^{-i(N-2)k}) \end{pmatrix} = 0. \tag{1.1.16}$$

We take a look at the first and last equations, which from now on will be referred to as the boundary/edge equations. We have

$$\begin{aligned} -E(C_+ e^{-i\varphi} + C_- e^{i\varphi}) \pm t_1 (C_+ e^{i\varphi} + C_- e^{-i\varphi}) = 0, \\ \mp E(C_+ e^{i\varphi} e^{i(N-2)k} + C_- e^{-i\varphi} e^{-i(N-2)k}) + t_1 (C_+ e^{-i\varphi} e^{i(N-2)k} + C_- e^{i\varphi} e^{-i(N-2)k}) = 0. \end{aligned} \tag{1.1.17}$$

These boundary equations are what makes the energy spectrum discrete as opposed to an infinite SSH chain that has continuous energy bands. We write (1.1.17) in matrix form

$$\begin{pmatrix} -Ee^{-i\varphi} \pm t_1 e^{i\varphi} & -Ee^{i\varphi} \pm t_1 e^{-i\varphi} \\ (\mp Ee^{i\varphi} + t_1 e^{-i\varphi}) e^{i(N-2)k} & (\mp Ee^{-i\varphi} + t_1 e^{i\varphi}) e^{-i(N-2)k} \end{pmatrix} \begin{pmatrix} C_+ \\ C_- \end{pmatrix} = 0. \tag{1.1.18}$$

We can considerably simplify this pair of equations by using the expression derived from the definition (1.1.12)

$$-Ee^{\pm i\varphi} \pm t_1 e^{\mp i\varphi} = \mp t_2 e^{\mp i\varphi} e^{\pm i2k}, \tag{1.1.19}$$

to get

$$\begin{pmatrix} e^{i\varphi}e^{-i2k} & e^{-i\varphi}e^{i2k} \\ e^{-i\varphi}e^{iNk} & e^{i\varphi}e^{-iNk} \end{pmatrix} \begin{pmatrix} C_+ \\ C_- \end{pmatrix} = 0. \tag{1.1.20}$$

Taking the determinant of this matrix, imposing it must vanish for nontrivial solutions, using (1.1.19) to simplify and defining the ratio of hopping parameters $r \equiv t_1/t_2$, we find the relation

$$rs_{N+2} + s_N = 0, \tag{1.1.21}$$

where we have used the shorthand $\sin(Ak) \equiv s_A$. We will discuss the solutions to this equation in the next section.

We can see from (1.1.20) that $C_\pm$ can take the form

$$\begin{pmatrix} C_+ \\ C_- \end{pmatrix} = \begin{pmatrix} e^{-i\varphi}e^{i2k} \\ -e^{i\varphi}e^{-i2k} \end{pmatrix}, \tag{1.1.22}$$

which we substitute in the general form of the wave function (1.1.15), reexpress the φ factors in terms of k using (1.1.19) and simplify to get the form

$$\left|\psi_\pm^{\text{bulk}}\right\rangle = \sum_{m=0}^{M-1} \Big\{(t_1 s_{2(m+1)} + t_2 s_{2m})|2m+1\rangle \; + E s_{2(m+1)}|2m+2\rangle\Big\}. \tag{1.1.23}$$

1.1.2. A complete set of solutions

We now want to verify that we have found a complete set of solutions. As the Hamiltonian has dimension $N \times N$, we expect to find N eigenstates and eigenenergies. To do so, we examine the k equation (1.1.21), which will provide us with the number of wavenumber solutions. Note that, for now, we still assume k to be real. This equation cannot be solved analytically, but can easily be solved graphically as shown in Fig. 1.4. We note that (1.1.21) depends on r and thus, the number of solutions will also be dependent on r. We define the parameter r_c on which the number of solutions depends

$$r_C = \frac{N}{N+2}, \tag{1.1.24}$$

which has been shown in [16], but rederived independently in [20]. As shown in Fig. 1.4, for $r > r_c$, there are N solutions for k in the range $[-\frac{\pi}{2}, \frac{\pi}{2}]$ as expected, while for $r < r_c$ there are only $N - 2$ solutions.

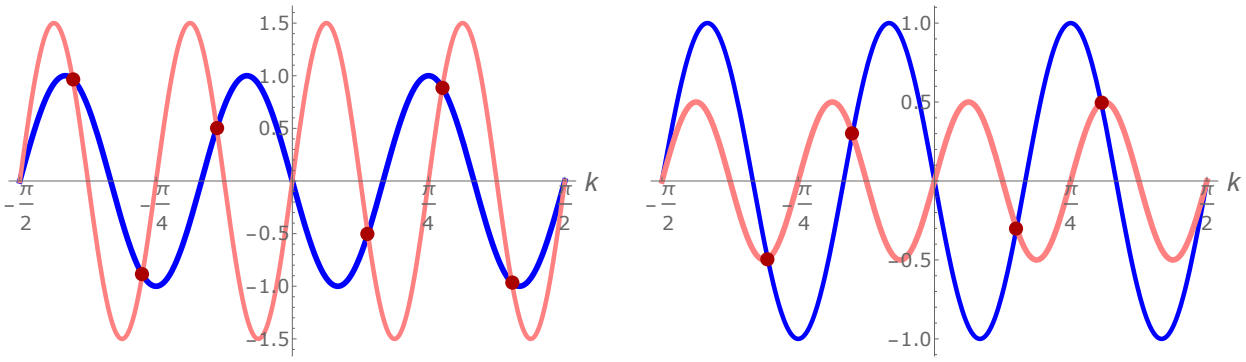

Fig. 1.4. Graphical solutions to the boundary condition (1.1.21) for N=6. The pink curve is $r \sin(N+2)k$ and the blue curve is $\sin(Nk)$. The case for $r > r_C$ is shown on the left; where there are $(N = 6)$ solutions and $r < r_C$ on the right where there are $(N - 2 = 4)$ solutions.

We must find these two missing solutions in order to complete the set. Letting k take complex values of the form $k \to \frac{\pi}{2} + i\kappa$, where κ is defined as positive, equation (1.1.21) becomes

$$r = \frac{\sinh(N\kappa)}{\sinh((N+2)\kappa)}. \tag{1.1.25}$$

In Fig. 1.5, we see that there are indeed no solutions for $r > r_c$ and two κ solutions for $r < r_c$.

We can now find the corresponding wave function for these complex-valued solutions by substituting $k \to \frac{\pi}{2} + i\kappa$ in the ansatz (1.1.3) and applying the same procedure as previously shown for the real-valued wavenumber. We find that the wave function takes the form

$$\left|\psi_{\pm}^{\text{edge}}\right\rangle = \sum_{m=0}^{M-1} (-1)^m \left\{ sh_{N-2m} |2m+1\rangle \pm sh_{2m+2} |2m+2\rangle \right\}, \tag{1.1.26}$$

where we have used the notation $\sinh(A\kappa) \to sh_A$. These solutions have near-zero-energy and are called edge states as they have an exponential form due to the hyperbolic sines. These will be discussed further in the next section.

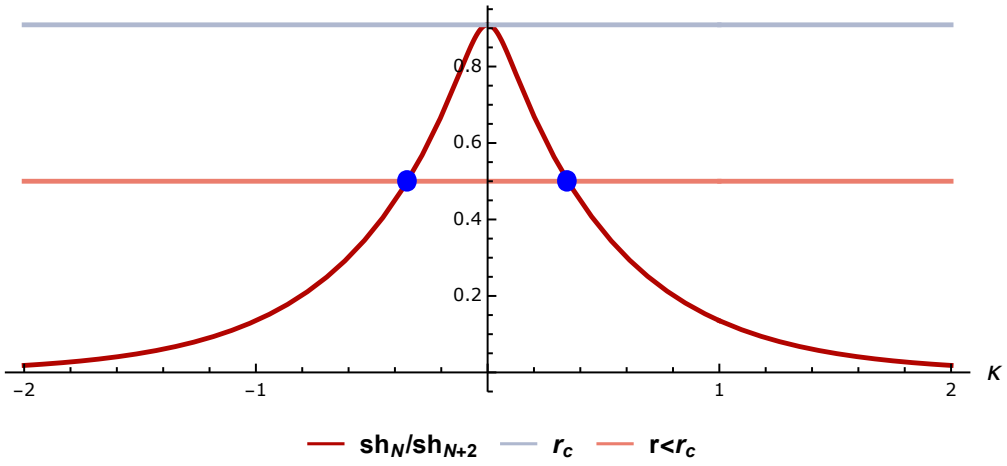

Fig. 1.5. Graphical solutions to the κ boundary condition (1.1.25) for $N = 20$. The pink curve shows $\sinh N\kappa / \sinh((N+2)\kappa)$, the grey curve corresponds to $r_c = 0.91$ and the pink curve is $r = 0.5$. we see that for $r < r_c$, there are two κ solutions while for $r > r_c$, there are no solutions.

1.1.3. Summary of Results

We have shown that for a chain with an even number of sites N, the topological phase of the system depends on r_c (1.1.24). For $r > r_c$, there are N solutions while for $r < r_c$, there are $N - 2$ bulk solutions. The two missing solutions are edge states and were found by letting k be complex-valued. For a chain with N odd, the critical parameter corresponds to $r = 1$ [20]. Since the dispersion relation (1.1.8) is symmetric, there must be an odd number of zero-energy states. In this case, we find $N - 1$ bulk states, hence there can only be one zero-energy state. For more details on this case, see [20]. We summarize both cases' results.

N **even**

with $r_C = \frac{N}{N+2}$

- $r > r_C$; N bulk solutions and no edge states
- $r < r_C$; N-2 bulk solutions and 2 edge states near $E = 0$

N odd

$\forall\ r$ there exist N-1 bulk solutions and 1 edge state with $E = 0$

- $r < 1$, left edge state
- $r > 1$, right edge state

Bulk solutions are delocalized oscillatory states which come in $\pm E$ pairs as a consequence of the chiral symmetry of the band structure [21]. Moreover, they can be antisymmetric or symmetric. There are N to $N-2$ bulk states depending on the parity of N and the value of r. An example of two bulk states is shown in Fig. 1.6.

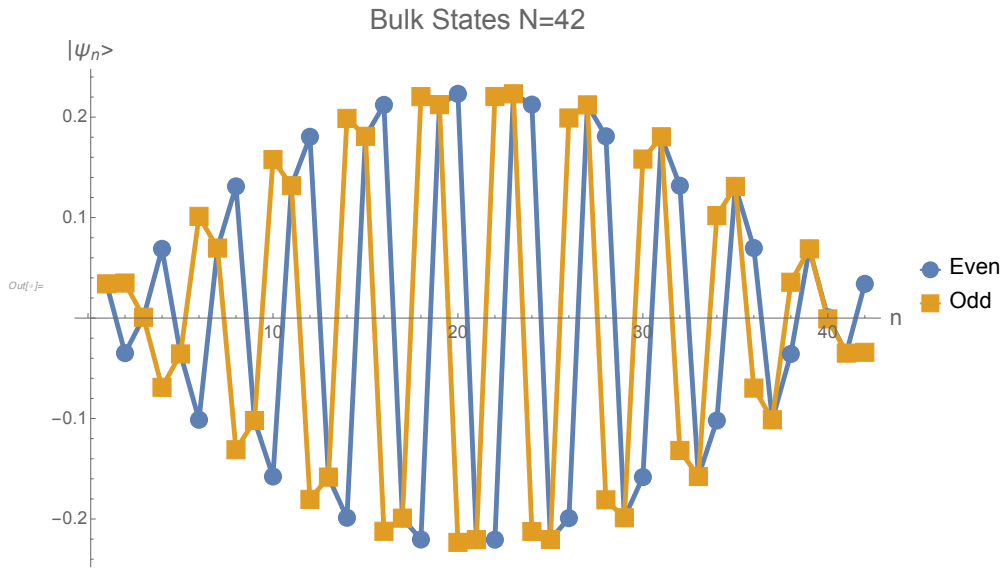

Fig. 1.6. A pair of SSH bulk states for $N = 42$. As expected, the electrons are delocalized throughout the bulk.

The more interesting solutions are the edge states, states that are exponentially localized at the boundaries of the chain. Fig. 1.7 shows the edge states for N even and N odd. For N even, the edge states exist simultaneously when $r < r_c$ and come in a symmetric-antisymmetric pair. These states have $E/t_2 = \pm 3.57628e^{-7}$ where the positive (negative) energy corresponds to the symmetric (antisymmetric) state.

For odd N, there is a single edge state for all values of r; the state is localized on the right (left) for $r < 1$ ($r > 1$).

For an even chain, the wavenumber solutions are given by (1.1.21) and if $r < r_c$, by (1.1.25). We then find the corresponding energy with (1.1.8). We show the energy spectrum of both

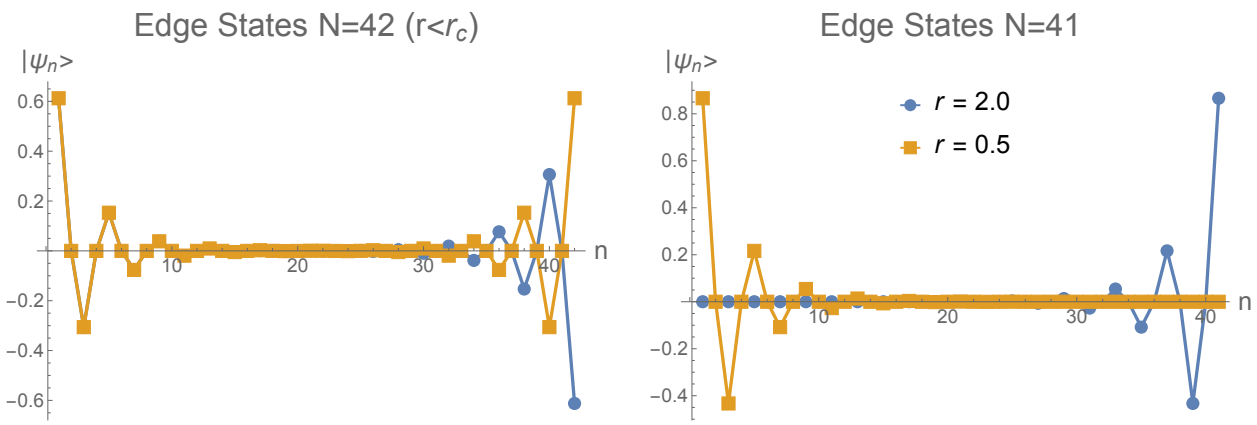

Fig. 1.7. Edge states for a finite SSH chain. On the left, edge modes for a N even chain; they exist simultaneously for $r < r_c$ with energies $E/t_2 = \pm 3.57628e^{-7}$. On the right, the two possible forms of the edge states for an N odd chain. The mode is localized on the left (right) when $r < 1$ ($r > 1$) and has $E = 0$.

even and odd SSH chains in Fig. 1.8 as a function of a new parameter, σ. We define $\sigma \equiv t_1$ and $1 - \sigma \equiv t_2$ such that $t_1 + t_2 = 1$. This parameter σ therefore takes values from zero to one. The topological parameter r can be expressed in terms of σ as $r = \sigma/(1-\sigma)$. The blue region in Fig. 1.8 shows the energy spectrum in the thermodynamic limit $N \to \infty$ given by the dispersion relation (1.1.8). Solid lines represent bulk states for all r. For an even chain, the dotted lines show edge states ($r < r_c$) transitioning to bulk states ($r > r_c$). The most striking feature certainly is that there are states in the band gap, which is defined in the thermodynamic limit, for $r < r_c$, which are the edge states (1.1.26). On the other hand, for the odd chain, the dotted line shows the edge state's presence for all values of r.

1.1.4. Building Intuition

We can understand the energy spectrum by taking a look at the limiting case ($t_1 = 0, t_2 = 1$) or $r = 0$ and ($t_1 = 1, t_2 = 0$) or $r \to \infty$. This analysis will be found useful throughout this work.

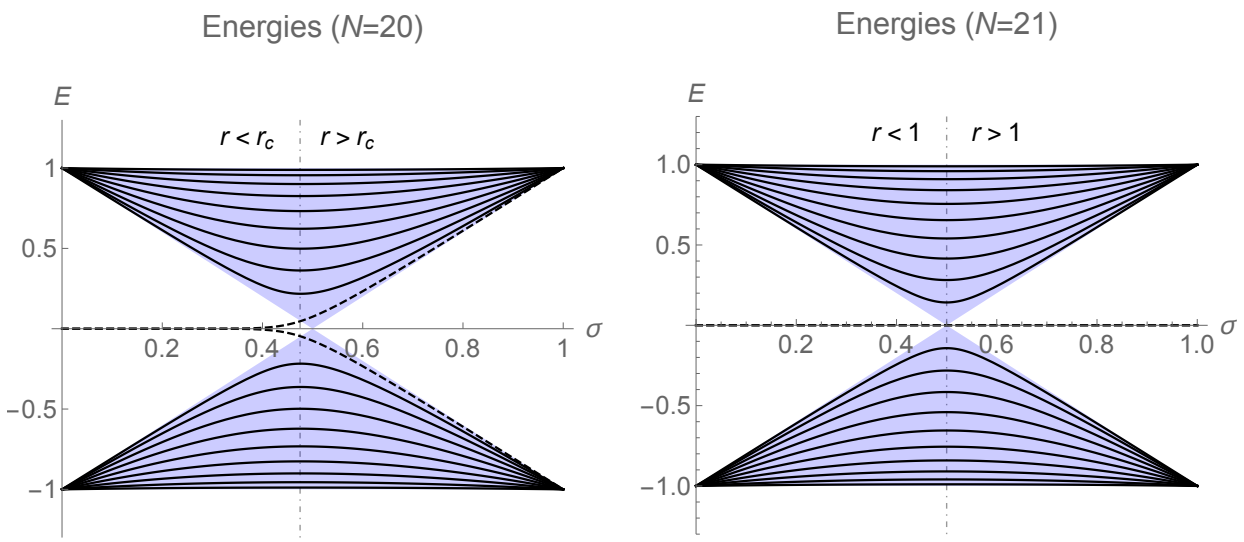

Fig. 1.8. Energy spectrum as a function of parameter σ for SSH chains of even ($N = 20$) on the left and odd ($N = 21$) parity on the right. We make the parametrization choice $t_1 = \sigma$ and $t_2 = 1 - \sigma$ such that $t_1 + t_2 = 1$ and σ takes values from zero to one. The dotted line shows the corresponding σ value for the transition point at $r = r_c$ ($r = 1$) for the even (odd) chain.

Even SSH Chain

We start with the even chain with $r = 0$ ($t_1 = 0, t_2 = 1$): the Hamiltonian (1.1.2) now describes a series of dimers in the bulk with a monomer at each end of the chain as shown in Fig. 1.9(a) and is given by

$$H_{SSH,Even} \to H_{monomer} \bigoplus_{i=1}^{M-1} H_{dimer,i} \bigoplus H_{monomer} \tag{1.1.27}$$

where M is the total number of unit cells of the chain and the monomer and dimer Hamiltonians are given by

$$H_{monomer} = \begin{bmatrix} 0 \end{bmatrix} \quad , \quad H_{dimer} = \begin{bmatrix} 0 & 1 \\ 1 & 0 \end{bmatrix} \quad . \tag{1.1.28}$$

Evidently, the monomers each only have energy solution $E = 0$ while the dimers each have eigenenergies ± 1. Since only the first and last sites support a zero-mode in that limit, the states will be localized at these sites while allowing for some tunneling throughout the bulk as we increase t_1 while still letting it be smaller than t_2. Moreover, in the $r = 0$ limit, the

chain's states for $E = 0$ will be superpositions of the monomers' eigenstates; there are two such combinations which are antisymmetric edge states. As we let t_1 increase but still be smaller than t_2, the two zero-modes gain small equal and opposite energies and the highly degenerate ± 1 eigenenergies broaden and join the bands as shown in Fig. 1.8.

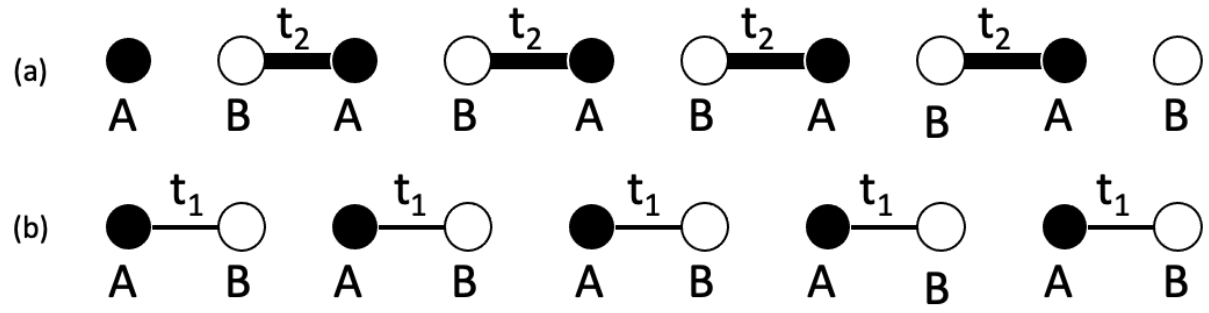

Fig. 1.9. SSH chain with $N = 10$ where we have imposed $\sigma = 0$ $(t_1 = 0, t_2 = 1)$ in (a): the system breaks up into a series of dimers with a monomer at each end. In (b),we have imposed $\sigma = 1$ $(t_1 = 1, t_2 = 0)$: the system breaks up into a series of dimers. Note that $\sigma = 0$ corresponds to $r = 0$ and $\sigma = 1$ corresponds to $r \to \infty$

Now we let $r \to \infty$, which corresponds to the limit $(t_1 = 1, t_2 = 0)$; the Hamiltonian (1.1.2) now describes an even chain broken up into a series of dimers as shown in Fig. 1.9(b) and given by

$$H_{SSH,Even} \to \bigoplus_{i=1}^{M} H_{dimer,i} \tag{1.1.29}$$

where M is the total number of unit cells. The only eigenergies are ± 1. Thus, we expect to have only bulk states with energies ± 1 when $r \to \infty$, which is indeed what we observe on the right end $(\sigma = 1)$ of the even chain's spectrum in Fig. 1.8. Moreover, we see that the near-zero-energy states transition to bulk states when $r \to \infty$ $(\sigma \to 1)$ as shown by the dotted lines in Fig. 1.8.

Odd SSH Chain

We do the same analysis for the odd SSH chain. Our convention consists of the first hopping parameter to be t_1 and the last, t_2, as shown in Fig. 1.10.

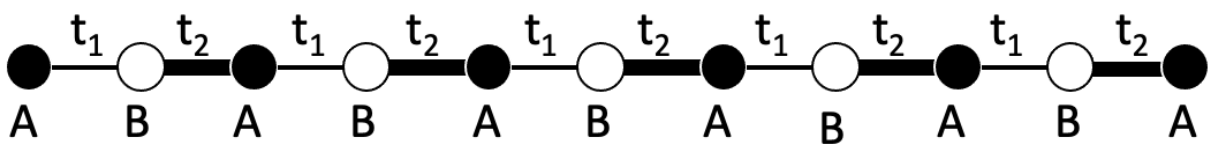

Fig. 1.10. Representation of an SSH Chain with $N = 11$ and alternating hopping parameters t_1 and t_2.

In the limiting case $r = 0$ $(t_1 = 0, t_2 = 1)$, the Hamiltonian now describes a chain of dimers except for the first site, which becomes a monomer as shown in Fig. 1.11(a). The Hamiltonian of this system is given by

$$H_{SSH,Odd} \rightarrow H_{monomer} \bigoplus_{i=1}^{M-1} H_{dimer,i} \tag{1.1.30}$$

The first site being a monomer, it is the only one to support a zero-energy state; we must have one left edge state for $r = 0$. The rest of the states have energies ± 1 as shown on the left of the odd chain's spectrum in Fig. 1.8. When we let t_1 take values larger but still smaller than t_2, the two highly degenerate ± 1 eigenenergies broaden and join the bands. The zero-energy mode remains as is required by the symmetry of the energy spectrum: this is indeed what we observe in Fig. 1.8. For the limiting case, $r \rightarrow \infty$ $(t_1 = 1, t_2 = 0)$, the

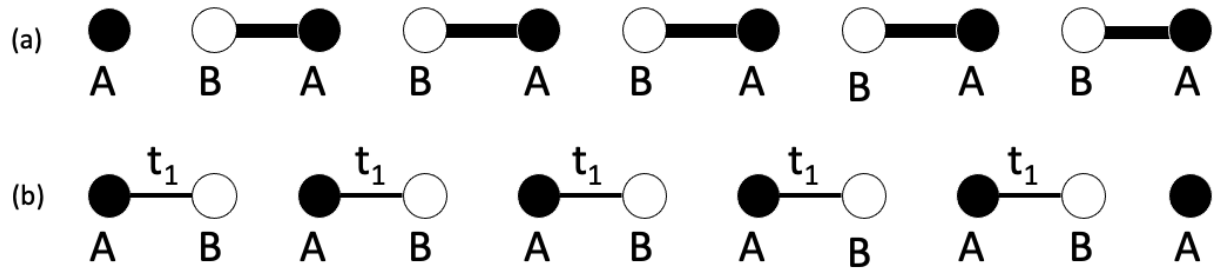

Fig. 1.11. SSH chain with $N = 11$ where we have imposed $(t_1 = 0, t_2 = 1)$ or $r = 0$ in (a): the system breaks up into a series of dimers and a single monomer at the left edge of the chain. In (b), we have imposed $(t_1 = 1, t_2 = 0)$ or $r \rightarrow \infty$: the system breaks up into a series of dimers and a single monomer at the right edge of the chain.

chain is once again a series of dimers and a single monomer, but this time it is the last site

that is a monomer as shown in Fig. 1.11(b). The Hamiltonian is now given by

$$H_{SSH,Odd} \rightarrow \bigoplus_{i=1}^{M-1} H_{dimer,i} \bigoplus H_{monomer} \tag{1.1.31}$$

The zero-energy state is only supported by the last site, and thus we have one right edge state for $r \rightarrow \infty$. The rest of the states are bulk states with energies ± 1 as we see on the right end of the odd chain's spectrum ($\sigma = 1$) in Fig. 1.8.

Chapter 2

Infinite SSH Chain with a Soliton

Before diving into the computational work of this chapter, we will discuss the SSH soliton. In the original papers [18, 19], it was found that the SSH model has solitonic modes, low-energy excitations confined to the soliton that travel along the chain with constant velocity and without dispersion. Most importantly, this provides a description of conducting polymers [7] as these modes allow for the transportation of charges along the chain. Without solitonic excitations, the model would describe an insulator. The soliton in question refers to a region that connects two different topological phases of the SSH chain and has been observed in many different engineered systems [23, 24, 25, 26, 27].

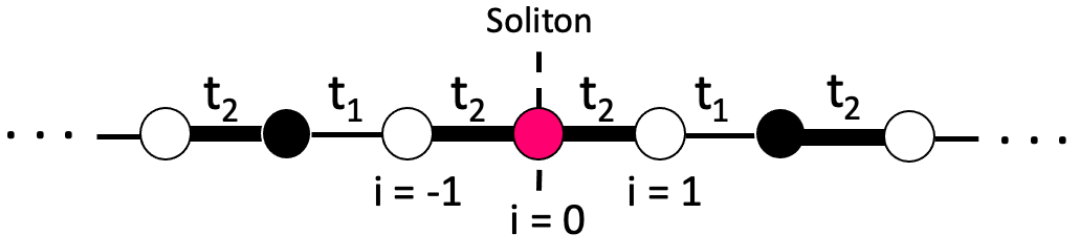

Fig. 2.1. Infinite SSH chain with repeated hopping parameter t_2 at the centre to make up the soliton. The central site is labeled by $i = 0$. The sites on the right chain segment are labeled by $i = (1, 2, 3, \dots)$ while the sites on the left are labeled by $i = (\text{-}1, \text{-}2, \text{-}3, \dots)$.

This chapter will provide derivations of electronic solutions for an infinite chain that has a domain wall as shown in Fig. 2.1 The original SSH papers gave the soliton a continous structure, while in this work we will consider a discrete domain wall which locally breaks the translational symmetry of the Hamiltonian. We introduce this domain wall by having two of

the same hopping parameters on each side of a single site. We will be using the terms soliton, interface, defect, and domain wall interchangeably. We choose hopping parameter t_2 to be repeated. There is no loss of generality in making this choice as we can always make the substitution $t_1 \leftrightarrow t_2$ in the final expressions to get the case where t_1 is repeated. Since the chain is infinite, the soliton is always central wherever it's located and we can view the chain as two semi-infinite SSH chains that are joined by a soliton site. We exploit the symmetry of the system by labeling the soliton site $i = 0$ and letting its wave function amplitude be a constant, B_0. Sites of the right chain segment are labeled by $i = (1, 2, 3, \dots)$ while sites on the left, by $i = (-1, -2, -3, \dots)$.

2.1. Real k Solutions

Firstly, we consider solutions that have a real wavenumber k that is in the range $[-\frac{\pi}{2}, \frac{\pi}{2}]$. Solutions with such a wavenumber will have energies withing the bands. As for the standard SSH chain, we start by writing the Schrödinger equation where we now denote the Hamiltonian by $H_{SSH,S}$ where the 's' stands for soliton

$$(H_{\mathrm{SSH,S}} - E)\,|\psi\rangle = 0. \tag{2.1.1}$$

In matrix form, with repeated hopping parameter t_2 in the middle, we have

$$\begin{pmatrix}
\ddots & \ddots & & & & & & & \\
\ddots & -E & t_2 & & & & & & \\
 & t_2 & -E & t_1 & & & & & \\
 & & t_1 & -E & t_2 & & & & \\
 & & & t_2 & -E & t_2 & & & \\
 & & & & t_2 & -E & t_1 & & \\
 & & & & & t_1 & -E & t_2 & \\
 & & & & & & t_2 & -E & \ddots \\
 & & & & & & & \ddots & \ddots
\end{pmatrix}
\begin{pmatrix}
\begin{pmatrix} B_L \\ A_L \end{pmatrix} e^{i2k} \\
\begin{pmatrix} B_L \\ A_L \end{pmatrix} \\
B_0 \\
\begin{pmatrix} A_R \\ B_R \end{pmatrix} \\
\begin{pmatrix} A_R \\ B_R \end{pmatrix} e^{i2k}
\end{pmatrix} = 0, \tag{2.1.2}$$

where we have defined the wave function as

$$|\psi\rangle = \begin{pmatrix} \vdots \\ \psi_{-3} = A_L e^{i2k} \\ \psi_{-2} = B_L \\ \psi_{-1} = A_L \\ \psi_0 = B_0 \\ \psi_1 = A_R \\ \psi_2 = B_R \\ \psi_3 = A_R e^{i2k} \\ \vdots \end{pmatrix}. \tag{2.1.3}$$

We can now solve for the wave functions by following the method used for the SSH chain, but we separate the chain into its right and left segments. The soliton site has index $i = 0$, the right (left) segment has positive (negative) site indices. We consider the right segment of the chain, which has two coupled bulk equations:

$$\begin{aligned} t_2 B_R - E A_R e^{i2k} + t_1 B_R e^{i2k} = 0, \\ t_1 A_R - E B_R + t_2 A_R e^{i2k} = 0. \end{aligned} \tag{2.1.4}$$

We notice that these equations are identical to the bulk equations of the standard SSH chain (1.1.6). We follow the same method as in Chapter 1 and obtain the same form for the wave function. This can be done for the left segment as well. We find both solutions and distinguish them by denoting the right bulk $|\psi_R\rangle$ and the left bulk $|\psi_L\rangle$

$$\begin{aligned} |\psi_{R\pm}\rangle = \sum_{m=0}^{\infty} \Big\{ \Big(C_+ e^{-i\varphi} e^{i2mk} + C_- e^{i\varphi} e^{-i2mk} \Big) |2m+1\rangle \\ \pm \Big(C_+ e^{i\varphi} e^{i2mk} + C_- e^{-i\varphi} e^{-i2mk} \Big) |2m+2\rangle \Big\}, \\ |\psi_{L\pm}\rangle = \sum_{m=0}^{\infty} \Big\{ \Big(D_+ e^{-i\varphi} e^{i2mk} + D_- e^{i\varphi} e^{-i2mk} \Big) |-(2m+1)\rangle \\ \pm \Big(D_+ e^{i\varphi} e^{i2mk} + D_- e^{-i\varphi} e^{-i2mk} \Big) |-(2m+2)\rangle \Big\}, \end{aligned} \tag{2.1.5}$$

where $C_\pm$ and $D_\pm$ are constants to be determined. We notice that attaching both of these wave functions will not describe the full chain as we are missing the soliton site $|0\rangle$. This site's amplitude will be included in the final form of the wave function.

We now consider the three central equations in (2.1.2) which result from joining the right

and left SSH chains to the soliton:

$$\begin{aligned} t_1\psi_{-2} - E\psi_{-1} + t_2\psi_0 &= 0, \\ t_2\psi_{-1} - E\psi_0 + t_2\psi_1 &= 0, \\ t_2\psi_0 - E\psi_1 + t_1\psi_2 &= 0. \end{aligned} \tag{2.1.6}$$

We use the bulk solutions (2.1.5) to rewrite these equations in terms of $C_\pm$ and $D_\pm$

$$\begin{aligned} \pm t_1(D_+e^{i\varphi} + D_-e^{-i\varphi}) - E(D_+e^{-i\varphi} + D_-e^{i\varphi}) + t_2B_0 &= 0, \\ t_2(D_+e^{-i\varphi} + D_-e^{i\varphi}) - EB_0 + t_2(C_+e^{-i\varphi} + C_-e^{i\varphi}) &= 0, \\ t_2B_0 - E(C_+e^{-i\varphi} + C_-e^{i\varphi}) \pm t_1(C_+e^{i\varphi} + C_-e^{-i\varphi}) &= 0. \end{aligned} \tag{2.1.7}$$

where we notice that we have three equations and five unknowns $C_\pm$, $D_\pm$ and B_0. We therefore have a family of solutions with two parameters. We can make a normalization choice to eliminate one parameter and are left with one unknown. Hence, there are two solutions per energy, which we will separate into symmetric and antisymmetric states as discussed in the section below.

On the Parity of Site Indices and Solutions

We can represent the site index parity $i \to -i$ in matrix form by an antidiagonal unit matrix. We call this transformation X with properties

$$X = \begin{bmatrix} 0 & 0 & 0 & 0 & 1 \\ 0 & 0 & 0 & 1 & 0 \\ 0 & 0 & 1 & 0 & 0 \\ 0 & 1 & 0 & 0 & 0 \\ 1 & 0 & 0 & 0 & 0 \end{bmatrix} \quad , \quad (X\psi)_i = \psi_{-i} \quad , \quad XHX = H, \tag{2.1.8}$$

where we consider $N = 5$, but the generalization to an infinite chain is straightforward. From this, we can easily see that if $|\psi\rangle$ is a solution to the Schrödinger equation (2.1.1), then $X|\psi\rangle$ is also a solution. Additionally, there are two possible classes of solutions; even solutions with $X|\psi\rangle = |\psi\rangle$ and odd solutions with $X|\psi\rangle = -|\psi\rangle$. We consider both in what follows.

Even Solutions

For even solutions, we have $\psi_i = \psi_{-i}$, which we can see from (2.1.7) corresponds to $C_\pm = D_\pm$. We also choose the normalization $B_0 = 1$. We make the substitution $D_\pm = C_\pm$ in all three equations (2.1.7). It is easy to see that the first equation ($i = -1$) is now equal to the third equation ($i = 1$), thus reducing the number of coupled equations to two

$$\begin{aligned} 2t_2(C_+e^{-i\varphi} + C_-e^{i\varphi}) &= E, \\ C_+(Ee^{-i\varphi} \mp t_1e^{i\varphi}) + C_-(Ee^{i\varphi} \mp t_1e^{-i\varphi}) &= t_2. \end{aligned} \tag{2.1.9}$$

where the first equation corresponds to $i = 0$ and the second, $i = 1$. We can simplify the latter by using the relation

$$Ee^{\pm i\varphi} \mp t_1e^{\mp i\varphi} = \pm t_2e^{\pm i2k}e^{\mp i\varphi}, \tag{2.1.10}$$

which can easily be derived from the φ definition (1.1.12). Using this relation, we rewrite (2.1.9)

$$\begin{aligned} 2t_2(C_+e^{-i\varphi} + C_-e^{i\varphi}) &= E, \\ C_+e^{-i2k}e^{i\varphi} + C_-e^{i2k}e^{-i\varphi} &= \pm 1. \end{aligned} \tag{2.1.11}$$

We write these in matrix form

$$\begin{pmatrix} e^{-i2k}e^{i\varphi} & e^{i2k}e^{-i\varphi} \\ 2t_2e^{-i\varphi} & 2t_2e^{i\varphi} \end{pmatrix} \begin{pmatrix} C_+ \\ C_- \end{pmatrix} = \begin{pmatrix} \pm 1 \\ E \end{pmatrix}, \tag{2.1.12}$$

for which we find the matrix'S determinant to be $\mp\frac{1}{E}4it_1t_2s_2$ where we have used the shorthand $s_A \equiv \sin Ak$. Since the determinant is non-vanishing, we can invert the matrix to solve for $C_\pm$, which yields

$$\begin{pmatrix} C_+ \\ C_- \end{pmatrix} = \frac{\mp E}{4it_1t_2s_2} \begin{pmatrix} 2t_2e^{i\varphi} & -e^{i2k}e^{-i\varphi} \\ -2t_2e^{-i\varphi} & e^{-i2k}e^{i\varphi} \end{pmatrix} \begin{pmatrix} \pm 1 \\ E \end{pmatrix}. \tag{2.1.13}$$

We multiply this out to get

$$\begin{pmatrix} C_+ \\ C_- \end{pmatrix} = \frac{\mp E}{4it_1t_2s_2} \begin{pmatrix} \pm 2t_2e^{i\varphi} - Ee^{i2k}e^{-i\varphi} \\ \mp 2t_2e^{-i\varphi} + Ee^{-i2k}e^{i\varphi} \end{pmatrix}, \tag{2.1.14}$$

or, using (2.1.10),

$$\begin{pmatrix} C_+ \\ C_- \end{pmatrix} = \frac{E}{4it_1t_2s_2} \begin{pmatrix} (t_1e^{i2k} - t_2)e^{i\varphi} \\ (t_2 - t_1e^{-i2k})e^{-i\varphi} \end{pmatrix}. \tag{2.1.15}$$

We combine the right and left segment solutions from (2.1.5); this gives the full solution

$$|\psi_{\text{even}}\rangle = |0\rangle + \sum_{m=0}^{\infty} \frac{E}{4it_1t_2s_2} \Big\{ \Big[(t_1e^{i2k} - t_2)e^{i2mk} + (t_2 - t_1e^{-i2k})e^{-i2mk}\Big] \Big[|2m+1\rangle \ +|-(2m+1)\rangle \ \Big] \\ \pm \Big[(t_1e^{i2k} - t_2)e^{i2\varphi}e^{i2mk} + (t_2 - t_1e^{-i2k})e^{-i2\varphi}e^{-i2mk}\Big] \Big[|2m+2\rangle \ +|-(2m+2)\rangle \ \Big] \Big\}. \tag{2.1.16}$$

We use the definition (1.1.12) to eliminate the φ dependence and simplify to obtain the final form of the solution:

$$|\psi_{\text{even}}\rangle = |0\rangle + \sum_{m=0}^{\infty} \frac{1}{2t_1t_2s_2} \Big\{ E(t_1s_{2m+2} - t_2s_{2m}) \Big[|2m+1\rangle \ +|-(2m+1)\rangle \ \Big] \\ +(t_1^2 - t_2^2)s_{2m+2} + t_1t_2(s_{2m+4} - s_{2m}) \Big[|2m+2\rangle \ +|-(2m+2)\rangle \ \Big] \Big\}. \tag{2.1.17}$$

Odd Solutions

For odd solutions, we have $\psi_i = -\psi_{-i}$, which we can see from the $i = 0$ equation in (2.1.7) corresponds to $B_0 = 0$ and therefore $C_\pm = -D_\pm$. Again, by making these substitutions in (2.1.7), we see that the $i = -1$ and $i = 1$ equations are equivalent. We use the latter

$$C_+(\pm t_1e^{i\varphi} - Ee^{-i\varphi}) + C_-(\pm t_1e^{-i\varphi} - Ee^{i\varphi}) = 0, \tag{2.1.18}$$

which we can further simplify by using relation (2.1.10) to obtain

$$C_+e^{-i2k}e^{i\varphi} + C_-e^{i2k}e^{-i\varphi} = 0, \\ \frac{C_+}{C_-} = \frac{-e^{i2k}e^{-i\varphi}}{e^{-i2k}e^{i\varphi}}, \tag{2.1.19}$$

so we can reexpress as

$$C_+ = -e^{i2k}e^{-i\varphi}, \\ C_- = e^{-i2k}e^{i\varphi}, \tag{2.1.20}$$

up to a normalization constant. From (2.1.5), this gives the solution

$$|\psi_{\text{odd}}\rangle = \sum_{m=0}^{\infty} \Big\{ (e^{-i2k}e^{i2\varphi}e^{-i2mk} - e^{i2k}e^{-i2\varphi}e^{i2mk}) \Big[|2m+1\rangle \ -|-(2m+1)\rangle \ \Big] \\ \pm (e^{-i2k}e^{-i2mk} - e^{i2k}e^{i2mk}) \Big[|2m+2\rangle \ -|-(2m+2)\rangle \ \Big] \Big\}. \tag{2.1.21}$$

We use the definition (1.1.12) to eliminate the φ dependence and simplify to obtain the final form of the solution:

$$|\psi_{\text{odd}}\rangle = \sum_{m=0}^{\infty} \Big\{ (t_1 s_{2m+2} + t_2 s_{2m}) \left[|2m+1\rangle \; -|-(2m+1)\rangle \; \right] + (E s_{2m+2}) \left[|2m+2\rangle \; -|-(2m+2)\rangle \; \right] \Big\}. \tag{2.1.22}$$

2.2. Complex k Solutions

We now perform a similar derivation as in the previous section, but this time considering a complex wavenumber $k \to \frac{\pi}{2} + i\kappa$. This leads to $e^{i2mk} \to (-1)^m e^{-2m\kappa}$. The wave functions now having an exponential behaviour, we can imagine a set of solutions decaying away from the central site. The energy of these solutions will be in the band gap. The Schrödinger equation in matrix form is now given by

$$\begin{pmatrix} \ddots & \ddots & & & & & & & \\ \ddots & -E & t_2 & & & & & & \\ & t_2 & -E & t_1 & & & & & \\ & & t_1 & -E & t_2 & & & & \\ & & & t_2 & -E & t_2 & & & \\ & & & & t_2 & -E & t_1 & & \\ & & & & & t_1 & -E & t_2 & \\ & & & & & & t_2 & -E & \ddots \\ & & & & & & & \ddots & \ddots \end{pmatrix} \begin{pmatrix} \vdots \\ \begin{pmatrix} B_L \\ A_L \end{pmatrix} e^{-4\kappa} \\ -\begin{pmatrix} B_L \\ A_L \end{pmatrix} e^{-2\kappa} \\ \begin{pmatrix} B_L \\ A_L \end{pmatrix} \\ B_0 \\ \begin{pmatrix} A_R \\ B_R \end{pmatrix} \\ -\begin{pmatrix} A_R \\ B_R \end{pmatrix} e^{-2\kappa} \\ \begin{pmatrix} A_R \\ B_R \end{pmatrix} e^{-4\kappa} \\ \vdots \end{pmatrix} = 0. \tag{2.2.1}$$

We have the following bulk equations for the right segment of the chain

$$\begin{aligned} t_2 B_R e^{2\kappa} + E A_R - t_1 B_R = 0, \\ t_1 A_R - E B_R - t_2 A_R e^{-2\kappa} = 0. \end{aligned} \tag{2.2.2}$$

Putting these into matrix form and requiring the determinant be equal to zero for a nontrivial solution leads to the dispersion relation

$$E^2 = t_1^2 + t_2^2 - 2t_1 t_2 \cosh(2\kappa). \tag{2.2.3}$$

We define φ, similarly to the real wavenumber case, as

$$|E|e^{\pm 2\varphi} \equiv (t_1 - t_2 e^{\mp 2\kappa}). \tag{2.2.4}$$

It is interesting to notice that this definition depends on the chosen relative size of the hopping parameters. This definition is valid for $t_1 > t_2$. However, we can do (and we have done) the following calculation with the definition valid for $t_1 < t_2$ and it leads to the same wave function. Using (2.2.4), we find that the following A_R and B_R satisfy (2.2.2)

$$\begin{pmatrix} A_R \\ B_R \end{pmatrix} = \begin{pmatrix} e^{-\varphi} \\ \pm e^{\varphi} \end{pmatrix}, \tag{2.2.5}$$

where the upper (lower) sign corresponds to the positive (negative) energy solutions. The ansatz is the same as the real-valued wavenumber case, but with $e^{i2mk} \to (-1)^m e^{-2m\kappa}$, such that

$$|\psi\rangle = \sum_{m=0}^{\infty} (-1)^m \Big(A|2m+1\rangle + B|2m+2\rangle \Big) e^{-2m\kappa}. \tag{2.2.6}$$

Using (2.2.5), we take a linear combination of positive and negative solutions for κ and φ to get

$$\begin{aligned} |\psi_{R\pm}\rangle = \sum_{m=0}^{\infty} (-1)^m \Big\{ &\Big(C_+ e^{-\varphi} e^{-2m\kappa} + C_- e^{\varphi} e^{2m\kappa} \Big) |2m+1\rangle \\ &\pm \Big(C_+ e^{\varphi} e^{-2m\kappa} + C_- e^{-\varphi} e^{2m\kappa} \Big) |2m+2\rangle \Big\}, \\ |\psi_{L\pm}\rangle = \sum_{m=0}^{\infty} (-1)^m \Big\{ &\Big(D_+ e^{-\varphi} e^{-2m\kappa} + D_- e^{\varphi} e^{2m\kappa} \Big) |-(2m+1)\rangle \\ &\pm \Big(D_+ e^{\varphi} e^{-2m\kappa} + D_- e^{-\varphi} e^{2m\kappa} \Big) |-(2m+2)\rangle \Big\}, \end{aligned} \tag{2.2.7}$$

where $C_\pm$ and $D_\pm$ are constants to be determined. As $m \to \infty$, the terms multiplied by C_- and D_- will also go to infinity. These solutions are not normalizable, hence we set C_- and D_- equal to zero to avoid this problem. The general form of the wave function becomes

$$\begin{aligned} |\psi_{R\pm}\rangle &= \sum_{m=0}^{\infty} C_+ e^{\varphi} e^{-2m\kappa} |2m+1\rangle \pm C_+ e^{-\varphi} e^{-2m\kappa} |2m+2\rangle, \\ |\psi_{L\pm}\rangle &= \sum_{m=0}^{\infty} D_+ e^{\varphi} e^{-2m\kappa} |-(2m+1)\rangle. \pm D_+ e^{-\varphi} e^{-2m\kappa} |-(2m+2)\rangle, \end{aligned} \tag{2.2.8}$$

where C_+ and D_+ are to be determined. We now write down the three coupled central equations

$$\begin{aligned} t_1\psi_{-2} - E\psi_{-1} + t_2\psi_0 &= 0, \\ t_2\psi_{-1} - E\psi_0 + t_2\psi_1 &= 0, \\ t_2\psi_0 - E\psi_1 + t_1\psi_2 &= 0, \end{aligned} \tag{2.2.9}$$

which we express in terms of C_+ and D_+ by using (2.2.8)

$$\begin{aligned} \pm t_1 D_+ e^{\varphi} - E D_+ e^{-\varphi} + t_2 B_0 &= 0, \\ t_2 D_+ e^{-\varphi} - E B_0 + t_2 C_+ e^{-\varphi} &= 0, \\ t_2 B_0 - E C_+ e^{-\varphi} \pm t_1 C_+ e^{\varphi} &= 0. \end{aligned} \tag{2.2.10}$$

Even Solutions

For the even solutions, we have $C_+ = D_+$ and make the normalization choice $B_0 = 1$ which yields the boundary equations

$$\begin{aligned} 2t_2 C_+ e^{-\varphi} &= E, \\ C_+ e^{2\kappa} e^{\varphi} &= \mp 1. \end{aligned} \tag{2.2.11}$$

Solving for C_+ we get two expressions

$$\begin{aligned} C_+ &= \frac{E e^{\varphi}}{2t_2}, \\ C_+ &= \mp e^{-\varphi} e^{-2\kappa}. \end{aligned} \tag{2.2.12}$$

Putting these two equations equal to one another, we obtain an expression for φ

$$|E| e^{2\varphi} = -2t_2 e^{-2\kappa}. \tag{2.2.13}$$

Using the φ definition (2.2.4), we get the following condition on κ

$$e^{-2\kappa} = -\frac{t_1}{t_2}, \tag{2.2.14}$$

which has no solutions for all values of t_1 and t_2 since κ is always positive. Therefore, it is tempting to conclude that there are no even solutions with an energy in the band gap. As will be discussed in section 2.2, this is not the case as the method we have been using until now to find all solutions to the Schrödinger equation (2.3.1) doesn't take into account solutions with zero-energy.

Odd Solutions

For the odd solutions, $B_0 = 0$ and $C_+ = -D_+$, thus producing the boundary condition

$$C_+(\pm t_1 e^{\varphi} - E e^{-\varphi}) = 0, \tag{2.2.15}$$

which leads to the expression

$$\pm t_1 e^{\varphi} - E e^{-\varphi} = 0. \tag{2.2.16}$$

Using this equation, we find the following expression for φ

$$|E| e^{-2\varphi} = t_1. \tag{2.2.17}$$

Using the φ definition (2.2.4), we get a condition on κ, given by

$$t_2 e^{2\kappa} = 0, \tag{2.2.18}$$

which has no physical solutions. Once again, we could conclude that there are no κ solutions for an energy in the band gap, but the method we have just used does not take into account solutions with $E = 0$. This will be discussed in the next section.

On the Zero-Mode

We take a look at the definition for φ when the wavenumber is complex

$$e^{\pm 2\varphi} \equiv \frac{1}{|E|}(t_1 - t_2 e^{\mp 2\kappa}). \tag{2.2.19}$$

If $E = 0$, it is clear that φ is undefined as the exponential tends to ∞. Our method of calculation thus breaks down for this case. Fortunately, we can find the solution nonetheless. Since $E = 0$ is located in the band gap, we know that the corresponding solution must have a complex wavenumber. We set $E = 0$ in the dispersion relation (2.2.3)

$$0 = t_1^2 + t_2^2 - 2t_1 t_2 \cosh 2k, \tag{2.2.20}$$

which can then be solved for κ such that

$$\kappa = \frac{1}{2} \operatorname{arcosh} [\frac{1}{2}(r + \frac{1}{r})], \tag{2.2.21}$$

which has one real and positive κ solution.

Odd Zero-Mode

To find the form of the zero-mode's wave function, we set $E = 0$ in the Schrödinger equation (2.3.1) to get

$$\begin{pmatrix} \ddots & \ddots & & & & & & & \\ \ddots & 0 & t_2 & & & & & & \\ & t_2 & 0 & t_1 & & & & & \\ & & t_1 & 0 & t_2 & & & & \\ & & & t_2 & 0 & t_2 & & & \\ & & & & t_2 & 0 & t_1 & & \\ & & & & & t_1 & 0 & t_2 & \\ & & & & & & t_2 & 0 & \ddots \\ & & & & & & & \ddots & \ddots \end{pmatrix} \begin{pmatrix} \vdots \\ \psi_{-4} \\ \psi_{-3} \\ \psi_{-2} \\ \psi_{-1} \\ \psi_0 \\ \psi_1 \\ \psi_2 \\ \psi_3 \\ \psi_4 \\ \vdots \end{pmatrix} = 0. \tag{2.2.22}$$

We look at the three central equations as well as three bulk equations to the right of the soliton

$$\begin{aligned} t_1\psi_{-2} + t_2\psi_0 &= 0, \\ t_2\psi_{-1} + t_2\psi_1 &= 0, \\ t_2\psi_0 + t_1\psi_2 &= 0, \\ t_1\psi_1 + t_2\psi_3 &= 0, \\ t_2\psi_2 + t_1\psi_4 &= 0, \\ t_1\psi_3 + t_2\psi_5 &= 0, \end{aligned} \tag{2.2.23}$$

where we note that each equation only has even or odd sites. We can rewrite equations (2.2.25) by considering the parity of the solution we are looking for. We start by considering an antisymmetric solution for which the amplitude of the soliton site is $\psi_0 = 0$ and $\psi_j = -\psi_{-j}$. The latter is confirmed for odd sites by the second equation in (2.2.25) where $\psi_1 = -\psi_{-1}$. Using our two constraints for antisymmetric solutions, we rewrite equations (2.2.25)

as

$$\begin{aligned} t_1\psi_{-2} = t_1\psi_2 = 0, \\ t_1\psi_1 + t_2\psi_3 = 0, \\ t_2\psi_2 + t_1\psi_4 = 0, \\ t_1\psi_3 + t_2\psi_5 = 0. \end{aligned} \tag{2.2.24}$$

Clearly, ψ_2 and ψ_{-2} must be equal to zero. Consequently, we see from the fifth equation that ψ_4 must also be equal to zero. This procedure can be applied to all the even site bulk equations and leads to the conclusion that $\psi_j = \psi_{-j} = 0$ for even j. We are left with two nontrivial equations

$$\begin{aligned} t_1\psi_1 + t_2\psi_3 = 0, \\ t_1\psi_3 + t_2\psi_5 = 0. \end{aligned} \tag{2.2.25}$$

From the first equation, we see that we can write ψ_3 in terms of ψ_1 and thus, with the second equation, we can also write ψ_5 in terms of ψ_1

$$\begin{aligned} \psi_3 = -\left(\frac{t_1}{t_2}\right)\psi_1, \\ \psi_5 = -\left(\frac{t_1}{t_2}\right)\psi_3 = \left(\frac{t_1}{t_2}\right)^2\psi_1. \end{aligned} \tag{2.2.26}$$

We can do this procedure for all odd site bulk equations and find that odd site amplitudes can all be expressed in terms of ψ_1. Doing so, we find the following form of the wave function for odd sites

$$\psi_{2m+1} = (-1)^m\left(\frac{t_1}{t_2}\right)^m\psi_1, \tag{2.2.27}$$

where m takes integer values from zero to infinity. We can now write the final form of the antisymmetric zero-mode solution, where we make the normalization choice $\psi_1 = 1$

$$|\psi_{\mathrm{E=0,odd}}\rangle = \sum_{m=0}^{\infty}(-1)^m\left(\frac{t_1}{t_2}\right)^m\Big[|2m+1\rangle - |-(2m+1)\rangle\Big], \tag{2.2.28}$$

which is only physical in the regime where $t_1 < t_2$ as this solution blows up as $m \to \infty$ for $t_1 > t_2$.

Even Zero-Mode

We now find the symmetric zero-mode wave function by imposing that $\psi_j = \psi_{-j}$ and making the normalization choice $\psi_0 = 1$ in equations (2.2.25), which reduce to five equations

$$\begin{aligned} t_2\psi_{-1} + t_2\psi_1 &= 0, \\ t_2 + t_1\psi_2 &= 0, \\ t_1\psi_1 + t_2\psi_3 &= 0, \\ t_2\psi_2 + t_1\psi_4 &= 0, \\ t_1\psi_3 + t_2\psi_5 &= 0. \end{aligned} \tag{2.2.29}$$

From the first equation, we see that ψ_1 can only be equal to ψ_{-1} if it is equal to zero. From the third equation, we see that ψ_3 must then also be equal to zero. As all odd site amplitudes can be expressed in terms of ψ_1, they must all vanish: $\psi_j = \psi_{-j} = 0$ for odd j. Now, we look at the even site equations: from the second equation, we can find ψ_2 in terms of t_1 and t_2, and thus, ψ_4

$$\begin{aligned} \psi_2 &= -\left(\frac{t_2}{t_1}\right), \\ \psi_4 &= -\left(\frac{t_2}{t_1}\right)\psi_2 = \left(\frac{t_2}{t_1}\right)^2. \end{aligned} \tag{2.2.30}$$

We can express all even site amplitudes in terms of ψ_2. Doing so, we find the following form of the wave function for even sites

$$\psi_{2m+2} = (-1)^{m+1}\left(\frac{t_2}{t_1}\right)^{m+1}, \tag{2.2.31}$$

where m takes integer values from zero to infinity. We can now write the final form of the symmetric zero-mode solution as

$$|\psi_{\mathrm{E=0,even}}\rangle = |0\rangle + \sum_{m=0}^{\infty}(-1)^m + 1\left(\frac{t_2}{t_1}\right)^m + 1\Big[|2m+2\rangle + |-(2m+2)\rangle\Big], \tag{2.2.32}$$

which is only valid in the regime where $t_1 > t_2$ as this solution will blow up as $m \to \infty$ if $t_1 < t_2$.

2.3. Imaginary k Solutions

We now consider an imaginary wavenumber $k \to i\kappa$, which leads to $e^{i2mk} \to e^{-2m\kappa}$. As for the solutions with a complex wavenumber, the exponential behaviour of the wave functions allows us to consider solutions that decay away from the soliton. The energy of these solutions will be outside the bands.

The Schrödinger equation in matrix form becomes

$$\begin{pmatrix}
\ddots & \ddots & & & & & & & \\
\ddots & -E & t_2 & & & & & & \\
 & t_2 & -E & t_1 & & & & & \\
 & & t_1 & -E & t_2 & & & & \\
 & & & t_2 & -E & t_2 & & & \\
 & & & & t_2 & -E & t_1 & & \\
 & & & & & t_1 & -E & t_2 & \\
 & & & & & & t_2 & -E & \ddots \\
 & & & & & & & \ddots & \ddots
\end{pmatrix}
\begin{pmatrix}
\vdots \\
\begin{pmatrix} B_L \\ A_L \end{pmatrix} e^{-4\kappa} \\
\begin{pmatrix} B_L \\ A_L \end{pmatrix} e^{-2\kappa} \\
\begin{pmatrix} B_L \\ A_L \end{pmatrix} \\
B_0 \\
\begin{pmatrix} A_R \\ B_R \end{pmatrix} \\
\begin{pmatrix} A_R \\ B_R \end{pmatrix} e^{-2\kappa} \\
\begin{pmatrix} A_R \\ B_R \end{pmatrix} e^{-4\kappa} \\
\vdots
\end{pmatrix} = 0. \tag{2.3.1}$$

The two coupled bulk equations are given by

$$\begin{aligned}
t_2 B_R e^{2\kappa} - E A_R + t_1 B_R = 0, \\
t_1 A_R - E B_R + t_2 A_R e^{-2\kappa} = 0,
\end{aligned} \tag{2.3.2}$$

which we put in matrix form and require the determinant to be equal to 0 to find the dispersion relation

$$E^2 = t_1^2 + t_2^2 + 2t_1 t_2 \cosh 2\kappa, \tag{2.3.3}$$

from which we define φ as

$$|E| e^{\pm 2\varphi} = (t_1 + t_2 e^{\pm 2\kappa}), \tag{2.3.4}$$

which is independent of whether $t_1 > t_2$ or $t_1 < t_2$. Using this definition, we find that the following expressions for A_R and B_R satisfy (2.3.2)

$$\begin{pmatrix} A_R \\ B_R \end{pmatrix} = \begin{pmatrix} e^{\varphi} \\ \pm e^{-\varphi} \end{pmatrix}. \tag{2.3.5}$$

We obtain the ansatz from taking its real-valued k counterpart and making the substitution $e^{i2mk} \to e^{-2m\kappa}$, which yields

$$|\psi\rangle = \sum_{m=0}^{\infty} \Big(A|2m+1\rangle + B|2m+2\rangle \Big) e^{-2m\kappa}. \tag{2.3.6}$$

By using A_R and B_R from (2.3.5) and by taking a linear combination of the positive and negative solutions for κ and φ, we get the solution

$$\begin{aligned} |\psi_{R\pm}\rangle = \sum_{m=0}^{\infty} \Big\{ & \Big(C_+ e^{\varphi} e^{-2m\kappa} + C_- e^{-\varphi} e^{2m\kappa} \Big) |2m+1\rangle \\ & \pm \Big(C_+ e^{-\varphi} e^{-2m\kappa} + C_- e^{\varphi} e^{2m\kappa} \Big) |2m+2\rangle \Big\}, \\ |\psi_{L\pm}\rangle = \sum_{m=0}^{\infty} \Big\{ & \Big(D_+ e^{\varphi} e^{-2m\kappa} + D_- e^{-\varphi} e^{2m\kappa} \Big) |-(2m+1)\rangle \\ & \pm \Big(D_+ e^{-\varphi} e^{-2m\kappa} + D_- e^{\varphi} e^{2m\kappa} \Big) |-(2m+2)\rangle \Big\}, \end{aligned} \tag{2.3.7}$$

where $C_\pm$ and $D_\pm$ are constants to be determined. As $m \to \infty$, the terms multiplied by C_- and D_- will also go to infinity. These solutions are not normalizable, hence we set C_- and D_- equal to zero to avoid this problem. The general form of the wave function becomes

$$\begin{aligned} |\psi_{R\pm}\rangle &= \sum_{m=0}^{\infty} \Big\{ C_+ e^{\varphi} e^{-2m\kappa} |2m+1\rangle \ \pm C_+ e^{-\varphi} e^{-2m\kappa} |2m+2\rangle \Big\}, \\ |\psi_{L\pm}\rangle &= \sum_{m=0}^{\infty} \Big\{ D_+ e^{\varphi} e^{-2m\kappa} |-(2m+1)\rangle \ \pm D_+ e^{-\varphi} e^{-2m\kappa} |-(2m+2)\rangle \Big\}, \end{aligned} \tag{2.3.8}$$

where the constants to be determined are now C_+ and D_+. We take a look at the three central equations (2.2.9), which we express in terms of C_+ and D_+

$$\begin{aligned} \pm t_1 D_+ e^{-\varphi} - E D_+ e^{\varphi} + t_2 B_0 &= 0, \\ t_2 D_+ e^{\varphi} - E B_0 + t_2 C_+ e^{\varphi} &= 0, \\ t_2 B_0 - E C_+ e^{\varphi} \pm t_1 C_+ e^{-\varphi} &= 0. \end{aligned} \tag{2.3.9}$$

Even Solutions

For even solutions, we have $C_+ = D_+$ and choose the normalization such that $B_0 = 1$, which leads to the coupled central equations

$$\begin{aligned} 2t_2 C_+ e^{\varphi} &= E, \\ C_+ e^{2\kappa} e^{-\varphi} &= \pm 1. \end{aligned} \tag{2.3.10}$$

Solving for C_+, we get the following two expressions

$$\begin{aligned} C_+ &= \frac{E e^{-\varphi}}{2t_2}, \\ C_+ &= \pm e^{\varphi} e^{-2\kappa}. \end{aligned} \tag{2.3.11}$$

Setting these expressions equal to one another, we get the following expression for φ

$$|E| e^{-2\varphi} = 2t_2 e^{-2\kappa}. \tag{2.3.12}$$

Using the φ definition (2.3.4), we get an equation for κ

$$e^{2\kappa} = \frac{t_2}{t_1}, \tag{2.3.13}$$

or, equivalently,

$$e^{-2\kappa} = \frac{t_1}{t_2}. \tag{2.3.14}$$

Since κ is positive, we must have $e^{2\kappa} > e^{-2\kappa}$ and therefore, $t_2 > t_1$. We therefore conclude that we have even solutions with an energy outside the bands only in the case where $t_2 > t_1$. We use κ equations (2.3.12) and (2.3.13) in the dispersion relation (2.3.3) to find the energy of the modes outside the bands

$$E^2 = 2(t_1^2 + t_2^2), \tag{2.3.15}$$

which is valid in the regime where $t_2 > t_1$. We now use the second equation in (2.3.11) for C_+ and substitute it into the general form of the solution (2.3.8) to find the final form of the wave function

$$\begin{aligned} |\psi_{\text{even}}\rangle = |0\rangle + \sum_{m=0}^{\infty} \Big\{ \frac{1}{E}(t_1 e^{-2(m+1)\kappa} + t_2 e^{-2m\kappa}) \Big[|2m+1\rangle + |-(2m+1)\rangle \Big] \\ \pm e^{-2(m+1)\kappa} \Big[|2m+2\rangle + |-(2m+2)\rangle \Big] \Big\}. \end{aligned} \tag{2.3.16}$$

Odd Solutions

For odd solutions, $B_0 = 0$ and $C_+ = -D_+$, therefore yielding the central equation

$$C_+(\pm t_1 e^{-\varphi} - E e^{\varphi}) = 0, \tag{2.3.17}$$

which allows us to obtain an expression for φ

$$|E| e^{2\varphi} = t_1 + t_2 e^{2\kappa}. \tag{2.3.18}$$

Using the φ definition (2.3.4), we get an equation for κ

$$t_2 e^{2\kappa} = 0, \tag{2.3.19}$$

which has no nontrivial solutions. Therefore, we conclude that there are no odd solutions with an energy outside the bands.

2.4. Discussion of the Energy Spectrum

We show the energy spectrum as a function of parameter σ for the infinite SSH chain with a soliton in Fig. 2.2. As we did for the energy spectrum of the finite SSH chain, we make the parametrization choice $\sigma = t_1$ and $1 - \sigma = t_2$ such that $t_1 + t_2 = 1$ and σ ranges from zero to one. The orange region corresponds to the infinite number of bulk states with energies within the bands. The two states in red with an energy outside the bands correspond to the even solutions found for an imaginary wavenumber in section 3.1.3. This state joins the bands when $t_1 = t_2$, which corresponds to $r = 1$ ($\sigma = 0.5$). Finally, we show the zero-mode in blue, which is an odd solution for $t_1 < t_2$ ($r < 1$), and an even solution for $t_1 > t_2$ ($r > 1$). We can understand the parity of the zero-mode by considering limiting cases of the hopping parameters t_1 and t_2. In Fig. 2.3(a), we show the chain in the limiting case $r = 0$ ($t_1 = 0$,$t_2 = 1$); the soliton becomes a trimer while the rest of the sites become dimers. We consider $r \to \infty$ ($t_1 = 1$,$t_2 = 0$) in Fig. 2.3(b), in which the soliton becomes a monomer while the rest of the sites become dimers. Firstly, we discuss the limiting case $r = 0$ ($t_1 = 0$,$t_2 = 1$) illustrated in Fig. 2.3(a). The Hamiltonian (3.1.14) reduces to

$$H_{SSH,S} \to \bigoplus_{i=-\infty}^{-1} H_{dimer,i} \bigoplus H_{trimer} \bigoplus_{i=1}^{\infty} H_{dimer,i} \tag{2.4.1}$$

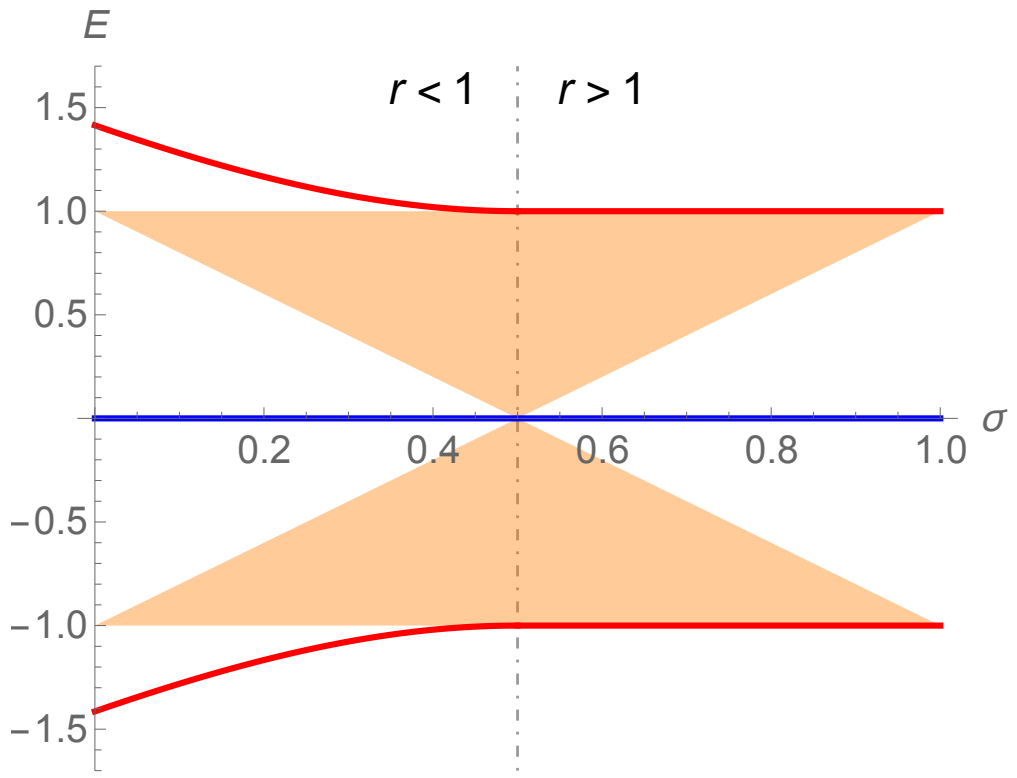

Fig. 2.2. Energy spectrum as a function of parameter σ for the infinite SSH chain with a soliton. We make the parametrization choice $t_1 = \sigma$ and $t_2 = 1 - \sigma$ such that $t_1 + t_2 = 1$ and σ takes values from zero to one. Highlighted in red are the high-energy states (imaginary k), highlighted in purple is the zero-mode (complex k) and in orange, the infinite bulk states.

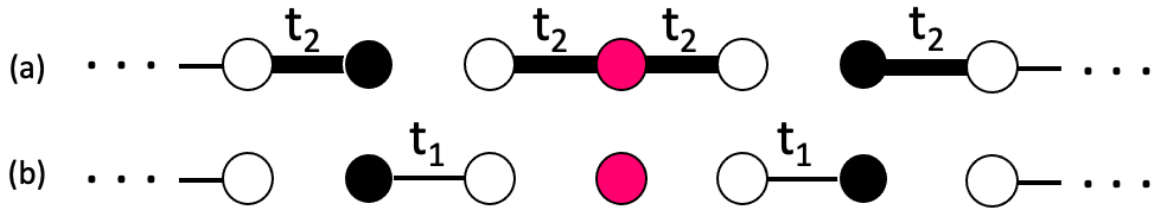

Fig. 2.3. Infinite SSH chain with a soliton where we have imposed $(t_1 = 0, t_2 = 1)$ in (a): the system breaks up into a trimer and an infinite series of dimers. In (b), we have imposed $(t_1 = 1, t_2 = 0)$: the system breaks up into a monomer and an infinite series of dimers.

where the dimer's Hamiltonian is given by (1.1.28). The trimer's Hamiltonian in matrix form is given by

$$H_{trimer} = \begin{bmatrix} 0 & 1 & 0 \\ 1 & 0 & 1 \\ 0 & 1 & 0 \end{bmatrix}, \tag{2.4.2}$$

which has eigenenergies 0 and $\pm\sqrt{2}$. The trimer's eigenstate corresponding to $E = 0$ is antisymmetric. The dimers each have eigenenergies ± 1. Therefore, only the trimer supports a zero-mode. As shown in Fig. 2.2, in the $r = 0$ ($\sigma = 0$) limit, we indeed only have states with energies zero, ± 1 and $\pm\sqrt{2}$. As we let $r \to 1$, the zero-energy state will no longer be purely localized at any site as this allows for tunneling along the chain. The zero-mode in the regime where $t_1 < t_2$ is therefore antisymmetric and is expected to decay away from the soliton, which is indeed what we have determined in section 2.2. Let's now discuss the trimer's other eigenenergies, $E = \pm\sqrt{2}$. Only the trimer supports these high energies and the corresponding eigenstates are symmetric. This allows us to conclude that we expect to have even solutions that have an energy outside the bands in the regime where $t_1 < t_2$. This is indeed what we found in section 2.3.

We now consider the limiting case $r \to \infty$ ($t_1 = 1$,$t_2 = 0$) for which the chain becomes an infinite series of dimers on each side of a monomer as shown in Fig. 2.3(b). The Hamiltonian (3.1.14) reduces to

$$H_{SSH,S} \to \bigoplus_{i=-\infty}^{-1} H_{dimer,i} \bigoplus H_{monomer} \bigoplus_{i=1}^{\infty} H_{dimer,i} \tag{2.4.3}$$

where the monomer's and dimer's Hamiltonians are given by (1.1.28). As was discussed in section 1.1.4, a monomer only has eigenenergy $E = 0$ and its corresponding eigenstate is symmetric. Moreover, dimers only have eigenenergies ± 1. Therefore, only the soliton site supports the zero-mode. As shown in Fig. 2.2, in the $r \to \infty$ ($\sigma = 1$) limit, we indeed only have states with energies zero and ± 1. As we let t_2 grow, but still be smaller than t_1 ($r > 1$), we expect the zero-energy state to no longer be completely localized at the soliton as we now allow for tunneling along the chain. The zero-mode in the regime where $t_1 > t_2$ is therefore symmetric and expected to decay away from the soliton, which is what we observed in section 2.2.

Chapter 3

Finite SSH Chain with a Central Soliton

In this chapter, we will find the solutions of a finite SSH chain with a central soliton. Once again, we impose that the repeated hopping parameter be t_2. Let the complete chain have a total number of sites N. We understand the system to be two finite SSH chains joined by the soliton site. There are two possible configurations: the two chain segments can have an even or odd number of sites α. Therefore, the total number of sites is $N = 2\alpha + 1$, which is an odd number regardless of the parity of α. If α is even (odd), the last hopping parameter of each chain segment is t_1 (t_2). We denote the former configuration as Φ_{12} as the edges' hopping parameter is t_1 and the domain wall's parameter is t_2. Similarly, we denote the configuration with t_2 at both the edges and the interface by Φ_{22}. The Φ_{12} configuration will be discussed in section 3.1 and the Φ_{22}, in section 3.2.

3.1. Φ_{12} Configuration

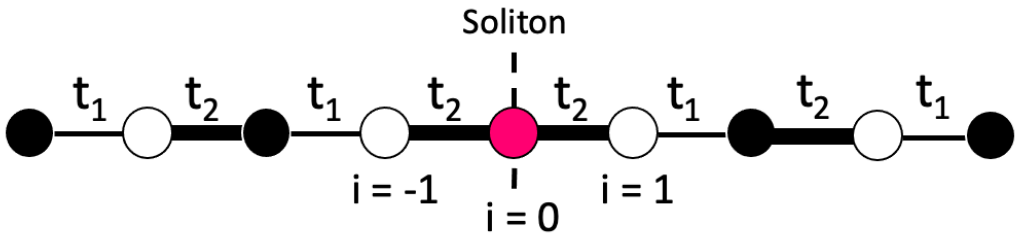

Fig. 3.1. Finite SSH chain with $N = 9$, repeated hopping parameters t_2 at the centre to make up the soliton and t_1 at its edges (Φ_{12} configuration) The central site is labeled by $i = 0$. The sites on the right chain segment are labeled by $i = (1, 2, 3, \ldots, \alpha)$ while the sites on the left are labeled by $i = (\text{-}1, \text{-}2, \text{-}3, \ldots, -\alpha)$). In this case, $\alpha = 4$ and the total number of unit cells on each chain segment is 2; in this case, the sum over m would run from 0 to $\beta = 1$.

As previously mentionned, this configuration of the chain has hopping parameters t_1 at its edges and t_2 as the repeated hopping parameter. We think of this system as two even-length SSH chains with α sites joined by a central site. The total length of the chain can take up values $N = 4n+1$ with $n = 1, 2, 3, \ldots$ A pair of sites (A,B) forms a unit cell, which is labeled by the index m. We run this index from 0 to $\frac{\alpha}{2} - 1 \equiv \beta$ to get the total number of unit cells.

3.1.1. Real k Solutions

We consider solutions with a real wavenumber k, which have energy within the bands. The Schrödinger equation in matrix form is given by

$$\begin{pmatrix}
-E & t_1 & & & & & & & & & & & \\
t_1 & -E & t_2 & & & & & & & & & & \\
 & \ddots & \ddots & \ddots & & & & & & & & & \\
 & & t_1 & -E & t_2 & & & & & & & & \\
 & & & t_2 & -E & t_1 & & & & & & & \\
 & & & & t_1 & -E & t_2 & & & & & & \\
 & & & & & t_2 & -E & t_2 & & & & & \\
 & & & & & & t_2 & -E & t_1 & & & & \\
 & & & & & & & t_1 & -E & t_2 & & & \\
 & & & & & & & & t_2 & -E & t_1 & & \\
 & & & & & & & & & \ddots & \ddots & \ddots & \\
 & & & & & & & & & & t_2 & -E & t_1 \\
 & & & & & & & & & & & t_1 & -E
\end{pmatrix}
\begin{pmatrix}
\begin{pmatrix} B_L \\ A_L \end{pmatrix} e^{i(\alpha-2)k} \\
\vdots \\
\begin{pmatrix} B_L \\ A_L \end{pmatrix} e^{i2k} \\
\begin{pmatrix} B_L \\ A_L \end{pmatrix} \\
B_0 \\
\begin{pmatrix} A_R \\ B_R \end{pmatrix} \\
\begin{pmatrix} A_R \\ B_R \end{pmatrix} e^{i2k} \\
\vdots \\
\begin{pmatrix} A_R \\ B_R \end{pmatrix} e^{i(\alpha-2)k}
\end{pmatrix} = 0, \tag{3.1.1}$$

where each side of the chain's last two sites' wave functions carry a factor $e^{i2mk} = e^{i(\alpha-2)k}$ as the last unit cell corresponds to index $m = \beta = \frac{\alpha}{2} - 1$. As the wave function only differs from (2.1.5) by the upper bound of the sum, we can directly write it in terms of $C_\pm$ and $D_\pm$

$$\begin{aligned}
|\psi_{R\pm}\rangle = \sum_{m=0}^{\beta} \Big\{ &\left(C_+ e^{-i\varphi} e^{i2mk} + C_- e^{i\varphi} e^{-i2mk}\right) |2m+1\rangle \\
&\pm \left(C_+ e^{i\varphi} e^{i2mk} + C_- e^{-i\varphi} e^{-i2mk}\right) |2m+2\rangle \Big\}, \\
|\psi_{L\pm}\rangle = \sum_{m=0}^{\beta} \Big\{ &\left(D_+ e^{-i\varphi} e^{i2mk} + D_- e^{i\varphi} e^{-i2mk}\right) |-(2m+1)\rangle \\
&\pm \left(D_+ e^{i\varphi} e^{i2mk} + D_- e^{-i\varphi} e^{-i2mk}\right) |-(2m+2)\rangle \Big\}.
\end{aligned} \tag{3.1.2}$$

We have five boundary conditions to consider: three which arise from the the juncture of the chains, which are given by (2.1.6), and two that come from the left and right edges of

the chain. We directly write the latter in terms of the constants $C_\pm$ and $D_\pm$ as

$$\begin{aligned} \mp E(D_+e^{i\varphi}e^{i(\alpha-2)k} + D_-e^{-i\varphi}e^{-i(\alpha-2)k}) + t_1(D_+e^{-i\varphi}e^{i(\alpha-2)k} + D_-e^{i\varphi}e^{-i(\alpha-2)k}) = 0, \\ t_1(C_+e^{-i\varphi}e^{i(\alpha-2)k} + C_-e^{i\varphi}e^{-i(\alpha-2)k}) \mp E(C_+e^{i\varphi}e^{i(\alpha-2)k} + C_-e^{-i\varphi}e^{-i(\alpha-2)k}) = 0. \end{aligned} \tag{3.1.3}$$

In the next sections, we will rewrite these equations according to the parity of the solutions.

Even Solutions

As per usual, when we consider even solutions to the Schrödinger equation, we have $C_\pm = D_\pm$ and we make the normalization choice $B_0 = 1$. This yields three nontrivial boundary equations since a pair of equations (2.1.6) reduce to the same equation, as do (3.1.3). These three equations are given by

$$\begin{aligned} 2t_2(C_+e^{-i\varphi} + C_-e^{i\varphi}) = E, \\ C_+(\pm t_1e^{i\varphi} - Ee^{-i\varphi}) + C_-(\pm t_1e^{-i\varphi} - Ee^{i\varphi}) = -t_2, \\ C_+(t_1e^{-i\varphi} \mp Ee^{i\varphi})e^{i(\alpha-2)k} + C_-(t_1e^{i\varphi} \mp Ee^{-i\varphi})e^{-i(\alpha-2)k} = 0. \end{aligned} \tag{3.1.4}$$

We can simplify the second and third equations using relation (2.1.10) to get the form

$$\begin{aligned} C_+e^{i\varphi}e^{-i2k} + C_-e^{-i\varphi}e^{i2k} = \pm 1, \\ C_+e^{-i\varphi}e^{i\alpha k} + C_-e^{i\varphi}e^{-i\alpha k} = 0. \end{aligned} \tag{3.1.5}$$

To solve for $C_\pm$, we rewrite these in matrix form as

$$\begin{pmatrix} e^{i\varphi}e^{-i2k} & e^{-i\varphi}e^{i2k} \\ e^{-i\varphi}e^{i\alpha k} & e^{i\varphi}e^{-i\alpha k} \end{pmatrix} \begin{pmatrix} C_+ \\ C_- \end{pmatrix} = \begin{pmatrix} \pm 1 \\ 0 \end{pmatrix}. \tag{3.1.6}$$

The matrix in this equation has determinant $\mp 2i/E(t_1s_{\alpha+2} + t_2s_\alpha)$. We invert this matrix and solve for the constants, yielding

$$\begin{pmatrix} C_+ \\ C_- \end{pmatrix} = \frac{E}{2i(t_1s_{\alpha+2} + t_2s_\alpha)} \begin{pmatrix} -e^{i\varphi}e^{-i\alpha k} \\ e^{-i\varphi}e^{i\alpha k} \end{pmatrix}. \tag{3.1.7}$$

These expressions for $C_\pm$ are substituted into (3.1.2) to find the final form of the wave function, which is given by

$$|\psi_{\text{even}}\rangle = |0\rangle + \sum_{m=0}^{\beta} \frac{1}{t_1 s_{\alpha+2} + t_2 s_\alpha} \Big\{ E s_{\alpha-2m} \Big[|2m+1\rangle + |-(2m+1)\rangle \Big] + (t_1 s_{\alpha-2m} + t_2 s_{\alpha-2m-2}) \Big[|2m+2\rangle + |-(2m+2)\rangle \Big] \Big\}. \tag{3.1.8}$$

As was done for a regular finite SSH chain (1.1.21), we are interested in finding a transcendental equation which can then be solved graphically to determine the number of solutions for real-valued wavenumber k. Here, we do so by using the expressions for $C_\pm$ (3.1.7) and substituting them in the first boundary equation in (3.1.4). After a few lines of algebra, we get the equation

$$r s_{\alpha+2} - s_\alpha = 0, \tag{3.1.9}$$

which has $\alpha - 2$ solutions for $r < r_c$ and α solutions for $r > r_c$, where $r_c = N/N+2$. We will discuss this further in Section (3.1.4.)

Odd Solutions

When considering odd solutions, we have $C_\pm = -D_\pm$, which gives $B_0 = 0$. Using these constraints to rewrite the boundary equations (2.1.6) and (3.1.3) yields the two following nontrivial conditions

$$\begin{aligned} C_+(\pm t_1 e^{i\varphi} - E e^{-i\varphi}) + C_-(\pm t_1 e^{-i\varphi} - E e^{i\varphi}) = 0, \\ C_+(t_1 e^{-i\varphi} \mp E e^{i\varphi}) e^{i(\alpha-2)k} + C_-(t_1 e^{i\varphi} \mp E e^{-i\varphi}) e^{-i(\alpha-2)k} = 0. \end{aligned} \tag{3.1.10}$$

We take the first equation, simplify using (2.1.10), and solve for the ratio of the constants to get

$$\begin{aligned} C_+ &= e^{-i\varphi} e^{i2k}, \\ C_- &= -e^{i\varphi} e^{-i2k}, \end{aligned} \tag{3.1.11}$$

up to normalization constant. From (3.1.2), we get the solution

$$|\psi_{\text{odd}}\rangle = \sum_{m=0}^{\beta} \Big\{ (t_1 s_{2m+2} + t_2 s_{2m}) \Big[|2m+1\rangle - |-(2m+1)\rangle \Big] + E s_{2m+2} \Big[|2m+2\rangle - |-(2m+2)\rangle \Big] \Big\}. \tag{3.1.12}$$

We substitute (3.1.11) in the second boundary equation in (3.1.10) and simplify to find the transcendental k equation

$$rs_{\alpha+2} + s_{\alpha} = 0, \tag{3.1.13}$$

which has $\alpha - 2$ solutions for $r < r_c$ and α solutions for $r > r_c$. This will be further discussed in section 3.2.4.

3.1.2. Complex k Solutions

A complex wavenumber $k \to \frac{\pi}{2} + i\kappa$ leads to the exponential $e^{i2mk} \to (-1)^m e^{-2m\kappa}$. The wave functions with a complex wavenumber will have energies in the band gap. The Schrödinger equation in matrix form (3.1.1) is now given by

$$\begin{pmatrix}
-E & t_1 & & & & & & & & & & \\
t_1 & -E & t_2 & & & & & & & & & \\
 & \ddots & \ddots & \ddots & & & & & & & & \\
 & & t_1 & -E & t_2 & & & & & & & \\
 & & & t_2 & -E & t_1 & & & & & & \\
 & & & & t_1 & -E & t_2 & & & & & \\
 & & & & & t_2 & -E & t_2 & & & & \\
 & & & & & & t_2 & -E & t_1 & & & \\
 & & & & & & & t_1 & -E & t_2 & & \\
 & & & & & & & & t_2 & -E & t_1 & \\
 & & & & & & & & & \ddots & \ddots & \ddots \\
 & & & & & & & & & & t_1 & -E
\end{pmatrix}
\begin{pmatrix}
\begin{pmatrix} B_L \\ A_L \end{pmatrix} e^{-(\alpha-2)\kappa} \\
\vdots \\
-\begin{pmatrix} B_L \\ A_L \end{pmatrix} e^{-2\kappa} \\
\begin{pmatrix} B_L \\ A_L \end{pmatrix} \\
B_0 \\
\begin{pmatrix} A_R \\ B_R \end{pmatrix} \\
-\begin{pmatrix} A_R \\ B_R \end{pmatrix} e^{-2\kappa} \\
\vdots \\
\begin{pmatrix} A_R \\ B_R \end{pmatrix} e^{-(\alpha-2)\kappa}
\end{pmatrix} = 0. \tag{3.1.14}$$

We have the same bulk equations as for the infinite chain with the soliton (2.2.2) and therefore, the same dispersion relation

$$E^2 = t_1^2 + t_2^2 - 2t_1 t_2 \cosh 2\kappa. \tag{3.1.15}$$

We define φ as follows

$$-|E|e^{2\varphi} \equiv (t_1 - t_2 e^{2\kappa}), \tag{3.1.16}$$

which is valid for $t_1 < t_2$, but, once again, yields the same solutions as the other possible definition. From (3.1.16), we find that A_R and B_R which satisfy (2.2.2) are given by

$$\begin{pmatrix} A_R \\ B_R \end{pmatrix} = \begin{pmatrix} -e^{\varphi} \\ \pm e^{-\varphi} \end{pmatrix}. \tag{3.1.17}$$

We have the same ansatz as for the infinite chain with complex k (2.2.6), but, since we have different expressions for A and B, the wave function takes the form

$$\begin{aligned}|\psi_{R\pm}\rangle = \sum_{m=0}^{\beta}(-1)^m \Big\{ &-\left(C_+e^{\varphi}e^{-2m\kappa} + C_-e^{-\varphi}e^{2m\kappa}\right)|2m+1\rangle \\ &\pm\left(C_+e^{-\varphi}e^{-2m\kappa} + C_-e^{\varphi}e^{2m\kappa}\right)|2m+2\rangle\Big\}, \\ |\psi_{L\pm}\rangle = \sum_{m=0}^{\beta}(-1)^m \Big\{ &-\left(D_+e^{\varphi}e^{-2m\kappa} + D_-e^{-\varphi}e^{2m\kappa}\right)|-(2m+1)\rangle \\ &\pm\left(D_+e^{-\varphi}e^{-2m\kappa} + D_-e^{\varphi}e^{2m\kappa}\right)|-(2m+2)\rangle\Big\},\end{aligned} \tag{3.1.18}$$

where $C_\pm$ and $D_\pm$ are constants to be determined. The three central boundary equations (2.2.9) become

$$\begin{aligned}&\pm t_1(D_+e^{-\varphi} + D_-e^{\varphi}) + E(D_+e^{\varphi} + D_-e^{-\varphi}) + t_2B_0 = 0, \\ &-t_2(D_+e^{\varphi} + D_-e^{-\varphi}) - EB_0 - t_2(C_+e^{\varphi} + C_-e^{-\varphi}) = 0 \\ &t_2B_0 + E(C_+e^{\varphi} + C_-e^{-\varphi}) \pm t_1(C_+e^{-\varphi} + C_-e^{\varphi}) = 0.\end{aligned} \tag{3.1.19}$$

From the left and right edges of the chain, we also have the two following conditions

$$\begin{aligned}&\mp E(D_+e^{-\varphi}e^{-(\alpha-2)\kappa} + D_-e^{\varphi}e^{(\alpha-2)\kappa}) - t_1(D_+e^{\varphi}e^{-(\alpha-2)\kappa} + D_-e^{-\varphi}e^{(\alpha-2)\kappa}) = 0, \\ &-t_1(C_+e^{\varphi}e^{-(\alpha-2)\kappa} + C_-e^{-\varphi}e^{(\alpha-2)\kappa}) \mp E(C_+e^{-\varphi}e^{-(\alpha-2)\kappa} + C_-e^{\varphi}e^{(\alpha-2)\kappa}) = 0.\end{aligned} \tag{3.1.20}$$

Even Solutions

The conditions for even solutions $C_\pm = D_\pm$ and $B_0 = 1$ lead to three nontrivial boundary equations given by

$$\begin{aligned}&-2t_2(C_+e^{\varphi} + C_-e^{-\varphi}) = E \\ &C_+(\pm t_1e^{-\varphi} + Ee^{\varphi}) + C_-(\pm t_1e^{\varphi} + Ee^{-\varphi}) = -t_2, \\ &C_+(-t_1e^{\varphi} \mp Ee^{-\varphi})e^{-(\alpha-2)\kappa}) + C_-(-t_1e^{-\varphi} \mp Ee^{\varphi})e^{(\alpha-2)\kappa}) = 0.\end{aligned} \tag{3.1.21}$$

With the definition (3.1.16), we find the relation

$$-t_1e^{\mp\varphi} \mp Ee^{\pm\varphi} = -t_2e^{\mp\varphi}e^{\pm2\kappa}, \tag{3.1.22}$$

which enables us to simplify the second and third equations of (3.1.21) to get the form

$$\begin{aligned}C_+e^{-\varphi}e^{2\kappa} + C_-e^{\varphi}e^{-2\kappa} &= \mp1 \\ C_+e^{\varphi}e^{-\alpha\kappa} + C_-e^{-\varphi}e^{\alpha\kappa} &= 0,\end{aligned} \tag{3.1.23}$$

which we put in matrix form

$$\begin{pmatrix} e^{-\varphi}e^{2\kappa} & e^{\varphi}e^{-2\kappa} \\ e^{\varphi}e^{-\alpha\kappa} & e^{-\varphi}e^{\alpha\kappa} \end{pmatrix} \begin{pmatrix} C_+ \\ C_- \end{pmatrix} = \begin{pmatrix} \mp 1 \\ 0 \end{pmatrix}. \tag{3.1.24}$$

We find the determinant of this matrix to be $-2/|E|(t_1 sh_{\alpha+2} + t_2 sh_\alpha)$. We invert the matrix and solve for $C_\pm$, which yields

$$\begin{pmatrix} C_+ \\ C_- \end{pmatrix} = \frac{E}{2(t_1 sh_{\alpha+2} + t_2 sh_\alpha)} \begin{pmatrix} e^{-\varphi}e^{\alpha\kappa} \\ -e^{\varphi}e^{-\alpha\kappa} \end{pmatrix}, \tag{3.1.25}$$

which are substituted in (3.1.18) to find the following solution,

$$\begin{aligned} |\psi_{\text{even}}\rangle = |0\rangle + \sum_{m=0}^{\beta} \frac{(-1)^m}{t_1 sh_{\alpha+2} - t_2 sh_\alpha} \Big\{ E sh_{\alpha-2m} \Big[|2m+1\rangle + |-(2m+1)\rangle \Big] \\ + (t_1 s_{\alpha-2m} - t_2 s_{\alpha-2m-2}) \Big[|2m+2\rangle + |-(2m+2)\rangle \Big] \Big\}. \end{aligned} \tag{3.1.26}$$

To find the equation that gives us the number of κ solutions for an even wave function, we substitute (3.1.25) in the first boundary equation of (3.1.21), simplify, and get the following transcendental equation

$$r sh_{\alpha+2} + 3 sh_\alpha = 0. \tag{3.1.27}$$

We find that this equation has no solutions for all r. It may seem like time was wasted by doing this computation, but there are two reasons for its importance. First of all, when we count all of the wavenumber solutions of the system at the end of this chapter, we need to find exactly $2\alpha+1 = N$ solutions. This means that we need to make sure that every possibility of a solution has been checked and accounted for. Secondly, and most importantly, the method of calculation that we have used up to now can't find the $E = 0$ solution of the system as was discussed in section 2.2. Once again, the $E = 0$ solution is located in the band gap and therefore has a complex wavenumber. Since the complex wavenumber dispersion relation for the finite chain is the same as for the infinite chain, (2.2.3), the κ solution for $E = 0$ is also the same, which is given by

$$\kappa = \frac{1}{2} \operatorname{arcosh} [\frac{1}{2}(r + \frac{1}{r})], \tag{3.1.28}$$

which has one real and positive κ solution. We will discuss the even parity of the zero-mode in section 3.1.4. With solution (3.1.26), we set $E = 0$ to find the wave function of the zero-mode

$$|\psi_{\mathrm{E}=0}\rangle = |0\rangle + \sum_{m=0}^{\beta} \frac{(-1)^m}{t_1 sh_{\alpha+2} - t_2 sh_{\alpha}} \Big\{ (t_1 sh_{\alpha-2m} - t_2 sh_{\alpha-2m-2}) \Big[|2m+2\rangle \; + |-(2m+2)\rangle \; \Big] \Big\}. \tag{3.1.29}$$

Odd Solutions

As we always do for odd solutions, we have $C_{\pm} = -D_{\pm}$ and therefore $B_0 = 0$. We have two nontrivial boundary equations simplified using (3.1.22), which are

$$\begin{aligned} C_+ e^{-\varphi} e^{2\kappa} + C_- e^{\varphi} e^{-2\kappa} = 0, \\ C_+ e^{\varphi} e^{-\alpha\kappa} + C_- e^{-\varphi} e^{\alpha\kappa} = 0. \end{aligned} \tag{3.1.30}$$

The first equation is used to find the ratio of C_+ and C_-, which lets us write

$$\begin{aligned} C_+ = -e^{-\varphi} e^{\alpha\kappa}, \\ C_- = e^{\varphi} e^{-\alpha\kappa}, \end{aligned} \tag{3.1.31}$$

up to a normalization constant. We substitute these expressions in (3.1.18) to find the following form of the solution

$$\begin{aligned} |\psi_{\mathrm{odd}}\rangle = \sum_{m=0}^{\beta} (-1)^m \Big\{ (t_1 sh_{2m+2} - t_2 sh_{2m}) \Big[|2m+1\rangle \; - |-(2m+1)\rangle \; \Big] \\ + E sh_{2m+2} \Big[|2m+2\rangle \; - |-(2m+2)\rangle \; \Big] \Big\}. \end{aligned} \tag{3.1.32}$$

Finally, we substitute the expressions (3.1.31) in the second boundary equation of (3.1.30) and find the following transcendental equation for κ

$$r sh_{\alpha+2} - sh_{\alpha} = 0, \tag{3.1.33}$$

which has 2 solutions for $r < r_c$ and no solutions for $r > r_c$.

3.1.3. Imaginary k Solutions

Considering the wavenumber to be imaginary $k \to i\kappa$ leads to the exponential $e^{i2mk} \to e^{-2m\kappa}$. Solutions with an imaginary wavenumber have energies outside the bands. The Schrödinger equation in matrix form becomes

$$\begin{pmatrix}
-E & t_1 & & & & & & & & & \\
t_1 & -E & t_2 & & & & & & & & \\
 & \ddots & \ddots & \ddots & & & & & & & \\
 & & t_1 & -E & t_2 & & & & & & \\
 & & & t_2 & -E & t_1 & & & & & \\
 & & & & t_1 & -E & t_2 & & & & \\
 & & & & & t_2 & -E & t_2 & & & \\
 & & & & & & t_2 & -E & t_1 & & \\
 & & & & & & & t_1 & -E & t_2 & \\
 & & & & & & & & \ddots & \ddots & \ddots \\
 & & & & & & & & & t_2 & -E & t_1 \\
 & & & & & & & & & & t_1 & -E
\end{pmatrix}
\begin{pmatrix}
\begin{pmatrix} B_L \\ A_L \end{pmatrix} e^{-(\alpha-2)\kappa} \\
\vdots \\
\begin{pmatrix} B_L \\ A_L \end{pmatrix} e^{-2\kappa} \\
\begin{pmatrix} B_L \\ A_L \end{pmatrix} \\
B_0 \\
\begin{pmatrix} A_R \\ B_R \end{pmatrix} \\
\begin{pmatrix} A_R \\ B_R \end{pmatrix} e^{-2\kappa} \\
\vdots \\
\begin{pmatrix} A_R \\ B_R \end{pmatrix} e^{-(\alpha-2)\kappa}
\end{pmatrix} = 0. \tag{3.1.34}$$

The two coupled bulk equations are still the same as for the infinite chain with a soliton, (2.3.2), and thus the dispersion relation is also the same. Again, we use the definition for φ (2.3.4) which yields the same form of the wave function as for the infinite chain case but with a finite upper bound β

$$\begin{aligned}
|\psi_{R\pm}\rangle = \sum_{m=0}^{\beta} \Big\{ &\left(C_+ e^{\varphi} e^{-2m\kappa} + C_- e^{-\varphi} e^{2m\kappa}\right) |2m+1\rangle \\
&\pm \left(C_+ e^{-\varphi} e^{-2m\kappa} + C_- e^{\varphi} e^{2m\kappa}\right) |2m+2\rangle \Big\}, \\
|\psi_{L\pm}\rangle = \sum_{m=0}^{\beta} \Big\{ &\left(D_+ e^{\varphi} e^{-2m\kappa} + D_- e^{-\varphi} e^{2m\kappa}\right) |-(2m+1)\rangle \\
&\pm \left(D_+ e^{-\varphi} e^{-2m\kappa} + D_- e^{\varphi} e^{2m\kappa}\right) |-(2m+2)\rangle \Big\}.
\end{aligned} \tag{3.1.35}$$

We have five boundary equations to consider; the three central conditions (2.3.9) and the two equations from the edges of the chain, given by

$$\begin{aligned} \mp E(D_+e^{-\varphi}e^{-(\alpha-2)\kappa} + D_-e^{\varphi}e^{(\alpha-2)\kappa}) + t_1(D_+e^{\varphi}e^{-(\alpha-2)\kappa} + D_-e^{-\varphi}e^{(\alpha-2)\kappa}) = 0, \\ t_1(C_+e^{\varphi}e^{-(\alpha-2)\kappa} + C_-e^{-\varphi}e^{(\alpha-2)\kappa}) \mp E(C_+e^{-\varphi}e^{-(\alpha-2)\kappa} + C_-e^{\varphi}e^{(\alpha-2)\kappa}) = 0. \end{aligned} \tag{3.1.36}$$

Even Solutions

From imposing $C_\pm = D_\pm$ and choosing $B_0 = 1$, we get the following three nontrivial boundary equations

$$\begin{aligned} 2t_2(C_+e^{\varphi} + C_-e^{-\varphi}) = E, \\ C_+(\pm t_1e^{-\varphi} - Ee^{\varphi}) + C_-(\pm t_1e^{\varphi} - Ee^{-\varphi}) = -t_2, \\ C_+(t_1e^{\varphi} \mp Ee^{-\varphi})e^{-(\alpha-2)\kappa} + C_-(t_1e^{-\varphi} \mp Ee^{\varphi})e^{(\alpha-2)\kappa} = 0, \end{aligned} \tag{3.1.37}$$

of which we simplify the second and third lines using (2.3.4) to get

$$\begin{aligned} C_+e^{-\varphi}e^{2\kappa} + C_-e^{\varphi}e^{-2\kappa} = \pm 1, \\ C_+e^{\varphi}e^{-\alpha\kappa} + C_-e^{-\varphi}e^{\alpha\kappa} = 0. \end{aligned} \tag{3.1.38}$$

We write these two in matrix form and find its determinant to be $-2/|E|(t_1sh_{\alpha+2} + t_2sh_\alpha)$. We invert the matrix and solve for $C_\pm$, which yields

$$\begin{pmatrix} C_+ \\ C_- \end{pmatrix} = \frac{E}{2(t_1sh_{\alpha+2} + t_2sh_\alpha)} \begin{pmatrix} e^{-\varphi}e^{\alpha\kappa} \\ -e^{\varphi}e^{-\alpha\kappa} \end{pmatrix}. \tag{3.1.39}$$

We use these expressions in (2.3.7) and simplify to find the final form of the solution

$$\begin{aligned} |\psi_{\text{even}}\rangle = |0\rangle + \sum_{m=0}^{\beta} \frac{1}{t_1sh_{\alpha+2} + t_2sh_\alpha} \Big\{ Esh_{\alpha-2m}\Big[|2m+1\rangle + |-(2m+1)\rangle \Big] \\ +(t_1sh_{\alpha-2m} + t_2sh_{\alpha-2m-2})\Big[|2m+2\rangle + |-(2m+2)\rangle \Big]\Big\}. \end{aligned} \tag{3.1.40}$$

All we have left to do is find the equation that will provide us with the number of κ solutions. We substitute (3.1.39) in the first boundary equation in (3.1.37) and find the relation

$$rsh_{\alpha+2} - sh_\alpha = 0, \tag{3.1.41}$$

which has 2 solutions for $r < r_c$ and no solutions for $r > r_c$.

Odd Solutions

As per usual, we have $C_\pm = -D_\pm$ which leads to $B_0 = 0$. We then have two nontrivial boundary equations given by

$$\begin{aligned} C_+ e^{-\varphi} e^{2\kappa} + C_- e^{\varphi} e^{-2\kappa} = 0, \\ C_+ e^{\varphi} e^{-\alpha\kappa} + C_- e^{-\varphi} e^{\alpha\kappa} = 0, \end{aligned} \tag{3.1.42}$$

of which we use the first equation to solve for the constants to get

$$\begin{aligned} C_+ = -e^{\varphi} e^{-2\kappa}, \\ C_- = e^{-\varphi} e^{2\kappa}, \end{aligned} \tag{3.1.43}$$

up to a normalization constant. Using these expressions in the second equation of (3.1.42), we find the transcendental equation

$$rsh_{\alpha+2} + sh_\alpha = 0, \tag{3.1.44}$$

which has no solutions for all r.

3.1.4. Discussion of States and the Energy Spectrum

We start by summarizing the number of solutions obtained graphically, as was done for a regular SSH chain, from all the transcendental equations found in the previous sections.

			$r < r_c$	$r > r_c$
Even Solutions	Real k	$rs_{\alpha+2} - s_\alpha = 0$	$\alpha - 2$	α
	Complex k	$rsh_{\alpha+2} + 3sh_\alpha = 0$	0	0
		$k = \frac{1}{2}\arccos\Big(-\frac{1}{2}\Big(r + \frac{1}{r}\Big)\Big)$	1	1
	Imaginary k	$rsh_{\alpha+2} - sh_\alpha = 0$	2	0
Odd Solutions	Real k	$rs_{\alpha+2} + s_\alpha = 0$	$\alpha - 2$	α
	Complex k	$rsh_{\alpha+2} - sh_\alpha = 0$	2	0
	Imaginary k	$rsh_{\alpha+2} + sh_\alpha = 0$	0	0
Total			$2\alpha + 1$	$2\alpha + 1$

Tableau 3.1. Summary of the number of solutions for the wavenumber k for the ϕ_{12} configuration

Real k

The solutions with real wavenumber k correspond to bulk states; oscillatory solutions that are expected in periodic materials as is shown in Fig. 3.2. Depending on the value of r, there can be from $(2\alpha - 4 = N - 5)$ to $(2\alpha = N - 1)$ of these states as will be discussed in the next section.

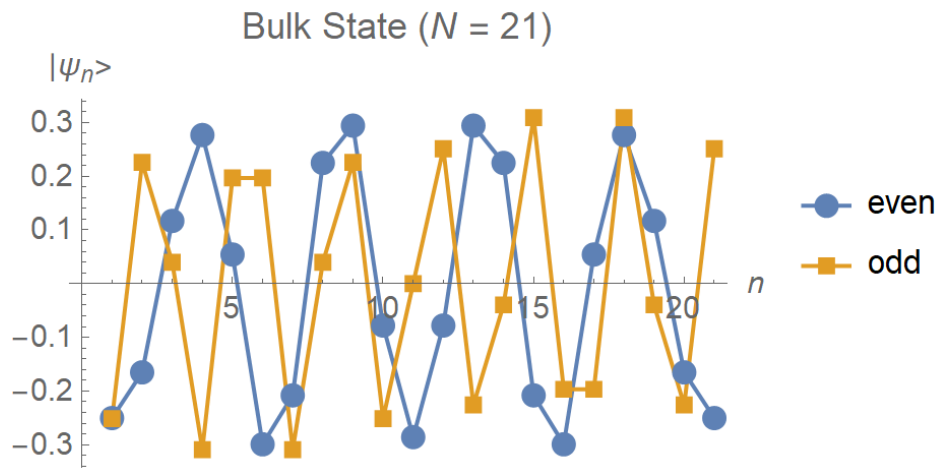

Fig. 3.2. In the Φ_{12} configuration, a pair of bulk states for a system of length $N = 21$. In blue, a symmetric state about the soliton and in orange, an antisymmetric state.

The Energy Spectrum

Before looking at the more interesting states we have found, let's discuss the energy spectrum as it will inform our future analysis. As was done for the regular SSH chain, we find the k solutions using the various transcendental equations, feed them to the corresponding dispersion relation and take the positive and negative root of the energy. Fig. 3.3. shows the energy spectrum of the Φ_{12} configuration as a function of parameter σ where we have defined $\sigma = t_1$ and $1 - \sigma = t_2$ such that $t_1 + t_2 = 1$.

For the regime where $r < r_c$, we have $(2\alpha - 4 = N - 5)$ bulk energy solutions. There is one solution with exactly $E = 0$ corresponding to the even solution with complex k. Additionally, we have two energy solutions that are near zero, which we call edge states and correspond to the two complex k odd solutions. Finally, we have two high-energy solutions which are associated with the imaginary k even solutions. For the regime where $r > r_c$, the high-energy and the near-zero-energy solutions transition to bulk states such that we indeed have $(2\alpha = N - 1)$ bulk energy solutions. The zero-energy mode stays and is still a complex k even solution. This differs from the regular SSH chain, which only has a pair of near-zero-energy edge states for a chain with even N and a single zero energy state for odd N; we have all three states in this system. Moreover, we have high-energy states, which are not present for the regular SSH chain, but were present in the infinite SSH chain with a soliton. Let's take a look at the limiting cases $(t_1 = 0, t_2 = 1)$ or $r = 0$ and $(t_1 = 1, t_2 = 0)$

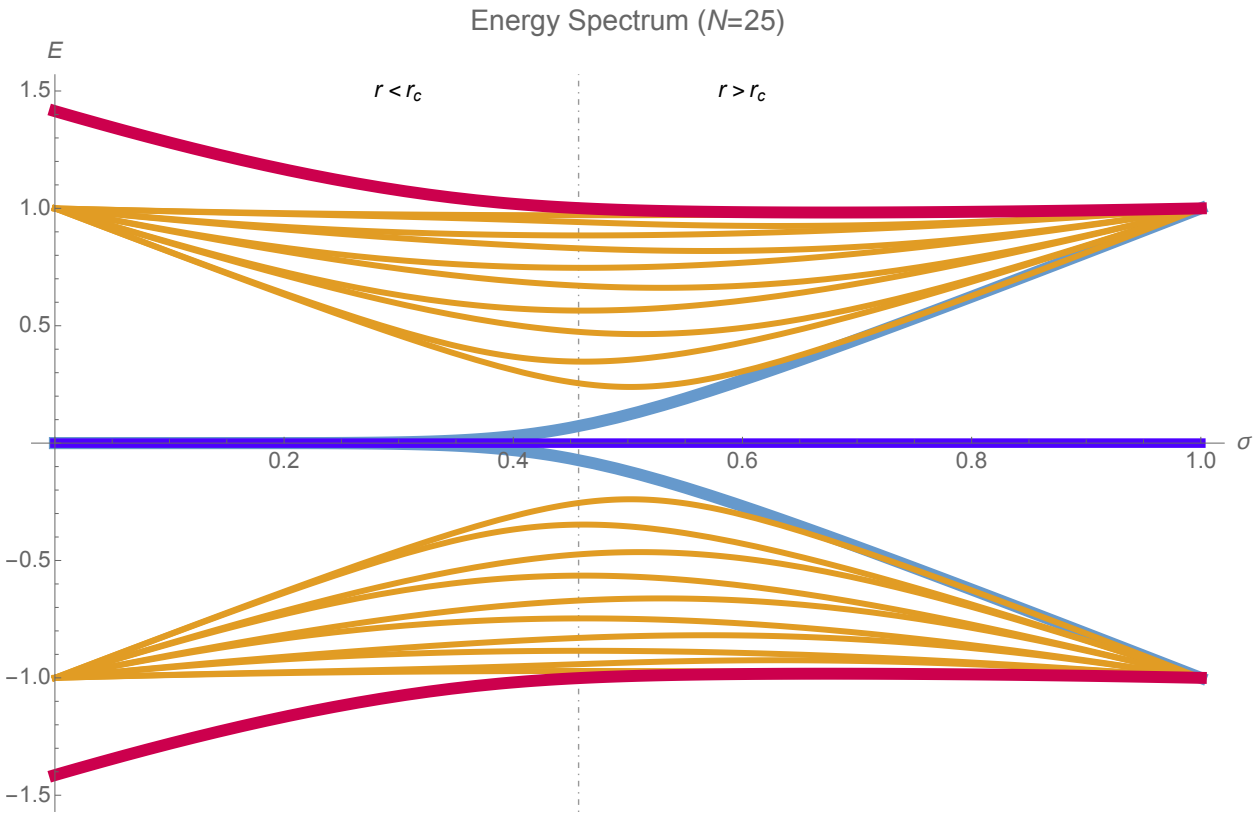

Fig. 3.3. Energy spectrum as a function of parameter σ for a finite SSH chain with a central soliton in the Φ_{12} configuration. We make the parametrization choice $t_1 = \sigma$ and $t_2 = 1 - \sigma$ such that $t_1 + t_2 = 1$ and σ takes values from zero to one. Highlighted in red are the high-energy solutions (imaginary k), in purple is the zero-energy midgap state (complex k), in blue are the edge states (complex k) and in orange are the bulk state (real k).

or $r \to \infty$ to intuitively understand the energy spectrum shown in Fig. 3.3. When $r = 0$, the chain has a central trimer, a series of dimers on both sides of this trimer and the edges of the chain become monomers as shown in Fig. 3.4(a). The Hamiltonian (3.1.1) becomes

$$H_{\Phi_{12}} \to H_{monomer} \bigoplus_{i=1}^{\frac{\alpha-2}{2}} H_{dimer,i} \bigoplus H_{trimer} \bigoplus_{i=1}^{\frac{\alpha-2}{2}} H_{dimer,i} \bigoplus H_{monomer} \tag{3.1.45}$$

where the monomer's and dimer's Hamiltonians are given by (1.1.28) and the trimer's Hamiltonian, by (2.4.2).

The trimer structure has three energy solutions: $\pm\sqrt{2}$ and 0. The dimers each have eigenenergies ± 1 and there are two monomers with zero-energy solutions. Let the number of dimers on each side of the central trimer be $D = \frac{\alpha-2}{2}$. There is therefore a number $4D$ of

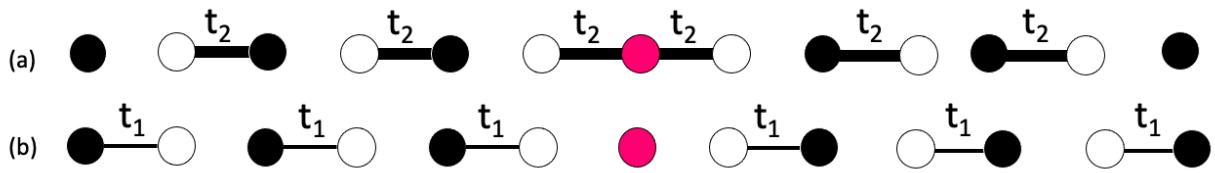

Fig. 3.4. SSH chain in the Φ_{12} configuration with $N = 13$ where, in (a), we have imposed $(t_1 = 0, t_2 = 1)$: the system breaks up into a central trimer, a series of dimers (D) and a monomer at each edge. In (b), we have imposed $(t_1 = 1, t_2 = 0)$: the system breaks up into a central monomer and a series of dimers $(D' = D + 1)$.

energy solutions from the dimers in the chain. If we add up the solutions from the trimer and the monomers, we have a total of $(4D + 5 = 2\alpha + 1 = N)$ energy solutions for the complete chain, as expected. By looking at the $r = 0$ $(\sigma = 0)$ end of the energy spectrum in Fig. 3.3, we indeed see the aforementioned behaviour.

Now, we consider the limiting case $(t_1 = 1, t_2 = 0)$; the chain has a central monomer and the rest of the chain breaks into dimers as shown in Fig. 3.4(b). The Hamiltonian (3.1.1) reduces to

$$H_{\Phi_{12}} \to \bigoplus_{i=1}^{\frac{\alpha}{2}} H_{dimer,i} \bigoplus H_{monomer} \bigoplus_{i=1}^{\frac{\alpha}{2}} H_{dimer,i} \tag{3.1.46}$$

where the monomer's and dimer's Hamiltonians are given by (1.1.28). Once again, the central monomer only has eigenenergy $E = 0$ and the dimers each have solutions of energy ± 1. On each side of the central site, there are $(D' = D + 1 = \frac{\alpha-2}{2} + 1)$ dimers since there is one more dimer per side in this case than there are in the previous limiting case. We therefore have $4(D + 1)$ energy solutions from the dimers and one solution from the monomer. In total, we have $(4D + 5 = N)$ solutions, as we should. This is indeed the behaviour when $r \to \infty$ $(\sigma = 1)$ as shown in Fig. 3.3; there is one zero energy state and all remaining energies correspond to bulk states.

Complex k

First, we discuss the zero-energy midgap state highlighted in purple in Fig. 3.3 and shown in Fig. 3.5.

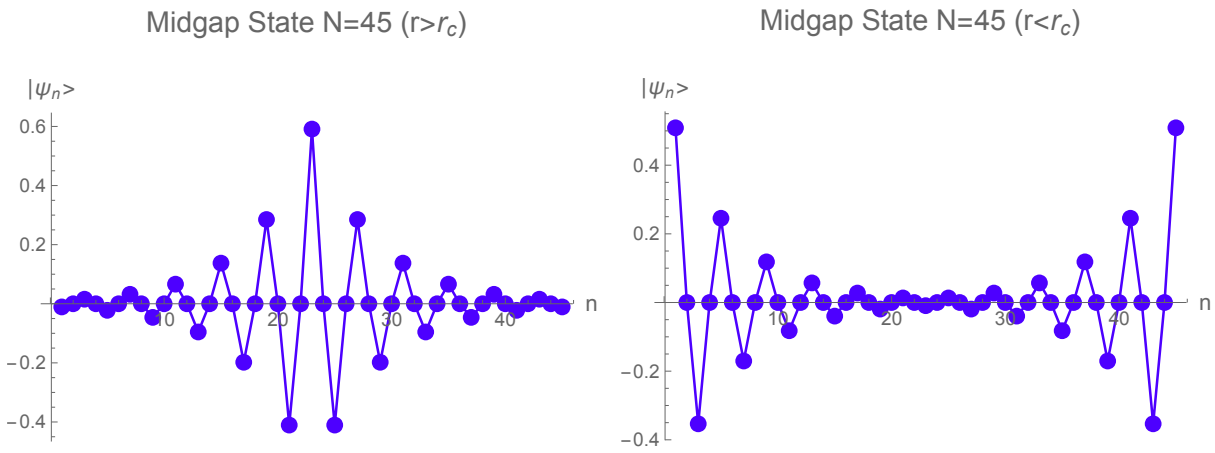

Fig. 3.5. In the Φ_{12} configuration, zero-energy midgap states for $r > r_c$ ($r < r_c$) on the left (right). Both states are symmetric about the central site.

The midgap state exists for all values of r, similarly to the odd SSH chain. For $r < r_c$, the state is localized at both ends of the chain while, for $r > r_c$, it is localized at the soliton. Both states are symmetric with respect to the central site. We can understand this behaviour by considering the limiting cases $r = 0$ and $r \to \infty$. We start with the limit $r \to \infty$ as it will inform our discussion of the other case. As shown in Fig. 3.4(b) and as discussed in the previous section, only the central monomer has a zero-energy solution. Therefore, when $r > r_c$, the zero-energy state will be localized at the central site and will exponentially fall off on each side of the soliton as tunneling between sites is allowed. Additionally, a monomer's $E = 0$ eigenstate is symmetric; this parity carries through when $r > r_c$, which is what we observe in Fig. 3.5. When $r < r_c$, the zero-energy midgap state is still present and stays even unlike the zero-mode of the infinite SSH chain with a soliton. We look at the opposite limiting case for which $r = 0$. The zero-energy solution is triply degenerate; there are therefore three corresponding states. The central trimer's zero-energy eigenstate is antisymmetric and there are zero-modes localized on the first and last sites of which we can choose even or odd combinations. Therefore, we can construct one symmetric state

with both monomers' eigenstates and two antisymmetric states with a superposition of all three wave functions. The even wave function is localized at both ends of the chain and, we expect that when we let $r < r_c$, it will exponentially die off towards the centre of the chain. This corresponds to the midgap state we observe in Fig. 3.5. The two other possible states for $r = 0$ are antisymmetric and purely localized at the soliton and at both edges; this description is very similar to the edge states as represented in Fig. 3.6.

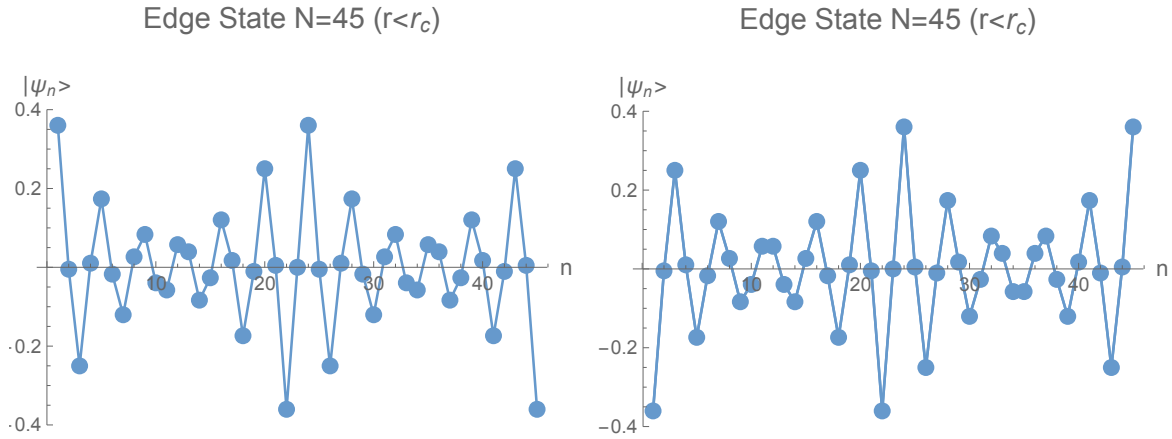

Fig. 3.6. In the Φ_{12} configuration, near-zero-energy edge states for $N = 45$. These edge states correspond to energies $E/t_2 = \pm 0.0007$.

As always, when we let r increase towards r_c, the states are not purely localized at any site anymore as this allows for tunneling through the rest of the chain. For $r > r_c$, these edge states become delocalized oscillatory bulk states.

Imaginary k

Lastly, we have high-energy states localized at the interface which only exist for $r < r_c$ and transition to bulk states for $r > r_c$ as highlighted in red in the spectrum shown in Fig. 3.3. The positive energy state is strictly positive while the negative energy state is oscillatory as shown in Fig. 3.7.

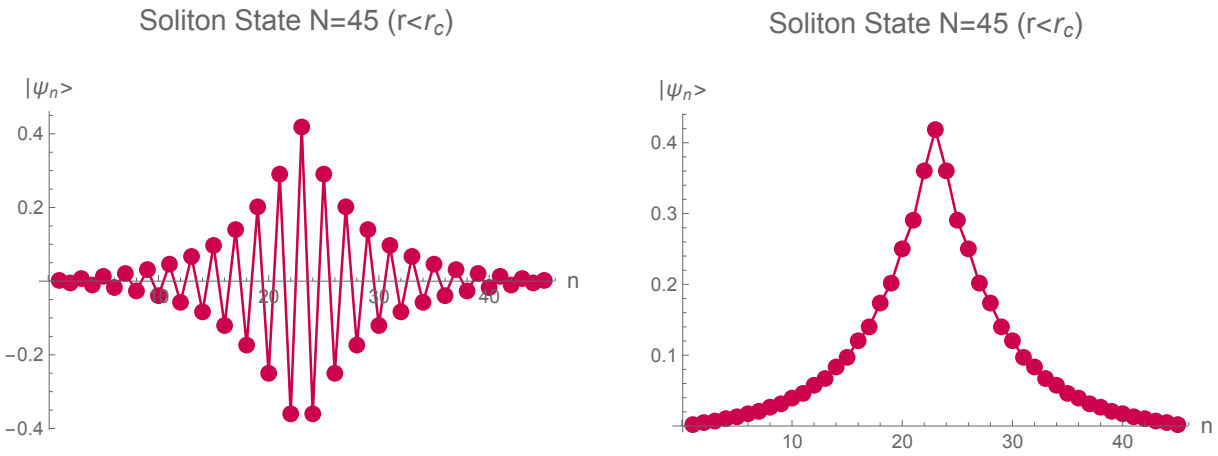

Fig. 3.7. In the Φ_{12} configuration, high-energy modes localized at the interface, which only exist in the regime $r < r_c$. This pair of symmetric states about the soliton has energies $E/t_2 = \pm 1.581$, with positive (negative) energy on the right (left).

Looking at the chain's form when $r = 0$, the high-energy states are only supported by the central trimer and are symmetric. Therefore, as $r < r_c$, we expect even wave functions that are localized at the soliton and that exponentially die off on both sides, which is what we see in Fig. 3.7. As the central trimer only exists in the $r < r_c$ regime, it is expected that these high-energy states delocalize throughout the bulk for $r > r_c$.

The Φ_{12} configuration was studied in the context of a spin chain in [8], which is related to the SSH model through the Jordan-Wigner transformation [28]. Results are in good agreement with the authors' findings of a single localized zero-energy state for $r > r_c$ as well as 5 localized states for $r < r_c$. However, there is a discrepancy with their observation of a triply-degenerate zero-energy state for $r < r_c$. This may be due to the choice of parameters in their study as our near-zero-energy edge states quickly tend to zero with large N and small r as shown in Fig. 3.3.

3.2. Φ_{22} Configuration

This configuration of the finite chain with a central soliton has t_2 at its edges and as the repeated hopping parameter. The system consists of two finite SSH chains with an odd number of sites α connected by a central interface site. The total length of the chain can take up values $N = 4n + 3$ with $n = 1, 2, 3, \ldots$ As usual, a unit cell consists of a pair of sites (A,B) labeled by the m index. We run this index from zero to $\frac{\alpha-1}{2}$ to get the total number of unit cells η.

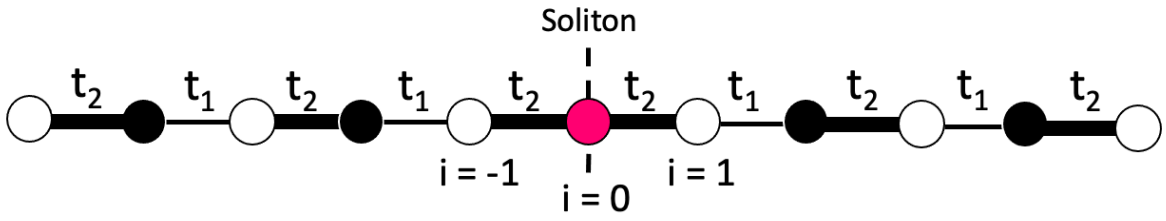

Fig. 3.8. Finite SSH chain with $N = 11$, repeated hopping parameters t_2 at the centre to make up the soliton and at its edges (Φ_{22} configuration). The central site is labeled by $i = 0$. The sites on the right chain segment are labeled by $i = (1, 2, 3, \ldots, \alpha)$ while the sites on the left are labeled by $i = (\text{-}1, \text{-}2, \text{-}3, \ldots, -\alpha)$). In this case, $\alpha = 5$ and the total number of unit cells on each chain segment is 3; in this case, the sum over m would run from 0 to $\eta = 2$ and we impose that the amplitude of the B site of the last unit cell be 0.

3.2.1. Real k Solutions

We consider electronic solutions with a real-valued wavenumber k which have energies within the bands. We start by writing the Schrödinger equation in matrix form as

$$\begin{pmatrix}
-E & t_2 & & & & & & & & & & \\
t_2 & -E & t_1 & & & & & & & & & \\
 & \ddots & \ddots & \ddots & & & & & & & & \\
 & & t_1 & -E & t_2 & & & & & & & \\
 & & & t_2 & -E & t_1 & & & & & & \\
 & & & & t_1 & -E & t_2 & & & & & \\
 & & & & & t_2 & -E & t_2 & & & & \\
 & & & & & & t_2 & -E & t_1 & & & \\
 & & & & & & & t_1 & -E & t_2 & & \\
 & & & & & & & & \ddots & \ddots & \ddots & \\
 & & & & & & & & & t_1 & -E & t_2 \\
 & & & & & & & & & & t_2 & -E
\end{pmatrix}
\begin{pmatrix}
A_L\, e^{i(\alpha-1)k_L} \\
\begin{pmatrix} B_L \\ A_L \end{pmatrix} e^{i(\alpha-3)k} \\
\vdots \\
\begin{pmatrix} B_L \\ A_L \end{pmatrix} e^{i2k} \\
\begin{pmatrix} B_L \\ A_L \end{pmatrix} \\
B_0 \\
\begin{pmatrix} A_R \\ B_R \end{pmatrix} \\
\begin{pmatrix} A_R \\ B_R \end{pmatrix} e^{i2k} \\
\vdots \\
\begin{pmatrix} A_R \\ B_R \end{pmatrix} e^{i(\alpha-3)k} \\
A_R\, e^{i(\alpha-1)k_R}
\end{pmatrix} = 0, \tag{3.2.1}$$

where each side of the chain's last site's wave function carries a factor $e^{i2mk} = e^{i(\alpha-1)k}$ as the last unit cell index is $m = \eta = \frac{\alpha-1}{2}$. The general form of the wave functions differs from the infinite chain's (2.1.5) only by the sum's upper bound: we immediately write in in terms of $C_\pm$ and $D_\pm$ as

$$
\begin{aligned}
|\psi_{R\pm}\rangle = \sum_{m=0}^{\eta=\frac{\alpha-1}{2}} \Big\{ \Big(C_+ e^{-i\varphi} e^{i2mk} + C_- e^{i\varphi} e^{-i2mk}\Big) |2m+1\rangle \\
\pm \Big(C_+ e^{i\varphi} e^{i2mk} + C_- e^{-i\varphi} e^{-i2mk}\Big) |2m+2\rangle \Big\} \\
|\psi_{L\pm}\rangle = \sum_{m=0}^{\eta=\frac{\alpha-1}{2}} \Big\{ \Big(D_+ e^{-i\varphi} e^{i2mk} + D_- e^{i\varphi} e^{-i2mk}\Big) |-(2m+1)\rangle \\
\pm \Big(D_+ e^{i\varphi} e^{i2mk} + D_- e^{-i\varphi} e^{-i2mk}\Big) |-(2m+2)\rangle \Big\},
\end{aligned}
\tag{3.2.2}
$$

where we impose that the site $|2\eta+2\rangle = |\alpha+1\rangle$ amplitude's be zero as the chain ends on an A sublattice site (as opposed to the usual B sublattice site). There are five boundary conditions to consider: three from the juncture of the chains (2.1.6) and two from the chain's edges

$$
\begin{aligned}
-E(D_+ e^{-i\varphi} e^{i(\alpha-1)k} + D_- e^{i\varphi} e^{-i(\alpha-1)k}) \pm t_2(D_+ e^{i\varphi} e^{i(\alpha-3)k} + D_- e^{-i\varphi} e^{-i(\alpha-3)k}) = 0, \\
\pm t_2(C_+ e^{i\varphi} e^{i(\alpha-3)k} + C_- e^{-i\varphi} e^{-i(\alpha-3)k}) - E(C_+ e^{-i\varphi} e^{i(\alpha-1)k} + C_- e^{i\varphi} e^{-i(\alpha-1)k}) = 0.
\end{aligned}
\tag{3.2.3}
$$

Even Solutions

Even solutions to the Schrödinger equation have $C_\pm = D_\pm$ and thus we can make the normalization choice $B_0 = 1$. We make these substitutions in the five boundary equations (2.1.6), (3.2.3) to get the following three nontrivial conditions

$$
\begin{aligned}
2t_2(C_+ e^{-i\varphi} + C_- e^{i\varphi}) = E, \\
C_+(\pm t_1 e^{i\varphi} - E e^{-i\varphi}) + C_-(\pm t_1 e^{-i\varphi} - E e^{i\varphi}) = -t_2, \\
C_+(-E e^{-i\varphi} \pm t_2 e^{i\varphi} e^{-i2k}) e^{i(\alpha-1)k} + C_-(-E e^{i\varphi} \pm t_2 e^{-i\varphi} e^{i2k}) e^{-i(\alpha-1)k} = 0.
\end{aligned}
\tag{3.2.4}
$$

of which we can simplify the second and third equations using (2.1.10) to get

$$
\begin{aligned}
C_+ e^{i\varphi} e^{-i2k} + C_- e^{-i\varphi} e^{i2k} = \pm 1 \\
C_+ e^{i\varphi} e^{i(\alpha-1)k} + C_- e^{-i\varphi} e^{-i(\alpha-1)k} = 0.
\end{aligned}
\tag{3.2.5}
$$

To solve for $C_\pm$, we rewrite these in matrix form

$$
\begin{pmatrix} e^{i\varphi} e^{i(\alpha-1)k} & e^{-i\varphi} e^{-i(\alpha-1)k} \\ e^{i\varphi} e^{-i2k} & e^{-i\varphi} e^{i2k} \end{pmatrix} \begin{pmatrix} C_+ \\ C_- \end{pmatrix} = \begin{pmatrix} 0 \\ \pm 1 \end{pmatrix}. \tag{3.2.6}
$$

The matrix has determinant $2is_{\alpha+1}$. We invert this matrix and solve for $C_\pm$, yielding

$$\begin{pmatrix} C_+ \\ C_- \end{pmatrix} = \frac{1}{2is_{\alpha+1}} \begin{pmatrix} \mp e^{-i\varphi} e^{-i(\alpha-1)k} \\ \pm e^{i\varphi} e^{i(\alpha-1)k} \end{pmatrix}. \tag{3.2.7}$$

We substitute these expressions in (3.2.2) and simplify to find the final form of the wave function, given by

$$\begin{aligned} |\psi_{\text{even}}\rangle = |0\rangle + \sum_{m=0}^{\eta} \frac{1}{s_{\alpha+1}} \Big\{ (t_1 s_{\alpha-1-2m} + t_2 s_{\alpha+1-2m}) \Big[|2m+1\rangle + |-(2m+1)\rangle \Big] \\ + E s_{\alpha-1-2m} \Big[|2m+2\rangle + |-(2m+2)\rangle \Big] \Big\}. \end{aligned} \tag{3.2.8}$$

We find the transcendental k equation by taking the expressions for $C_\pm$ (3.2.7) and substituting them in the boundary equation that links the 3 central sites of the chain (3.2.4). After simplifying, this yields

$$s_{\alpha-1} - s_{\alpha+3} + \left(\frac{1}{r} - r\right) s_{\alpha+1} = 0, \tag{3.2.9}$$

which has $\alpha - 1$ solutions for all values of r.

Odd Solutions

Odd solutions must have $C_\pm = -D_\pm$ and therefore $B_0 = 0$. When imposing these conditions, we obtain two nontrivial boundary equations

$$\begin{aligned} C_+(\pm t_1 e^{i\varphi} - E e^{-i\varphi}) + C_-(\pm t_1 e^{-i\varphi} - E e^{i\varphi}) = 0, \\ C_+(\pm t_2 e^{i\varphi} e^{-i2k} - E e^{-i\varphi}) e^{i(\alpha-1)k} + C_-(\pm t_2 e^{-i\varphi} e^{i2k} - E e^{i\varphi}) e^{-i(\alpha-1)k} = 0, \end{aligned} \tag{3.2.10}$$

which we simplify using relation (2.1.10) to get

$$\begin{aligned} C_+ e^{i\varphi} e^{-i2k} + C_- e^{-i\varphi} e^{i2k} = 0, \\ C_+ e^{i\varphi} e^{i(\alpha-1)k} + C_- e^{-i\varphi} e^{-i(\alpha-1)k} = 0. \end{aligned} \tag{3.2.11}$$

We use the first equation to solve for the ratio of C_+ and C_-, which yields

$$\begin{aligned} C_+ &= e^{-i\varphi} e^{i2k}, \\ C_- &= -e^{i\varphi} e^{-i2k}, \end{aligned} \tag{3.2.12}$$

up to a normalization constant. We use these expressions to rewrite the wave function (3.2.2), which results in the following final form of the solution

$$\begin{aligned} |\psi_{\text{odd}}\rangle = \sum_{m=0}^{\eta} \Big\{ &(t_1 s_{2m+2} + t_2 s_{2m}) \Big[|2m+1\rangle \; - |-(2m+1)\rangle \; \Big] \\ &+ E s_{2m+2} \Big[|2m+2\rangle \; - |-(2m+2)\rangle \; \Big] \Big\}. \end{aligned} \tag{3.2.13}$$

Substituting the expressions (3.2.12) in the second boundary equation of (3.2.11), and simplifying, we find the following transcendental equation

$$s_{\alpha+1} = 0, \tag{3.2.14}$$

which has $\alpha - 1$ solutions for all values of r.

3.2.2. Complex k Solutions

We now take the wavenumber to be complex with the form $k \to \frac{\pi}{2} + i\kappa$, for which the exponential factor now becomes $e^{i2mk} \to (-1)^m e^{-2m\kappa}$. Solutions with a complex wavenumber have energies in the band gap. The Schrödinger equation in matrix form is given by

$$\begin{pmatrix}
-E & t_2 & & & & & & & & & & \\
t_2 & -E & t_1 & & & & & & & & & \\
 & \ddots & \ddots & \ddots & & & & & & & & \\
 & & t_1 & -E & t_2 & & & & & & & \\
 & & & t_2 & -E & t_1 & & & & & & \\
 & & & & t_1 & -E & t_2 & & & & & \\
 & & & & & t_2 & -E & t_2 & & & & \\
 & & & & & & t_2 & -E & t_1 & & & \\
 & & & & & & & t_1 & -E & t_2 & & \\
 & & & & & & & & \ddots & \ddots & \ddots & \\
 & & & & & & & & & t_1 & -E & t_2 \\
 & & & & & & & & & & t_2 & -E
\end{pmatrix}
\begin{pmatrix}
A_L\, e^{-(\alpha-1)\kappa} \\
-\begin{pmatrix} B_L \\ A_L \end{pmatrix} e^{-(\alpha-3)\kappa} \\
\vdots \\
-\begin{pmatrix} B_L \\ A_L \end{pmatrix} e^{-2\kappa} \\
\begin{pmatrix} B_L \\ A_L \end{pmatrix} \\
B_0 \\
\begin{pmatrix} A_R \\ B_R \end{pmatrix} \\
-\begin{pmatrix} A_R \\ B_R \end{pmatrix} e^{-2\kappa} \\
\vdots \\
-\begin{pmatrix} A_R \\ B_R \end{pmatrix} e^{-(\alpha-3)\kappa} \\
A_R\, e^{-(\alpha-1)\kappa}
\end{pmatrix} = 0, \tag{3.2.15}$$

where the last unit cell has factor $(-1)^m e^{-2m\kappa} \to (-1)^\eta e^{-2\eta\kappa} = e^{-2(\frac{(\alpha-1)}{2})\kappa} = e^{-(\alpha-1)\kappa}$ since η is an even number. Similarly the second to last unit cell has index $m \to \eta - 1$, which yields the exponential factor $-e^{-(\alpha-3)\kappa}$. We have the same bulk equations as for the infinite chain with the central soliton (2.2.2) and therefore, the same dispersion relation (2.2.3). As it has been discussed in previous sections, there are two possible definitions for φ, which yield the same solution; we use the definition used in the Φ_{12} configuration (3.1.16) and therefore the values of A and B given by (3.1.17). The general form of the wave function only differs from (3.1.18) by the upper bound on the sum, such that the wave function takes the following

form

$$
\begin{aligned}
|\psi_{R\pm}\rangle = \sum_{m=0}^{\eta} (-1)^m \Big\{ &- \left(C_+ e^{\varphi} e^{-2m\kappa} + C_- e^{-\varphi} e^{2m\kappa} \right) |2m+1\rangle \\
&\pm \left(C_+ e^{-\varphi} e^{-2m\kappa} + C_- e^{\varphi} e^{2m\kappa} \right) |2m+2\rangle \Big\}, \\
|\psi_{L\pm}\rangle = \sum_{m=0}^{\eta} (-1)^m \Big\{ &- \left(D_+ e^{\varphi} e^{-2m\kappa} + D_- e^{-\varphi} e^{2m\kappa} \right) | -(2m+1)\rangle \\
&\pm \left(D_+ e^{-\varphi} e^{-2m\kappa} + D_- e^{\varphi} e^{2m\kappa} \right) | -(2m+2)\rangle \Big\},
\end{aligned}
\tag{3.2.16}
$$

where the values of constants $C_\pm$ and $D_\pm$ will differ depending on the parity of the solutions. In addition to the three boundary equations from the bulk (2.1.6), we have two conditions that account for the left and right edges of the chain

$$
\begin{aligned}
&E(D_+ e^{\varphi} e^{-(\alpha-1)\kappa} + D_- e^{-\varphi} e^{(\alpha-1)\kappa}) \mp t_2 (D_+ e^{-\varphi} e^{-(\alpha-3)\kappa} + D_- e^{\varphi} e^{(\alpha-3)\kappa}) = 0, \\
&\mp t_2 (C_+ e^{-\varphi} e^{-(\alpha-3)\kappa} + C_- e^{\varphi} e^{(\alpha-3)\kappa}) + E(C_+ e^{\varphi} e^{-(\alpha-1)\kappa} + C_- e^{-\varphi} e^{(\alpha-1)\kappa}) = 0.
\end{aligned}
\tag{3.2.17}
$$

Even Solutions

For even solutions, $C_\pm = D_\pm$ and we set $B_0 = 1$. These conditions yield three nontrivial boundary equations given by

$$
\begin{aligned}
-2t_2 (C_+ e^{\varphi} + C_- e^{-\varphi}) &= E, \\
C_+ (\pm t_1 e^{-\varphi} + E e^{\varphi}) + C_- (\pm t_1 e^{\varphi} + E e^{-\varphi}) &= -t_2, \\
C_+ (E e^{\varphi} \mp t_2 e^{-\varphi} e^{2\kappa}) e^{-(\alpha-1)\kappa} + C_- (E e^{-\varphi} \mp t_2 e^{\varphi} e^{-2\kappa}) e^{(\alpha-1)\kappa} &= 0,
\end{aligned}
\tag{3.2.18}
$$

of which we simplify the second and third equations using (3.1.22) to get

$$
\begin{aligned}
C_+ e^{-\varphi} e^{2\kappa} + C_- e^{\varphi} e^{-2\kappa} &= \mp 1, \\
C_+ e^{-\varphi} e^{-(\alpha-1)\kappa} + C_- e^{\varphi} e^{(\alpha-1)\kappa} &= 0.
\end{aligned}
\tag{3.2.19}
$$

We express these in matrix form as

$$
\begin{pmatrix} e^{-\varphi} e^{-(\alpha-1)\kappa} & e^{\varphi} e^{(\alpha-1)\kappa} \\ e^{-\varphi} e^{2\kappa} & e^{\varphi} e^{-2\kappa} \end{pmatrix} \begin{pmatrix} C_+ \\ C_- \end{pmatrix} = \begin{pmatrix} 0 \\ \mp 1 \end{pmatrix}. \tag{3.2.20}
$$

The matrix has determinant $-2sh_{\alpha+1}$. We invert this matrix and solve for $C_\pm$, which yields

$$
\begin{pmatrix} C_+ \\ C_- \end{pmatrix} = \frac{\mp 1}{2sh_{\alpha+1}} \begin{pmatrix} e^{\varphi} e^{(\alpha-1)\kappa} \\ -e^{-\varphi} e^{-(\alpha-1)\kappa} \end{pmatrix}. \tag{3.2.21}
$$

We substitute these expressions for $C_\pm$ in (3.2.16) to obtain the final form of the wave function, which is given by

$$|\psi_{\text{even}}\rangle = E|0\rangle + \sum_{m=0}^{\eta} \frac{(-1)^m}{sh_{\alpha+1}} \Big\{ (t_2 sh_{\alpha+1-2m} - t_1 sh_{\alpha-1-2m}) \Big[|2m+1\rangle + |-(2m+1)\rangle \Big] - E sh_{\alpha-1-2m} \Big[|2m+2\rangle + |-(2m+2)\rangle \Big] \Big\}. \tag{3.2.22}$$

We now find the transcendental κ equation. We use the expressions for $C_\pm$ (3.2.21) in the first boundary equation of (3.2.18) to find

$$sh_{\alpha+3} - sh_{\alpha-1} + \Big(\frac{1}{r} - r\Big) sh_{\alpha+1} = 0, \tag{3.2.23}$$

which has no solutions for $r < 1$ and two solutions for $r > 1$.

Odd Solutions

For antisymmetric solutions, we have $C_\pm = -D_\pm$ which leads to the constraint $B_0 = 0$. These two conditions give us the two following nontrivial boundary equations

$$\begin{aligned} C_+(\pm t_1 e^{-\varphi} + E e^{\varphi}) + C_-(\pm t_1 e^{\varphi} + E e^{-\varphi}) &= 0, \\ C_+(E e^{\varphi} \mp t_2 e^{-\varphi} e^{2\kappa}) e^{-(\alpha-1)\kappa} + C_-(E e^{-\varphi} \mp t_2 e^{\varphi} e^{-2\kappa}) e^{(\alpha-1)\kappa} &= 0, \end{aligned} \tag{3.2.24}$$

which are simplified using relation (3.1.22) to get the form

$$\begin{aligned} C_+ e^{-\varphi} e^{2\kappa} + C_- e^{\varphi} e^{-2\kappa} &= 0, \\ C_+ e^{-\varphi} e^{-(\alpha-1)\kappa} + C_- e^{\varphi} e^{(\alpha-1)\kappa} &= 0. \end{aligned} \tag{3.2.25}$$

We use the second equation to solve for the ratio of $C_\pm$ and get

$$\begin{aligned} C_+ &= -e^{\varphi} e^{(\alpha-1)\kappa}, \\ C_- &= e^{-\varphi} e^{-(\alpha-1)\kappa}, \end{aligned} \tag{3.2.26}$$

up to a normalization constant. These are substituted in (3.2.16) to find the final form of the wave function, which is given by

$$|\psi_{\text{odd}}\rangle = \sum_{m=0}^{\eta} (-1)^m \Big\{ (t_1 sh_{\alpha-1-2m} - t_2 sh_{\alpha+1-2m}) \Big[|2m+1\rangle - |-(2m+1)\rangle \Big] + sh_{\alpha-1-2m} \Big[|2m+2\rangle - |-(2m+2)\rangle \Big] \Big\}. \tag{3.2.27}$$

We substitute the expressions for $C_{\pm}$ (3.2.26) in the first boundary equation in (3.2.25) to get the transcendental κ equation

$$sh_{\alpha+1} = 0, \tag{3.2.28}$$

which has no solutions for all values of r. However, as discussed in section (2.2), this does not include the $E = 0$ solution. Since the dispersion relation is the same as for the Φ_{12} configuration, the κ solution for the zero-mode is also the same, given by (2.2.21). We will discuss the odd parity of the zero-energy solution in section (3.2.4).To find the form of the wave function of the zero-mode, we impose $E = 0$ in (3.2.27) and get

$$|\psi_{\mathrm{E}=0}\rangle = \sum_{m=0}^{\eta} (-1)^m \Big\{ (t_1 sh_{\alpha-1-2m} - t_2 sh_{\alpha+1-2m}) \Big[|2m+1\rangle \; - | - (2m+1)\rangle \; \Big] \Big\}. \tag{3.2.29}$$

3.2.3. Imaginary k Solutions

Considering solutions with an imaginary wavenumber $k \to i\kappa$ results in the exponential form $e^{i2mk} \to e^{-2m\kappa}$. Solutions with an imaginary wavenumber have energies outside the bands. The Schrödinger equation in matrix form is given by

$$\begin{pmatrix}
-E & t_2 & & & & & & & & & & \\
t_2 & -E & t_1 & & & & & & & & & \\
 & \ddots & \ddots & \ddots & & & & & & & & \\
 & & t_1 & -E & t_2 & & & & & & & \\
 & & & t_2 & -E & t_1 & & & & & & \\
 & & & & t_1 & -E & t_2 & & & & & \\
 & & & & & t_2 & -E & t_2 & & & & \\
 & & & & & & t_2 & -E & t_1 & & & \\
 & & & & & & & t_1 & -E & t_2 & & \\
 & & & & & & & & t_2 & -E & t_1 & \\
 & & & & & & & & & t_1 & -E & t_2 \\
 & & & & & & & & & & t_2 & -E
\end{pmatrix}
\begin{pmatrix}
A_L\, e^{-(\alpha-1)\kappa} \\
\begin{pmatrix} B_L \\ A_L \end{pmatrix} e^{-(\alpha-3)\kappa} \\
\vdots \\
\begin{pmatrix} B_L \\ A_L \end{pmatrix} e^{-2\kappa} \\
\begin{pmatrix} B_L \\ A_L \end{pmatrix} \\
B_0 \\
\begin{pmatrix} A_R \\ B_R \end{pmatrix} \\
\begin{pmatrix} A_R \\ B_R \end{pmatrix} e^{-2\kappa} \\
\vdots \\
\begin{pmatrix} A_R \\ B_R \end{pmatrix} e^{-(\alpha-3)\kappa} \\
A_R\, e^{-(\alpha-1)\kappa}
\end{pmatrix} = 0. \tag{3.2.30}$$

The bulk equations are the same as for the infinite chain with the soliton (2.3.2), hence the dispersion relation is also identical. We also use the same definition for φ (2.3.4). All of this makes for the same general form of the wave function in terms of constants $C_\pm$ and $D_\pm$ except for the upper bound on the sum such that the wave function is now given by

$$
\begin{aligned}
|\psi_{R\pm}\rangle = \sum_{m=0}^{\eta} \Big\{ \Big(C_+ e^{\varphi} e^{-2m\kappa} + C_- e^{-\varphi} e^{2m\kappa} \Big) |2m+1\rangle \\
\pm \Big(C_+ e^{-\varphi} e^{-2m\kappa} + C_- e^{\varphi} e^{2m\kappa} \Big) |2m+2\rangle \Big\}, \\
|\psi_{L\pm}\rangle = \sum_{m=0}^{\eta} \Big\{ \Big(D_+ e^{\varphi} e^{-2m\kappa} + D_- e^{-\varphi} e^{2m\kappa} \Big) |-(2m+1)\rangle \\
\pm \Big(D_+ e^{-\varphi} e^{-2m\kappa} + D_- e^{\varphi} e^{2m\kappa} \Big) |-(2m+2)\rangle \Big\}.
\end{aligned}
\tag{3.2.31}
$$

In addition to the three central boundary equations (2.3.9), we have two conditions which account for the left and right edges of the chain, which are

$$
\begin{aligned}
-E(D_+ e^{\varphi} e^{-(\alpha-1)\kappa} + D_- e^{-\varphi} e^{(\alpha-1)\kappa}) \pm t_2 (D_+ e^{-\varphi} e^{-(\alpha-3)\kappa} + D_- e^{\varphi} e^{(\alpha-3)\kappa}) = 0, \\
\pm t_2 (C_+ e^{-\varphi} e^{-(\alpha-3)\kappa} + C_- e^{\varphi} e^{(\alpha-3)\kappa}) - E(C_+ e^{\varphi} e^{-(\alpha-1)\kappa} + C_- e^{-\varphi} e^{(\alpha-1)\kappa}) = 0.
\end{aligned}
\tag{3.2.32}
$$

Even Solutions

As we know well by now, even solutions have $C_\pm = D_\pm$ and we make the normalization choice $B_0 = 1$. With these constraints, we have three nontrivial boundary equations, given by

$$
\begin{aligned}
2t_2 (C_+ e^{\varphi} + C_- e^{-\varphi}) = E, \\
C_+(-Ee^{\varphi} \pm t_1 e^{-\varphi}) + C_-(-Ee^{-\varphi} \pm t_1 e^{\varphi}) = -t_2, \\
C_+(-Ee^{\varphi} \pm t_2 e^{-\varphi} e^{2\kappa}) e^{-(\alpha-1)\kappa} + C_-(-Ee^{-\varphi} \pm t_2 e^{\varphi} e^{-2\kappa}) e^{(\alpha-1)\kappa} = 0,
\end{aligned}
\tag{3.2.33}
$$

of which we simplify the last two equations by using (2.3.4) to get

$$
\begin{aligned}
C_+ e^{-\varphi} e^{2\kappa} + C_- e^{\varphi} e^{-2\kappa} = \pm 1, \\
C_+ e^{-\varphi} e^{-(\alpha-1)\kappa} + C_- e^{\varphi} e^{(\alpha-1)\kappa} = 0.
\end{aligned}
\tag{3.2.34}
$$

We take these two equations and express them in matrix form and find the determinant to be $-2sh_{\alpha+1}$. We invert this matrix and solve for $C_\pm$, which yields

$$
\begin{pmatrix} C_+ \\ C_- \end{pmatrix} = \frac{\mp 1}{2sh_{\alpha+1}} \begin{pmatrix} -e^{\varphi} e^{(\alpha-1)\kappa} \\ e^{-\varphi} e^{-(\alpha-1)\kappa} \end{pmatrix}. \tag{3.2.35}
$$

We substitute these expressions in the wave function (3.2.31) to find its final form

$$|\psi_{\text{even}}\rangle = E|0\rangle + \sum_{m=0}^{\eta} \frac{1}{sh_{\alpha+1}} \Big\{ (t_1 sh_{\alpha-1-2m} + t_2 sh_{\alpha+1-2m}) \Big[|2m+1\rangle + |-(2m+1)\rangle \Big] + E sh_{\alpha-1-2m} \Big[|2m+2\rangle + |-(2m+2)\rangle \Big] \Big\}. \tag{3.2.36}$$

The final step in our computation is to find the transcendental κ equation. We use the expressions for $C_\pm$ (3.2.35) in the first boundary equation in (3.2.33) and simplify to find

$$sh_{\alpha-1} - sh_{\alpha+3} + \Big(\frac{1}{r} - r\Big) sh_{\alpha+1} = 0, \tag{3.2.37}$$

which has 2 solutions for $r < 1$ and no solutions for $r > 1$.

Odd Solutions

Odd solutions have $C_\pm = -D_\pm$ which leads to the condition $B_0 = 0$. From these two constraints, we obtain the two following nontrivial boundary equations

$$\begin{aligned} C_+(-Ee^{\varphi} \pm t_1 e^{-\varphi}) + C_-(-Ee^{-\varphi} \pm t_1 e^{\varphi}) = 0, \\ C_+(-Ee^{\varphi} \pm t_2 e^{-\varphi} e^{2\kappa}) e^{-(\alpha-1)\kappa} + C_-(-Ee^{-\varphi} \pm t_2 e^{\varphi} e^{-2\kappa}) e^{(\alpha-1)\kappa} = 0, \end{aligned} \tag{3.2.38}$$

which we can simplify by using relation (2.3.4) to get the form

$$\begin{aligned} C_+ e^{-\varphi} e^{2\kappa} + C_- e^{\varphi} e^{-2\kappa} = 0, \\ C_+ e^{-\varphi} e^{-(\alpha-1)\kappa} + C_- e^{\varphi} e^{(\alpha-1)\kappa} = 0. \end{aligned} \tag{3.2.39}$$

We use the first equation to solve for the ratio of $C_\pm$ which enables us to write

$$\begin{aligned} C_+ = -e^{\varphi} e^{-2\kappa}, \\ C_- = e^{-\varphi} e^{2\kappa}, \end{aligned} \tag{3.2.40}$$

up to a normalization constant. We substitute these expressions in the first boundary equation in (3.2.39) to find the transcendental equation

$$sh_{\alpha+1} = 0, \tag{3.2.41}$$

which has no solutions for all values of r.

3.2.4. Discussion of States and the Energy Spectrum

To the best of our knowledge, the Φ_{22} configuration's localized states have not been reported in the literature. We start by summarizing the number of solutions obtained numerically from all the transcendental equations found in the previous sections.

			$r<1$	$r>1$
Even Solutions	Real k	$s_{\alpha-1}+s_{\alpha+3}+\left(\frac{1}{r}-r\right)s_{\alpha+1}=0$	$\alpha-1$	$\alpha-1$
	Complex k	$sh_{\alpha+3}-sh_{\alpha-1}+\left(\frac{1}{r}-r\right)sh_{\alpha+1}=0$	0	2
	Imaginary k	$sh_{\alpha-1}-sh_{\alpha+3}+\left(\frac{1}{r}-r\right)sh_{\alpha+1}=0$	2	0
Odd Solutions	Real k	$s_{\alpha+1}=0$	$\alpha-1$	$\alpha-1$
	Complex k	$sh_{\alpha+1}=0$	0	0
		$k=\frac{1}{2}\arccos\left(-\frac{1}{2}\left(r+\frac{1}{r}\right)\right)$	1	1
	Imaginary k	$sh_{\alpha+1}=0$	0	0
Total			$2\alpha+1$	$2\alpha+1$

Tableau 3.2. Summary of the number of solutions for the wavenumber k for the ϕ_{22} configuration

Real k

The solutions with real wavenumber k correspond to bulk states as shown in Fig. 3.9. There are $(2\alpha-2=N-3)$ of these states for all values of r.

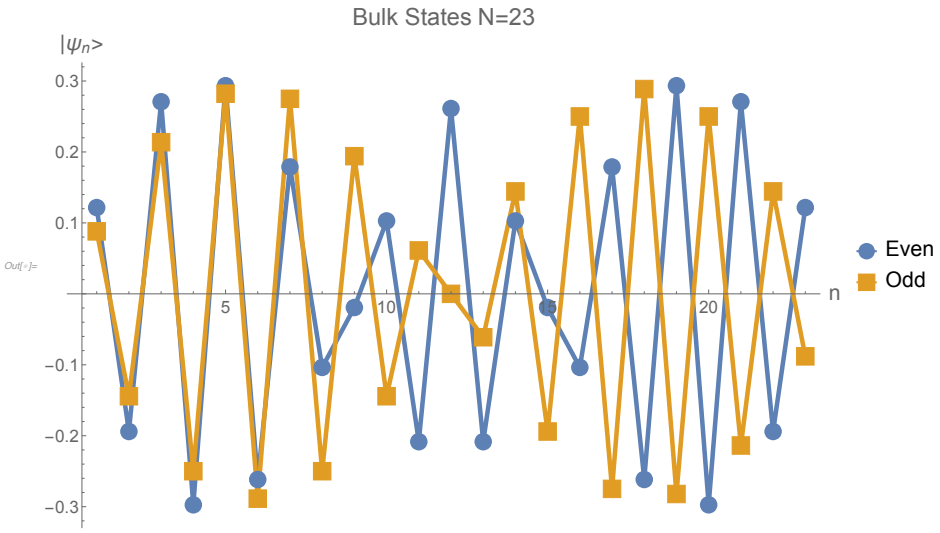

Fig. 3.9. In the Φ_{22} configuration, a pair of bulk states for a system of length $N = 23$. In blue, a symmetric state around the soliton and in orange, an antisymmetric state.

The Energy Spectrum

As we've done for the Φ_{12} configuration, let's discuss the energy spectrum before moving on to the more intriguing states. As was done for the regular SSH chain, we find the k solutions using the various transcendental equations, feed them to the corresponding dispersion relation and take the positive and negative root of the energy. Fig. 3.10 shows the energy spectrum of the Φ_{22} configuration as a function of parameter σ where we have defined $\sigma = t_1$ and $1-\sigma = t_2$ such that $t_1 + t_2 = 1$. We show the separation of the regimes where $r < 1$ and $r > 1$ by a dotted line. For the regime where $r < 1$, we have $(2\alpha - 2 = N - 3)$ bulk energy solutions. There is one solution with exactly $E = 0$ corresponding to the odd solution with complex k. Additionally, we have two high-energy solutions which are associated with the imaginary k even solutions.For the regime where $r > 1$, the high-energy solutions transition to bulk states and two bulk energy solutions transition to near-zero-energy solutions (edge states). This leaves us with $(2\alpha - 2 = N - 3)$ bulk solutions. The zero-energy mode stays and is still a complex k even solution. Let's take a look at the limiting cases $(t_1 = 0, t_2 = 1)$ or $r = 0$ and $(t_1 = 1, t_2 = 0)$ or $r \to \infty$ to intuitively understand the energy spectrum shown in Fig. 3.10. When $r = 0$, the chain breaks into a central trimer and a series of dimers as

shown in Fig. 3.11(a). The Hamiltonian (3.2.30) now takes the form

$$H_{\Phi_{22}} \to \bigoplus_{i=1}^{\frac{\alpha-1}{2}} H_{dimer,i} \bigoplus H_{trimer} \bigoplus_{i=1}^{\frac{\alpha-1}{2}} H_{dimer,i} \tag{3.2.42}$$

where the dimer's Hamiltonian is given by (1.1.28) and the trimer's, by (2.4.2).

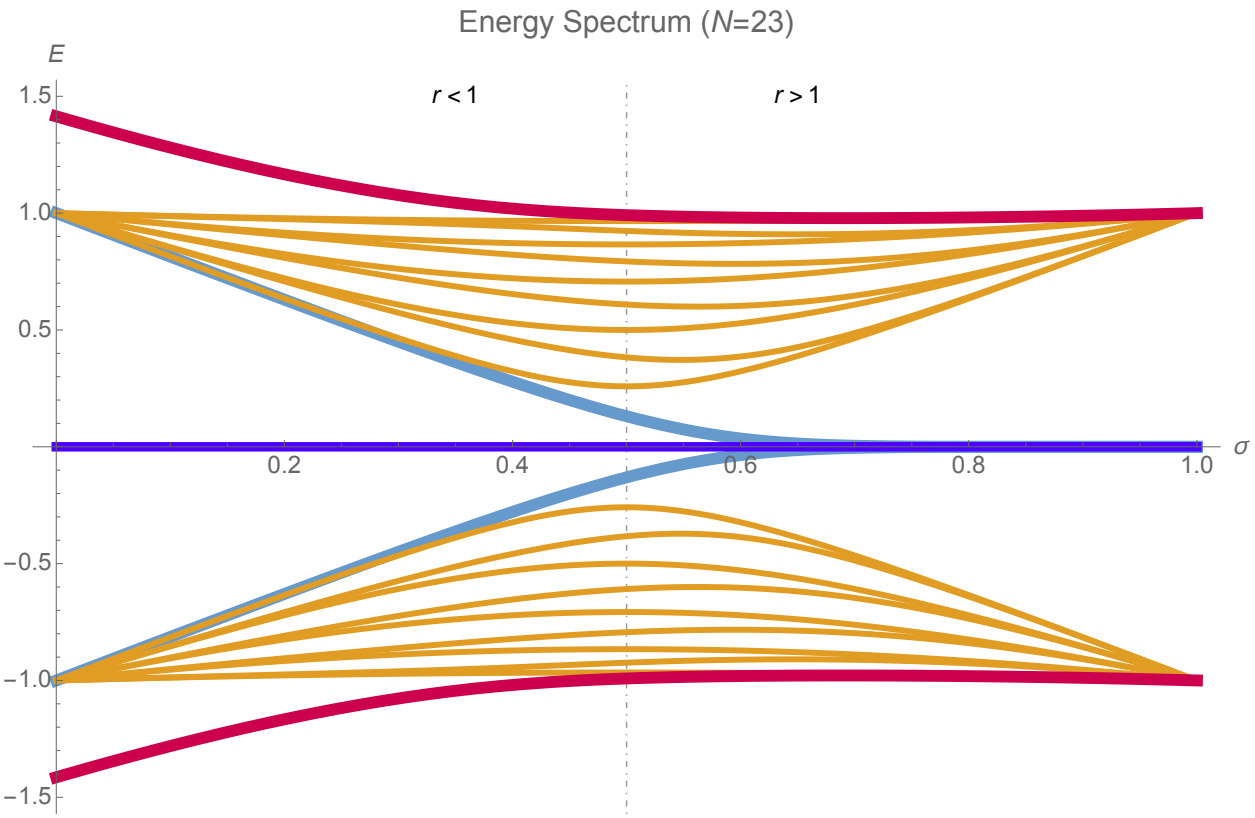

Fig. 3.10. Energy spectrum as a function of topological parameter r for a finite SSH chain with a central soliton in the Φ_{22} configuration. Highlighted in red are the high-energy solutions (imaginary k),in purple is the zero-energy midgap state (complex k), in blue are the edge states (complex k) and in orange are the bulk state (real k).

The trimer structure has three energy solutions: one zero-energy and two high-energy solutions, $\pm\sqrt{2}$. The dimers each have eigenenergies ± 1. Let the number of dimers on each side of the central trimer be $D = \frac{\alpha-1}{2}$. There are therefore $4D$ energy solutions that come from the dimers. If we add the solutions from the trimer, we have a total of $(4D+3 = 2\alpha+1 = N)$ energy solutions for the total chain, as expected. By looking at the $r = 0$ ($\sigma = 0$) end of the energy spectrum in Fig. 3.10, we see the aforementioned energy solutions. Now, we consider the limiting case $r \to \infty$; the chain has a central monomer, a series of dimers on each chain

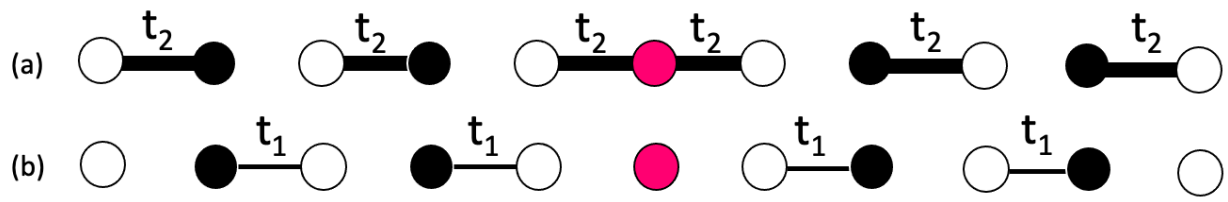

Fig. 3.11. SSH chain in the Φ_{22} configuration with $N = 11$ where we have imposed $(t_1 = 0, t_2 = 1)$ in (a): the system breaks up into a central trimer and a series of dimers (D). In (b), we have imposed $(t_1 = 1, t_2 = 0)$: the system breaks up into a central monomer, a series of dimers (D) and a monomer at each edge.

segment and a monomer at each edge as illustrated in Fig. 3.11(b). The Hamiltonian (3.2.30) is now given by

$$H_{\Phi_{22}} \to H_{monomer} \bigoplus_{i=1}^{\frac{\alpha-1}{2}} H_{dimer,i} \bigoplus H_{monomer} \bigoplus_{i=1}^{\frac{\alpha-1}{2}} H_{dimer,i} \bigoplus H_{monomer} \tag{3.2.43}$$

where the monomer's and dimer's Hamiltonians are given by (1.1.28). Once again, the three monomers each have energy $E = 0$ and the dimers can each have, ± 1. On each side of the central site, there are $D = \frac{\alpha-1}{2}$ dimers. We therefore have $(4D + 3 = N)$ solutions, as we should find. This is indeed the behaviour when $r \to \infty$ $(\sigma = 1)$; there is precisely one zero-energy state that remains and two states that break away from the bulk to approach zero as $r \to \infty$ $(\sigma \to 1)$. All remaining energies must be bulk states as we observe in Fig. 3.10 at $\sigma = 1$.

Complex k

We start by discussing the zero-energy midgap state highlighted in purple in Fig. 3.10 and shown in Fig. 3.12.

The midgap state exists for all values of r, similarly to the odd SSH chain, but takes different forms depending on which topological regime we're in, as depicted in Fig. 3.12. For $r > 1$, the wave function is localized at both edges of the chain while it is localized at the soliton for $r < 1$. Both states are antisymmetric; the state has the same parity for all values of r. We understand this behaviour by taking a look at the limiting cases where we let $r = 0$ and $r \to \infty$. We start with the case where $r = 0$; as shown in Fig. 3.11(a), the chain

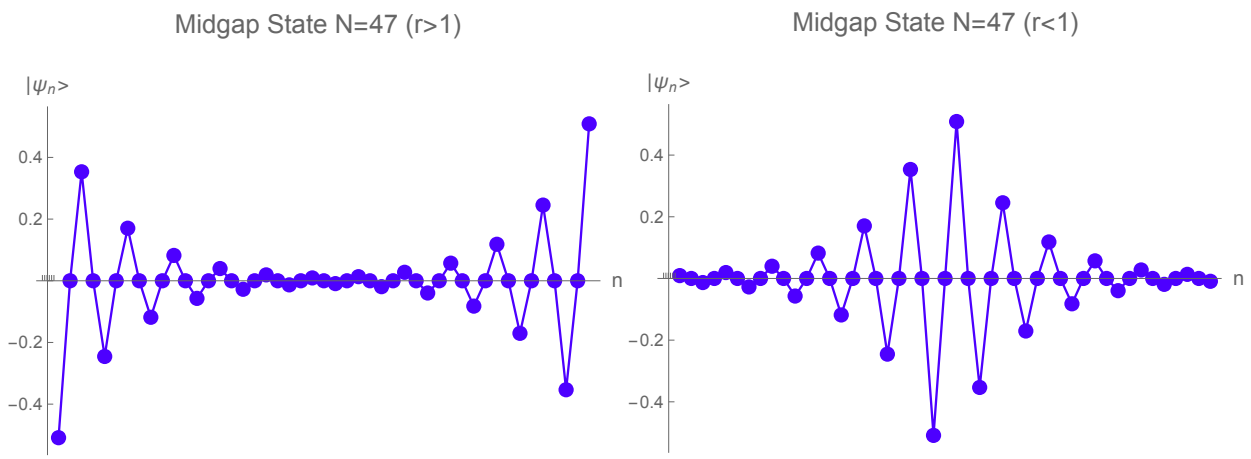

Fig. 3.12. In the Φ_{22} configuration, zero-energy midgap states for $r > 1$ ($r < 1$) on the left (right). Both states are antisymmetric about the central site.

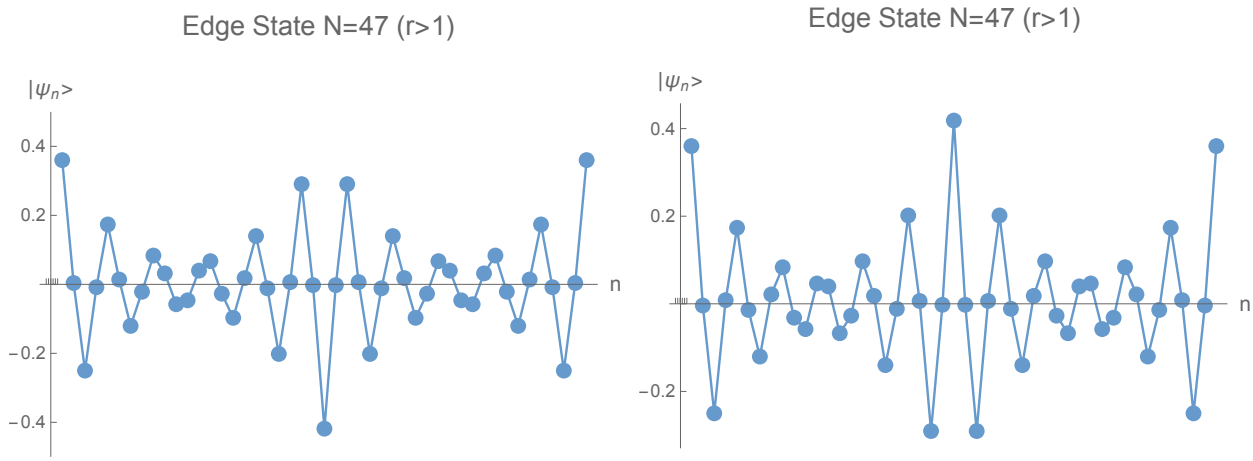

Fig. 3.13. In the Φ_{22} configuration, near-zero-energy edge states for $N = 47$. These edge states correspond to energies $E/t_2 = \pm 0.009$.

is broken up into a series of dimers on each side of a central trimer. This trimer is the only structure in the chain that supports a zero-energy mode. Therefore, when $r < 1$, the zero-energy state must be localized at the central defect and will exponentially die off on both sides as there will be hybridization across the rest of the chain. Moreover, a trimer's zero-energy eigenstate is antisymmetric; the state must then be antisymmetric when $r < 1$ and this parity carries through when $r > 1$, which is what we observe in Fig. 3.12. When $r \to \infty$, the zero-energy state is three times degenerate as the chain has three monomers that

each have one zero-energy solution. Thus, there are three corresponding states of the chain. The monomers' eigenstates are all symmetric. As we have just mentioned, the midgap state stays antisymmetric; we can only build an antisymmetric state by using the edges' monomers' states. We get a state that is localized at both edges; one side being negative while the other is positive. As we let $r < 1$, we expect this behaviour, but with some tunneling along the chain, which is what we observe in Fig. 3.12. There are two symmetric states left which are a combination of all three monomers' eigenstates. This pair of solutions is localized at both edges as well as at the soliton; they're edge states. As we allow $r < 1$, we expect this behaviour as well as some hybridization along the chain; this is what is depicted in Fig. 3.13. As expected, the edge states only exist for $r < 1$ as they delocalize into the bulk for $r > 1$.

Imaginary k

Lastly, we have high-energy states that are identical to the Φ_{12} configuration's states as shown in Fig. 3.14. This is to be expected as, once again, the high-energy modes are only supported by the central trimer which is solely present in the $r < 1$ regime.

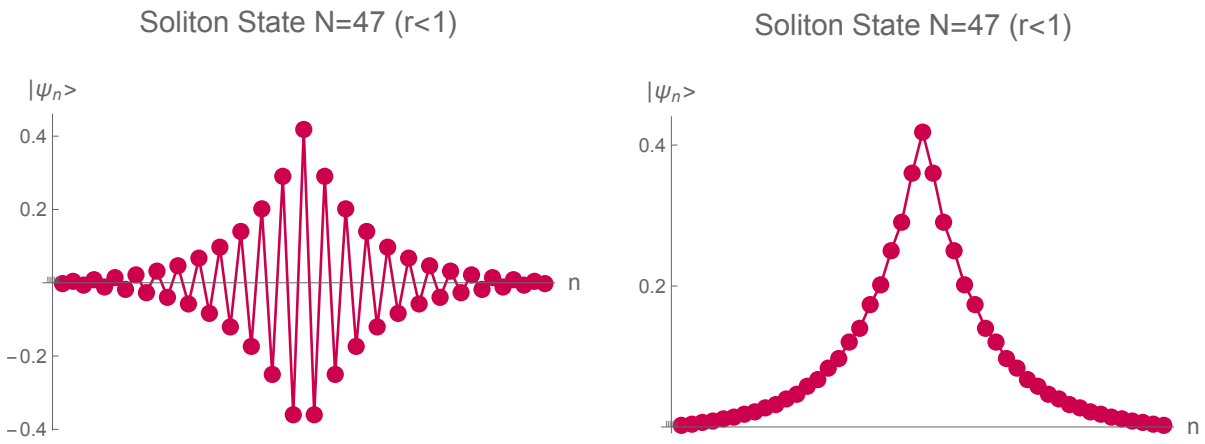

Fig. 3.14. In the Φ_{22} configuration, high-energy modes localized at the interface, which only exist in the regime $r > 1$. This pair of antisymmetric states about the soliton has energies $E/t_2 = \pm 1.722$. The state with positive (negative) energy is on the right (left).

These states delocalize into the bulk for $r > 1$ as shown in Fig. 3.10.

Conclusion

Topological insulators and related materials are at the forefront of today's condensed matter physics and quantum information research. Topological modes arising from defects are promising platforms for quantum computing architectures and quantum devices [29, 30, 31, 32]. Additionally, protected topological states have encouraged a boost in the development of photonics technology [33, 34, 35, 36, 37, 38]. In particular, solitonic modes are observed to be robust excitations in the face of deformations and disorder [39].

We began this work by providing a review of the SSH model through the calculation and discussion of the chain's energy solutions and wave functions. We showed that the existence of solutions with a complex wavenumber, which are localized modes called edge states, is necessary in order to have a complete set of solutions. We intuitively understood the model's solutions by using limiting cases of the topological parameter r that break the chain's edges into dimers or monomers. In Chapter 2, we added a soliton to an infinite SSH chain and derived all solutions to the Schrödinger equation, which included solutions with a real, complex, and imaginary wavenumber. These computations provided us with the tools to tackle the finite SSH model with a central soliton. We give a complete analysis of both possible configurations of the chain Φ_{12} and Φ_{22}. In the Φ_{12} configuration, there are $N-5$ ($r<1$) to $N-1$ ($r>1$) bulk states. For $r<1$, we have found one zero-energy state localized at the chain's boundaries, two edge states localized both at the boundaries and at the interface as well as two high-energy solitonic modes. For $r>1$, there is a zero-energy state localized at the soliton. In the Φ_{22} configuration, there are $N-3$ bulk states for all values of r. For $r<1$, there exists one zero-energy state localized at the domain wall and there are two high-energy solitonic modes. In the $r>1$ regime, there is still a zero-energy mode, but it is localized at the edges and there are two edge states localized at both the soliton and at the chain's physical edges. It is interesting to note that unlike the SSH model, the near-zero-energy

edge states are not only localized at the edges, but also at the soliton. We were able to explain this behaviour by looking at the chain in the limiting cases when the topological parameter r is zero or infinite; the central soliton either becomes a monomer or a trimer and can support zero-energy modes. The high-energy modes localized at the soliton were understood using the same reasoning. Our results for the Φ_{12} configuration were found to be in good agreement with a SSH-analogous spin chain model [8] while the Φ_{22} configuration doesn't seem to have been reported in the literature. This completes the summary of the work that was presented.

Let us conclude with the logical next step beyond this work. In [20], it was shown that a qubit can serve as detector (probe) of topological edge states by studying its dynamics. In the work we presented, the finite SSH chain with a soliton has topological states located at the soliton. It would be interesting to extend the work in [20] and study the dynamics of a qubit attached to the model we have analysed as well as a system modeling an environment. The goal, of course, would not to simply probe the known characteristics of the localized modes in these solvable models. Rather, the fact that the probe was shown in [20] to be sensitive to the existence of localized states suggests its use in more complicated models to find and characterize any such modes that may exist.

References

[1] K. v. Klitzing, G. Dorda, and M. Pepper. "New Method for High-Accuracy Determination of the Fine-Structure Constant Based on Quantized Hall Resistance". In: *Physical Review Letters* 45.6 (Aug. 1980). Publisher: American Physical Society, pp. 494–497. DOI: 10.1103/PhysRevLett.45.494. URL: https://link.aps.org/doi/10.1103/PhysRevLett.45.494 (visited on 11/23/2022).

[2] Jing Wang and Shou-Cheng Zhang. "Topological states of condensed matter". en. In: *Nature Materials* 16.11 (Nov. 2017). Number: 11 Publisher: Nature Publishing Group, pp. 1062–1067. ISSN: 1476-4660. DOI: 10.1038/nmat5012. URL: https://www.nature.com/articles/nmat5012 (visited on 11/23/2022).

[3] Xin-Tao He et al. "A silicon-on-insulator slab for topological valley transport". en. In: *Nature Communications* 10.1 (Feb. 2019). Number: 1 Publisher: Nature Publishing Group, p. 872. ISSN: 2041-1723. DOI: 10.1038/s41467-019-08881-z. URL: https://www.nature.com/articles/s41467-019-08881-z (visited on 11/22/2022).

[4] Meng Xiao et al. "Geometric phase and band inversion in periodic acoustic systems". en. In: *Nature Physics* 11.3 (Mar. 2015). Number: 3 Publisher: Nature Publishing Group, pp. 240–244. ISSN: 1745-2481. DOI: 10.1038/nphys3228. URL: https://www.nature.com/articles/nphys3228 (visited on 11/22/2022).

[5] Yu-Gui Peng et al. "Experimental demonstration of anomalous Floquet topological insulator for sound". en. In: *Nature Communications* 7.1 (Nov. 2016). Number: 1 Publisher: Nature Publishing Group, p. 13368. ISSN: 2041-1723. DOI: 10.1038/ncomms13368. URL: https://www.nature.com/articles/ncomms13368 (visited on 11/22/2022).

[6] Yoshinori Tokura, Kenji Yasuda, and Atsushi Tsukazaki. "Magnetic topological insulators". en. In: *Nature Reviews Physics* 1.2 (Feb. 2019). Number: 2 Publisher: Nature Publishing Group, pp. 126–143. ISSN: 2522-5820. DOI: 10.1038/s42254-018-0011-

5. URL: https://www.nature.com/articles/s42254-018-0011-5 (visited on 11/22/2022).

[7] W. P. Su, J. R. Schrieffer, and A. J. Heeger. "Solitons in Polyacetylene". In: *Phys. Rev. Lett.* 42 (25 June 1979), pp. 1698–1701. DOI: 10.1103/PhysRevLett.42.1698. URL: https://link.aps.org/doi/10.1103/PhysRevLett.42.1698.

[8] Marta P. Estarellas, Irene D'Amico, and Timothy P. Spiller. "Topologically protected localised states in spin chains". In: *Scientific Reports* 7.1 (Mar. 2017). arXiv:1609.07516 [quant-ph], p. 42904. ISSN: 2045-2322. DOI: 10.1038/srep42904. URL: http://arxiv.org/abs/1609.07516 (visited on 11/22/2022).

[9] Marcos Atala et al. "Direct Measurement of the Zak phase in Topological Bloch Bands". In: *Nature Physics* 9.12 (Dec. 2013). arXiv:1212.0572 [cond-mat, physics:quant-ph], pp. 795–800. ISSN: 1745-2473, 1745-2481. DOI: 10.1038/nphys2790. URL: http://arxiv.org/abs/1212.0572 (visited on 11/22/2022).

[10] Martin Leder et al. "Real-space imaging of a topologically protected edge state with ultracold atoms in an amplitude-chirped optical lattice". en. In: *Nature Communications* 7.1 (Oct. 2016). Number: 1 Publisher: Nature Publishing Group, p. 13112. ISSN: 2041-1723. DOI: 10.1038/ncomms13112. URL: https://www.nature.com/articles/ncomms13112 (visited on 11/22/2022).

[11] M. Lohse et al. "A Thouless quantum pump with ultracold bosonic atoms in an optical superlattice". en. In: *Nature Physics* 12.4 (Apr. 2016). Number: 4 Publisher: Nature Publishing Group, pp. 350–354. ISSN: 1745-2481. DOI: 10.1038/nphys3584. URL: https://www.nature.com/articles/nphys3584 (visited on 11/22/2022).

[12] Shuta Nakajima et al. "Topological Thouless pumping of ultracold fermions". en. In: *Nature Physics* 12.4 (Apr. 2016). Number: 4 Publisher: Nature Publishing Group, pp. 296–300. ISSN: 1745-2481. DOI: 10.1038/nphys3622. URL: https://www.nature.com/articles/nphys3622 (visited on 11/22/2022).

[13] J. Zak. "Berry's phase for energy bands in solids". In: *Physical Review Letters* 62.23 (June 1989). Publisher: American Physical Society, pp. 2747–2750. DOI: 10.1103/PhysRevLett.62.2747. URL: https://link.aps.org/doi/10.1103/PhysRevLett.62.2747 (visited on 11/23/2022).

[14] Weiwei Zhu et al. “Zak phase and band inversion in dimerized one-dimensional locally resonant metamaterials”. In: *Physical Review B* 97.19 (May 2018). Publisher: American Physical Society, p. 195307. DOI: 10.1103/PhysRevB.97.195307. URL: https://link.aps.org/doi/10.1103/PhysRevB.97.195307 (visited on 11/23/2022).

[15] Henning Schomerus. “Topologically protected midgap states in complex photonic lattices”. EN. In: *Optics Letters* 38.11 (June 2013). Publisher: Optica Publishing Group, pp. 1912–1914. ISSN: 1539-4794. DOI: 10.1364/OL.38.001912. URL: https://opg.optica.org/ol/abstract.cfm?uri=ol-38-11-1912 (visited on 11/23/2022).

[16] P. Delplace, D. Ullmo, and G. Montambaux. “Zak phase and the existence of edge states in graphene”. In: *Physical Review B* 84.19 (Nov. 2011). Publisher: American Physical Society, p. 195452. DOI: 10.1103/PhysRevB.84.195452. URL: https://link.aps.org/doi/10.1103/PhysRevB.84.195452 (visited on 11/23/2022).

[17] R. Jackiw and C. Rebbi. “Solitons with fermion number ½”. en. In: *Physical Review D* 13.12 (June 1976), pp. 3398–3409. ISSN: 0556-2821. DOI: 10.1103/PhysRevD.13.3398. URL: https://link.aps.org/doi/10.1103/PhysRevD.13.3398 (visited on 11/23/2022).

[18] W. P. Su, J. R. Schrieffer, and A. J. Heeger. “Soliton excitations in polyacetylene”. In: *Phys. Rev. B* 22 (4 Aug. 1980), pp. 2099–2111. DOI: 10.1103/PhysRevB.22.2099. URL: https://link.aps.org/doi/10.1103/PhysRevB.22.2099.

[19] A. J. Heeger et al. “Solitons in conducting polymers”. In: *Rev. Mod. Phys.* 60 (3 July 1988), pp. 781–850. DOI: 10.1103/RevModPhys.60.781. URL: https://link.aps.org/doi/10.1103/RevModPhys.60.781.

[20] M. Zaimi et al. “Detecting topological edge states with the dynamics of a qubit”. In: *Physics Letters A* 388 (2021), p. 127035. ISSN: 0375-9601. DOI: https://doi.org/10.1016/j.physleta.2020.127035. URL: https://www.sciencedirect.com/science/article/pii/S0375960120309026.

[21] Bo-Hung Chen and Dah-Wei Chiou. “An elementary rigorous proof of bulk-boundary correspondence in the generalized Su-Schrieffer-Heeger model”. In: *Physics Letters A* 384.7 (Mar. 2020). arXiv:1705.06913 [cond-mat], p. 126168. ISSN: 03759601. DOI: 10.1016/j.physleta.2019.126168. URL: http://arxiv.org/abs/1705.06913 (visited on 11/24/2022).

[22] J. K. Asbóth, L. Oroszlány, and Pályi A. *A Short Course on Topological Insulators*. Springer International Publishing, 2016, pp. 1–39.

[23] Felix Bleckmann et al. "Spectral imaging of topological edge states in plasmonic waveguide arrays". In: *Physical Review B* 96.4 (July 2017). Publisher: American Physical Society, p. 045417. DOI: 10.1103/PhysRevB.96.045417. URL: https://link.aps.org/doi/10.1103/PhysRevB.96.045417 (visited on 11/23/2022).

[24] Gyungchoon Go et al. "Realization of Su-Schrieffer-Heeger states based on metamaterials of magnetic solitons". In: *Physical Review B* 101.13 (Apr. 2020). Publisher: American Physical Society, p. 134423. DOI: 10.1103/PhysRevB.101.134423. URL: https://link.aps.org/doi/10.1103/PhysRevB.101.134423 (visited on 11/23/2022).

[25] Md Nurul Huda et al. "Tuneable topological domain wall states in engineered atomic chains". en. In: *npj Quantum Materials* 5.1 (Mar. 2020). Number: 1 Publisher: Nature Publishing Group, pp. 1–5. ISSN: 2397-4648. DOI: 10.1038/s41535-020-0219-3. URL: https://www.nature.com/articles/s41535-020-0219-3 (visited on 11/23/2022).

[26] M. Bello, C. E. Creffield, and G. Platero. "Long-range doublon transfer in a dimer chain induced by topology and ac fields". In: *Scientific Reports* 6.1 (Sept. 2016). arXiv:1510.01379 [cond-mat, physics:quant-ph], p. 22562. ISSN: 2045-2322. DOI: 10.1038/srep22562. URL: http://arxiv.org/abs/1510.01379 (visited on 11/23/2022).

[27] Shaochun Lin et al. "Dynamic Observation of Topological Soliton States in a Programmable Nanomechanical Lattice". In: *Nano Letters* 21.2 (Jan. 2021). Publisher: American Chemical Society, pp. 1025–1031. ISSN: 1530-6984. DOI: 10.1021/acs.nanolett.0c04121. URL: https://doi.org/10.1021/acs.nanolett.0c04121 (visited on 11/24/2022).

[28] Ruben Verresen, Roderich Moessner, and Frank Pollmann. "One-Dimensional Symmetry Protected Topological Phases and their Transitions". In: *Physical Review B* 96.16 (Oct. 2017). arXiv:1707.05787 [cond-mat], p. 165124. ISSN: 2469-9950, 2469-9969. DOI: 10.1103/PhysRevB.96.165124. URL: http://arxiv.org/abs/1707.05787 (visited on 11/23/2022).

[29] Fabio L. Pedrocchi and David P. DiVincenzo. "Majorana Braiding with Thermal Noise". In: *Physical Review Letters* 115.12 (Sept. 2015). Publisher: American Physical Society,

p. 120402. DOI: 10.1103/PhysRevLett.115.120402. URL: https://link.aps.org/doi/10.1103/PhysRevLett.115.120402 (visited on 11/24/2022).

[30] François Konschelle and Fabian Hassler. "Effects of nonequilibrium noise on a quantum memory encoded in Majorana zero modes". In: *Physical Review B* 88.7 (Aug. 2013). Publisher: American Physical Society, p. 075431. DOI: 10.1103/PhysRevB.88.075431. URL: https://link.aps.org/doi/10.1103/PhysRevB.88.075431 (visited on 11/24/2022).

[31] N. Y. Yao et al. "Topologically protected quantum state transfer in a chiral spin liquid". en. In: *Nature Communications* 4.1 (Mar. 2013). Number: 1 Publisher: Nature Publishing Group, p. 1585. ISSN: 2041-1723. DOI: 10.1038/ncomms2531. URL: https://www.nature.com/articles/ncomms2531 (visited on 11/24/2022).

[32] Sankar Das Sarma, Michael Freedman, and Chetan Nayak. "Majorana Zero Modes and Topological Quantum Computation". In: *npj Quantum Information* 1.1 (Dec. 2015). arXiv:1501.02813 [cond-mat], p. 15001. ISSN: 2056-6387. DOI: 10.1038/npjqi.2015.1. URL: http://arxiv.org/abs/1501.02813 (visited on 11/24/2022).

[33] Daria Smirnova et al. "Nonlinear topological photonics". In: *Applied Physics Reviews* 7.2 (June 2020). Publisher: American Institute of Physics, p. 021306. DOI: 10.1063/1.5142397. URL: https://aip.scitation.org/doi/full/10.1063/1.5142397 (visited on 11/24/2022).

[34] Alexander B. Khanikaev and Gennady Shvets. "Two-dimensional topological photonics". en. In: *Nature Photonics* 11.12 (Dec. 2017). Number: 12 Publisher: Nature Publishing Group, pp. 763–773. ISSN: 1749-4893. DOI: 10.1038/s41566-017-0048-5. URL: https://www.nature.com/articles/s41566-017-0048-5 (visited on 11/24/2022).

[35] Shukai Ma and Steven M. Anlage. "Microwave applications of photonic topological insulators". en. In: *Applied Physics Letters* 116.25 (June 2020), p. 250502. ISSN: 0003-6951, 1077-3118. DOI: 10.1063/5.0008046. URL: http://aip.scitation.org/doi/10.1063/5.0008046 (visited on 11/24/2022).

[36] Ling Lu, John D. Joannopoulos, and Marin Soljačić. "Topological states in photonic systems". en. In: *Nature Physics* 12.7 (July 2016). Number: 7 Publisher: Nature Publishing Group, pp. 626–629. ISSN: 1745-2481. DOI: 10.1038/nphys3796. URL: https://www.nature.com/articles/nphys3796 (visited on 11/24/2022).

[37] Nicolas Pernet et al. “Gap solitons in a one-dimensional driven-dissipative topological lattice”. en. In: *Nature Physics* 18.6 (June 2022). Number: 6 Publisher: Nature Publishing Group, pp. 678–684. ISSN: 1745-2481. DOI: 10.1038/s41567-022-01599-8. URL: https://www.nature.com/articles/s41567-022-01599-8 (visited on 11/24/2022).

[38] Minkyung Kim, Zubin Jacob, and Junsuk Rho. “Recent advances in 2D, 3D and higher-order topological photonics”. en. In: *Light: Science & Applications* 9.1 (July 2020). Number: 1 Publisher: Nature Publishing Group, p. 130. ISSN: 2047-7538. DOI: 10.1038/s41377-020-0331-y. URL: https://www.nature.com/articles/s41377-020-0331-y (visited on 11/24/2022).

[39] E. J. Meier, F. A. An, and B. Gadway. “Observation of the topological soliton state in the Su–Schrieffer–Heeger model”. In: *Nature Communications* 7 (1 2016). DOI: 10.1038/ncomms13986.